UNIVERSITAT DE BARCELONA

Modeling the gravitational clustering in hierarchical scenarios of structure formation

Alberto Manrique Oliva

Departament d'Astronomia i Meteorologia

Universitat the Barcelona

MODELING THE GRAVITATIONAL CLUSTERING IN HIERARCHICAL SCENARIOS OF STRUCTURE FORMATION

Memoria presentada por
Alberto Manrique Oliva
para optar al título de
Doctor en Ciencias Físicas

Barcelona, Septiembre de 1995

Contents

1

PREFACE

Theoretical and observational data on galaxy clustering suggest an increasingly accepted trend on how cosmic objects form and evolve. According to this view, there is a hierarchy in structure formation that starts with early, low-massive objects and finishes with late, massive ones, these latter arising from the gravitational clustering of the former.

It is generaly believed that the first objects, as well as their subsequent clusterings, have their origin in small amplitude density inhomogeneities which have grown by gravitational instability as the universe expanded. Several mechanisms have been proposed to explain the genesis and properties of primordial fluctuations. The theory of inflation predicts the generation of adiabatic density perturbations with a spatial Gaussian distribution completely characterized by the correlation function. Topological defect models claim that the motion of cosmic strings is able to imprint non-Gaussian isocurvature density perturbations in the matter.

In the early univers, the tight coupling between baryons and photons inhibits the growth of barionic density perturbations until the epoch of recombination ($z_{rec} \approx 1000$). Since then, the perturbation amplitude grows exclusively driven by gravitation. The situation changes drastically if a great amount

of non-barionic dark matter is considered. As this matter does not interact with radiation, its density perturbations starts growing much earlier, especially when the univers enters the matter dominated era ($z_{eq} \gg z_{rec}$ for high Ω). After recombination baryons 'fall into' dark matter fluctuations so that baryonic perturbations rapidly catch up non-barionic ones . The existence of a large fraction of non-baryonic dark matter seems to be confirmed from both galaxy clustering data.

The evolution of density inhomogeneities in an expanding univers passes through two distinct stages. In the linear regime the perturbation expands while its amplitude increases. Owing to the independence of the Fourier modes, the set of equations governing the amplitude evolution can be solved analitically. For high amplitudes the perturbations enter the non-linear regime (the Fourier modes are coupled together), begin to collapse and finally virialize giving rise to a newborn object. Unfortunately, this latter regime has no general exact solution, and the only accurate way to follow the non-linear evolution of perturbations is by means of numerical simulations. But this procedure does not provide a modeling of gravitational clustering because of two reasons. On one hand, N-body and hydrodynamics methods use up large amounts of CPU time, preventing one from the probe of the whole parameter space. On the other hand, the present state-of-the-art numerical simulations have not reached yet a sufficient wide dynamic range to properly study the clustering process.

Observational data on the distant univers are rapidly becoming numerous and detailed. Comparison with those avalaible on the nearby univers harbors important information on the formation and evolution of cosmic objects. Our capability of interpreting these observations and extracting accurate cosmological implications depends on the existence of a detailed model of gravitational clustering. This long-standing necessity was alleviated by the seminal work of Press & Schechter (1974; hereafter PS), who proposed an innovative method, founded on features of the linear density field, capable of giving the mass distribution of collapsed objects. Although their formalism is poorly justified, the derived mass function fits the corresponding quantity from N-body simulations

reasonably well. This amazing outcome suggests that the PS formalism is able to describe the real clustering process, fact which has motivated a series of papers devoted to properly justify the method. The most popular of them has been the solution brought by Bond et al. (1991; henceforward BCEK), known as the excursion set formalism. Recently, based on this formalism, Lacey & Cole (1993) have calculated some interesting quantities related to the growth history of collapsed objects, such as the merger and accretion rates and the survival and formation times, which complete the gravitational clustering view.

But the hierarchical clustering picture drawn by the PS formalism assumes all points of the linear density field as seeds of relaxed objects at some epoch. However it is expected from the simple spherical collapse model that maxima of the density field (peaks) are physically better motivated seeds. A detailed modeling of the gravitational clustering in the peak model framework would therefore be more justified than that given by the PS formalism. The construction of such a model is the main goal of this work.

The construction of such a model is the main goal of this work. The idea arised as a natural consequence of the theoretical work developed by the Cosmology Group of the University of Barcelona on the morphological segregation of galaxies. Its chief contribution to this topic has been made from the evolutive viewpoint (Solanes, Salvador-Solé, & Sanromà 1989, Salvador-Solé, Sanromà, & Jordana 1989, Sanromà, & Salvador-Solé 1990, Solanes, & Salvador-Solé 1992), which suppose that galaxies change their shape due to interactions with the environment. Nonetheless, it was deemed interesting to tackle with the genetic approach, which assumes that shapes are not altered but already determined by the environment before galaxy formation. In order to model an innate morphological segregation, it is necessary to introduce a specific formation scenario; the most suitable and simplest one is the biased galaxy formation, which states that earlier galaxies arise from higher peaks of the linear density field. With the aid of the statistics of maxima in three-dimensional Gaussian fields developed by Bardeen et al. (1986; hereafter BBKS), Manrique (1992) computed the population fraction between disk and elliptical galaxies as a function of the density in non-relaxed environments.

The extension of the model to relaxed objects required an accurate specification of their physical and statistical properties. Since at that moment there was no justified quantity available in the peak model framework, the immediate task was to build a formalism which would permit us to carry out this enterprise. As the work went on, it turn out to be that our formalism was powerful enough to account not only for the derivation of the mass function, but for a complete description of the hierarchical clustering. This definively set off the topic of my Ph. D. Thesis.

What was born as a necessary tool to model the morphological segregation in relaxed environments has turn into a new research line, which has already yielded three papers in refereed journals (Manrique, & Salvador-Solé 1995a, Salvador-Solé, & Manrique 1995, Manrique, & Salvador-Solé 1995b), and with a great amount of applications. It is expected that it will serve to set, on a physical ground, dynamical quantities roughly determined, such as the collapse threshold for galaxies of different shapes, fact which will give new insights into the morphological segregation phenomenon. On the other hand, it will complement the interesting work that is being currently developed by our group on the detection and characterization of substructure (Sanromà, & Salvador-Solé 1989, Salvador-Solé, & Sanromà 1989, Salvador-Solé, Sanromà, & González-Casado 1993, Salvador-Solé, González-Casado, & Solanes 1993, González-Casado, Solanes, & Salvador-Solé 1993, Gonzalez-Casado, Mamon, & Salvador-Solé 1994, Gonzalez-Casado, Serna, Alimi, & Salvador-Solé 1995), playing a key role in the cosmological implications.

In Chapter 1 we review the foundations of gravtinsta the

2

COSMOLOGICAL PERTURBATIONS

This chapter is devoted to show the cosmological framework in which structures form and evolve. It approximately follows the lines developed in § 2 and § 3 of the review by Varun & Coles (1995). It contains a brief description of the unperturbed univers, a general discusion on the linear evolution of density perturbations, and some insight in the non-linear regime by means of the spherical collapse model. Finally, a simple formalism to obtain the statistics of virialized objects from the linear field is presented. The reader is encouraged to consult the textbooks on Cosmology by Weinberg (1972), Misner, Thorne, & Wheeler (1973), Zel'dovich & Novikov (1983), and Peebles (1993) as fundamental sources for further information about these subjects.

2.1 FRW Models

Modern Cosmology is founded on the Cosmological Principle and Einstein's field equations. The Cosmological Principle assumes that the univers is spa-

tially homogeneous and isotropic, in other words, physical properties do not change with position or direction. Homogeneity seems to be confirmed by measurements of peculiar velocities of galaxies on very large-scales, as well as radio sources count studies. On the other hand, the high degree smoothness of the Cosmic Background Radiation (CBR) is an unmistakable signature of an isotropic univers.

According to Einstein's equations, the dynamics of the whole universe is linked to its energy content

$$G_{\mu\nu} = 8\pi G T_{\mu\nu}, \tag{2.1}$$

where $G_{\mu\nu}$ $(\mu, \nu = 0, 1, 2, 3)$ is a tensor formed by the metric $g_{\mu\nu}$ and its two first derivatives, and $T_{\mu\nu}$ is the energy-momentum tensor. The line element associated to the metric for a homogeneous and isotropic univers in comoving polar spherical coordinates and cosmic time has the general form [1]

$$ds^2 = g_{\mu\nu} dx^\mu dx^\nu = dt^2 - a^2(t) \left(\frac{dr^2}{1 - kr^2} + r^2 d\theta^2 + r^2 \sin^2\theta d\phi^2 \right), \tag{2.2}$$

where $a(t)$ is a unknown function of time called the *cosmic scale factor* and k is a constant which determines the space curvature and takes the values -1, 0, and 1 for the hyperbolic, euclidian (flat) and spherical cases respectively. This kind of metric is known as the *Robertson-Walker metric*.

The universe as a whole can be approximately regarded as a perfect fluid. In this case the energy-momentum tensor adopts a diagonal form, with components $T_{00} = \rho$, $T_{\alpha\beta} = -P\delta_{\alpha\beta}$ $(\alpha, \beta = 1, 2, 3)$, being ρ the energy density and P the pressure. This brings the Einstein equations to

$$\begin{aligned} 3\frac{\ddot{a}}{a} &= -4\pi G(\rho + 3P) + \Lambda, \\ \frac{\ddot{a}}{a} + 2\frac{\dot{a}^2}{a^2} + 2\frac{k}{a^2} &= 4\pi G(\rho - P) + \Lambda, \end{aligned} \tag{2.3}$$

[1] As usual, the velocity of light c is set to unity.

where Λ is the cosmological constant. Eliminating $\ddot{a}$ in the former equations and taking into account the Bianchi identities, equations (2.3) are equivalent to

$$\left(\frac{\dot{a}}{a}\right)^2 + \frac{k}{a^2} = \frac{8\pi G}{3}\rho + \frac{\Lambda}{3}, \tag{2.4}$$

$$\frac{d}{da}(\rho a^3) = -3Pa^2. \tag{2.5}$$

Where equation (2.5) is the energy conservation equation. Equation (2.5) allows one to obtain the energy density ρ as a function of the scale factor a provided a relation between the variables ρ and P (an equation of state) is supplied. If the energy density of the universe is dominated by relativistic particles (radiation dominated era), the relation $P = \rho/3$ holds and (2.5) gives $\rho \propto a^{-4}$, whereas if the energy density is dominated by non-relativistic particles (matter dominated era), then $P = 0$ and $\rho \propto a^{-3}$. Using these results in (2.4), we can precisely determine the behavior of the scale factor for all time. The set made up by equations (2.4), (2.5), and the equation of state is known as *Friedman's equations*, and models based on this set are named *Friedman-Robertson-Walker (FRW) models*.

It is possible to explore the evolutive history of the univers by studying the sign of the time derivatives of the scale factor even without specifying a definite equation of state. For instance, taking $\Lambda = 0$ the first of equations (2.3) states that acceleration $\ddot{a}/a$ is negative as long as $(\rho + 3P) > 0$. Since $a > 0$ by definition and observation tell us that $\dot{a}/a > 0$ (the univers is expanding), then the function $a(t)$ must have reached the zero value at some finite time in the past. If we take $a(t = 0) = 0$, then the present time t_0, i.e., the time elapsed since this singularity, measures the age of the univers. To see the role played by the constant k, equation (2.4) can be rewritten (with $\Lambda = 0$) as

$$\dot{a}^2 + k = \frac{8\pi G}{3}\rho a^2. \tag{2.6}$$

Provided that the pressure P does not become negative, the density ρ decrease with increasing scale factor, being a^{-3} the least favorable decaying law, so when $a \to \infty$, the right hand side of (2.6) tends to zero at least as fast as a^{-1}. For $k = -1$, the square velocity $\dot{a}^2$ is positive definite and $a(t)$ is a monotonic

increasing function with asymptotic behavior

$$\lim_{t\to\infty} a(t) = t \tag{2.7}$$

(open univers). For $k = 0$ (flat univers) $\dot{a}^2$ is still positive definite and $a(t)$ goes on increasing but slower than t. Finally, for $k = 1$ the scale factor increases with time, stops growing when the expansion velocity becomes zero and begin to decrease owing to the negative acceleration (closed univers).

2.1.1 Cosmological parameters

We have already introduced the cosmological constant Λ which was initially invoked by Einstein to obtain a static univers. Nowadays it is called on to solve several timing problems such as the age of the univers or the onset of structure formation. In the context of quantum field theory, a positive cosmological constant corresponds to a vacuum energy density. To see the gravitational effects driven by the cosmological constant, let us imagine the univers uniformly filled with an ideal "vacuum fluid", with energy density ρ_{vac} and pressure P_{vac}. The equation of state for such a fluid is (Weinberg 1992) $\rho_{vac} = -P_{vac}$, which means that $(\rho_{vac} + 3P_{vac}) < 0$, and, according to the first of equations (2.3), $\ddot{a} > 0$. So, we have found that the gravity of a vacuum is not attractive, as for ordinary matter, but repulsive. Such repulsion arise from the fact that the vacuum pressure is negative and participates in the the gravitational intreraction as another component. Therefore, adding a cosmological constant to Einstein's equations causes the expansion rate of the universe to slow down.

Another relevant parameter in Cosmology is the Hubble parameter, defined as $H = \dot{a}/a$, which measures the expansion rate at a given epoch. It has dimensions of invers time, so H^{-1} sets a characteristic time, and H^{-1} times the velocity of light sets a characteristic length. *The Hubble time* gives the typical age of the univers, and *The Hubble length* the scale of the observable univers (the distance covered by a light signal since the initial singularity [2]).

[2]This quantity it is also known as the particle horizon in a pure FRW univers.

At the present epoch, galaxies, which take part in the overall expansion, are moving away from us at a velocity $v_r = H_0 r$, where H_0 is the Hubble constant (the Hubble parameter at $t = t_0$) and r is the distance to the galaxy. Due to the recessional velocity, the light emitted by these galaxies experiences a shift towards low frequencies. If this redshift is interpreted as Doppler effect then [3]

$$z = \frac{\Delta\lambda}{\lambda} = v_r, \tag{2.8}$$

so $z = H_0 r$, and the Hubble constant can be determined by measuring distances and redshifts. Unfortunately, the estimates of the Hubble constant are still quite uncertain owing to the dificulty in establishing the absolute distance to an object. Since the time of Hubble, who obtained $H_0 = 550$ km/s/Mpc, the value has been lowered by a factor of ten. Current measures yield values between 50 km/s/Mpc and 80 km/s/Mpc. Methods using Type Ia supernovae as standard candles favour the first value, whereas methods based on the Tully-Fisher relation for spirals calibrated by observations of Cepheid variable stars in several nearby galaxies favour the second value. In order to manage this uncertainty, which is propagated to physical quantities depending on the expansion rate, it is usual to express the Hubble constant in terms of the dimensionless factor

$$h = \frac{H_0}{100\,\mathrm{km/s/Mpc}}. \tag{2.9}$$

The third parameter playing a key role in the dynamics of the univers is the density parameter Ω, defined as

$$\Omega \equiv \frac{\rho}{\rho_{cr}} = \frac{8\pi G\rho}{3H^2}. \tag{2.10}$$

[3] This is a simplified interpretation, because the light frequency is also affected by the gravitational field of the univers. The deviation from a pure Doppler redshift is more marked for increasingly distant objects. In terms of the scale factor,

$$z = \frac{\Delta\lambda}{\lambda} = \frac{a_0}{a(t)} - 1.$$

It gives the energy density of the univers (associated to matter, radiation, and cosmological constant) in units of the critical density ρ_{cr}. For a vanishing cosmological constant, ρ_{cr} is the density that leads to a flat univers (see equation [2.6]). At the present time, the energy density associated to relativistic particles (i.e., radiation plus massless neutrinos) is $\Omega_{0,r} = 4.2\,10^{-5}$, while the baryon density derived from Big Bang nucleosynthesis models and observations indicating primordial abundances of light isotopes spans the range $0.01 \leq \Omega_b h^2 \leq 0.02$, so the current density parameter only have significant contribution from matter (and possibly from the cosmological constant).

Several methods are employed to directly evaluate the density parameter. The most straightforward one is to measure the luminosity of galaxies and estimate the ratio M/L. Given the average luminosity density $\mathcal{L}$ in the waveband used to determine the mass-to-light ratio, the mass density of visible matter is simply given by

$$\rho_{vis} = \frac{M}{L}\mathcal{L}. \tag{2.11}$$

This method gives $0.002 \leq \Omega_{vis} h \leq 0.006$ for galaxies. Comparing this interval with the one corresponding to Ω_b, it turns out to be that a great amount of baryonic matter in galaxies does not emit. The existence of dark matter matter in the univers is kown since the 1930's, when Zwicky pointed out that more mass than the visible one was needed to mantain galaxy clusters bounded.

Methods relying on dynamics allow estimates of the mass density on large scales. On galaxy clusters scales, the most usual method of estimating masses and M/L ratios has been to apply the virial theorem, which states that $M_{tot} \propto \langle v^2 \rangle / \langle r_{ij}^2 \rangle$ where $\langle v^2 \rangle$ is the velocity dispersion of the galaxies in the cluster, and r_{ij} is the separation between them. This method assumes that galaxies trace the cluster mass and the galaxy velocity distribution is isotropic. Typical inferred values of the matter density in galaxy clusters imply $\Omega_{cluster} \sim 0.1-0.2$. It is well known that clusters of galaxies contain great amounts of hot gas. If the gas is in hydrostatic equilibrium, it can be used to directly map the cluster mass distribution

$$M_{tot}(r) = -\frac{kT(r)}{G\mu m_p}\left(\frac{d\ln n}{d\ln r} + \frac{d\ln T}{d\ln r}\right), \tag{2.12}$$

where μ is the mean molecular weight of the gas, and $n(r)$ and $T(r)$ are the gas density and temperature profiles. Cluster masses inferred from X-ray observations are comparable to but about 30% less than virial estimates. On scales of order $50\,h^{-1}$ Mpc, cosmic density estimates are based on the comparison between the density perturbation field and the peculiar velocity field, sampled in the same volume (Dekel 1994). If both arise gravitationally, then the proportionality between them depends on the growth rate of density perturbations, which in turn depends on Ω (see § 2.2). This method gives values greater than 0.5 for the density parameter. Notice that in this case some sort of non-baryonic dark matter is needed to account for the value of Ω.

Other methods devised to estimate mass distributions are based on gravitational lensing. On small scales, microlensing effects are expected to uncover the presence of a large quantity of MACHOS (Massive Compact Halo Objects) which would be responsible for dark matter in galactic halos (Alcock et al. 1993; Aubourg et al. 1993; and Udalski et al. 1993). On larger scales, observations inside galaxy clusters of gravitational arcs and arclets, produced by the defection of light emitted by foreground sources, are allowing the mapping of the matter distribution which make up the gravitational lens (Fort & Mellier 1994; Kneib et al. 1995).

There is a strong theoretical prejudice that favours the value $\Omega_0 = 1$ for the current density parameter. Although observations clearly point towards values lower than unity, they are only one order of magnitude away from the preferred one. This fact means that at nucleosynthesis epoch the density parameter must have been unity with an accuracy of 10^{-17}. Theorists cannot stand this amazing fine-tunning and called on inflation [4] (Guth 1981) as an effective mechanism to produce a flat univers. The discrepancy between Ω_m and Ω_0 (assumed to be one) can be alleviated by introducing the cosmological constant. At the present epoch equation (2.4) adopts the form

$$\frac{k}{a_0^2} + 1 = \frac{8\pi G}{3H_0^2}\rho_m + \frac{\Lambda}{3H_0^2}. \tag{2.13}$$

[4] Besides, inflation is able to explain the causality problem and the generation of small density perturbations with Gaussian probability distribution.

For a flat univers $k = 0$, and defining $\Omega_\Lambda = \Lambda/3H_0^2$ we are lead to

$$1 = \Omega_m + \Omega_\Lambda \tag{2.14}$$

In order to mantain the usual notation, Ω_0 and ρ_0 will stand hereafter for the matter contribution to the density parameter and cosmic density at the present time.

2.1.2 The Age of the Universe

Solving equations (2.4) and (2.5), with the aid of an equation of state, we can obtain the current cosmic time t_0. Since at this epoch the universe is completely dominated by matter, the pressure can be neglected in front of the mass density. At the present instant both quantities are given by equations (2.3)

$$\begin{aligned} \rho_0 &= \frac{3}{8\pi G}\left(\frac{k}{a_0^2} + H_0^2 - \frac{\Lambda}{3}\right), \\ P_0 &= -\frac{1}{8\pi G}\left[\frac{k}{a_0^2} + H_0^2(1 - 2q_0) - \Lambda\right], \end{aligned} \tag{2.15}$$

where $q_0 = (-a\ddot{a}/\dot{a}^2)_0$ is the deceleration parameter, which measures the rate at which the gravitational attraction of the matter is slowing down the overall expansion at $t = t_0$. Taking into account that in a matter dominated univers $P = 0$, then the second of the equations leads to the relation

$$\frac{k}{a_0^2} = (2q_0 - 1)H_0^2 + \Lambda, \tag{2.16}$$

and substituting this expresion for the k/a_0^2 term in the first of equations (2.15) we obtain

$$\frac{\rho_0}{\rho_{cr}} = 2q_0 + \frac{2}{3}\frac{\Lambda}{H_0^2}. \tag{2.17}$$

The dynamics of the univers at the matter-dominated era is governed by the Friedmann equation (2.4) with the density ρ proprtional to a^{-3}. If the

cosmological constant vanishes, then this equation can be solve analytically. Therefore, we initially consider this case in order to get close expressions for t_0, and later on we will discuss the effects caused by the inclusion of a cosmological constant. The first step is to write equation (2.4) in terms of the present density ρ_0 and the ratio $a_0/a(t)$

$$\left(\frac{a_0}{a}\right)^2\left(\frac{\dot{a}}{a}\right)^2+\left(\frac{a_0}{a}\right)^2\frac{k}{a_0^2}=\left(\frac{a_0}{a}\right)^3\frac{8\pi G}{3}\rho_0. \tag{2.18}$$

We use equations (2.16) and (2.17), to write the latter equation in terms of the Hubble constant and the density parameter

$$\left(\frac{\dot{a}}{a}\right)^2+(\Omega_0-1)H_0^2=\Omega_0H_0^2\left(\frac{a_0}{a}\right). \tag{2.19}$$

Isolating dt and integrating both sides with the initial condition $t(a/a_0 \ll 1) = 0$ leads to the following formal solution

$$t=\frac{1}{H_0}\int_0^{a/a_0}dx\left(1-\Omega_0-\frac{\Omega_0}{x}\right)^{-1/2}. \tag{2.20}$$

In particular, the age of the univers can be obtained for $a/a_0 = 1$. The explicit solutions for the closed, flat, and open cosmological models are respectively

$$\begin{aligned} t_0H_0 &= \frac{\Omega_0}{2(\Omega_0-1)^{3/2}}\left[\cos^{-1}\left(\frac{2}{\Omega_0}-1\right)-\frac{2}{\Omega_0}\sqrt{\Omega_0-1}\right], \\ t_0H_0 &= \frac{2}{3}, \\ t_0H_0 &= \frac{\Omega_0}{2(1-\Omega_0)^{3/2}}\left[\frac{2}{\Omega_0}\sqrt{1-\Omega_0}-\cosh^{-1}\left(\frac{2}{\Omega_0}-1\right)\right]. \end{aligned} \tag{2.21}$$

These results show that the age of the univers increases monotonically with decreasing density parameter, reaching the limit $t_0 = H_0^{-1}$ for $\Omega_0 = 0$.

The inclusion of a positive cosmological constant crucially alters the expansion history of the univers, in such a way that the scale factor a increases very slowly at the present time. The solution for the spatially flat model has the form

$$\frac{a(t)}{a_0}=\left(\frac{\Omega_0}{\Omega_\Lambda}\right)^{\frac{1}{3}}\sinh^{\frac{2}{3}}\left(\frac{3\Omega_\Lambda^{1/2}H_0t}{2}\right). \tag{2.22}$$

At later times, when the matter density becomes negligible, it approaches the exponential de Sitter solution, $a(t) \sim \exp(\sqrt{\Lambda/3}\, t)$ (see [2.4] with $k = 0$). This fine-tuning in the increasing behavior of the scale factor causes the age of the univers to be greater than in the $\Lambda = 0$ case. For values in the intervals $k \leq 0$, $0 \leq \Omega_0 \leq 1$, and $\Omega_0 - 3\Omega_\Lambda/7 \leq 1$ an accurate approximation is

$$t_0 = \frac{2}{3H_0} \frac{\sinh^{-1}(\sqrt{(1-\Omega_a)/\Omega_a})}{\sqrt{1-\Omega_a}} \tag{2.23}$$

where $\Omega_a = \Omega_0 - 0.3\,(\Omega_0 + \Omega_\Lambda) + 0.3$.

From the practical viewpoint, three methods have been used to estimate the age of the univers: nuclear cosmochronology, the cooling of nearby white dwarfs, and the dating of the older globular clusters of the galaxy. The first method is based on the radioactive decay of heavy elements formed in supernovae by rapid neutron capture. Measures of element abundance ratios lead to an age of the univers ranging between 10 and 20 Gyr, but there is large uncertainty owing to the unknown element history. Age estimates from the cooling of white dwarfs in the neighborhood of the Sun are based on the existence of a lower limit to their temperature. Although cooler white dwarfs can be detected, none have been found yet. This fact suggests that they have not had enough time to cool to lower temperatures, which implies an estimate of 9 Gyr for the age of the Galactic disk (about 11 Gyr for the age of the univers). The last method takes advantage of the fact that, since stars in globular clusters formed at the same time, their evolution is only sensitive to the initial mass distribution. Then the age of globular clusters can be inferred by studying their stellar populations. This method gives a lower limit for the age of the univers in the interval 11 to 15 Gyr. Although the dating of globular clusters may be affected by uncertainties in the distance determination or the possible stellar mass loss, it is expected that these effects only reduce the former limit in 1 Gyr.

2.2 Gravitational Instability: Linear Theory

The FRW equations describe an unperturbed univers, but it is widely believed that the complex cosmic structures we observe and analize today would not have existed without the presence of primordial small density perturbations. Those sites in which the density was greater than the average had gravitational potentials slightly stronger, causing the surrounding matter to stream towards them. In this way, overdense regions became more overdense and underdense regions more underdense. This is the basic idea of gravitational instability. Therefore, it is extremely interesting to introduce small departures from homogeneity and isotropy which are suposed to be the seeds of future galaxies and other structures. First, we should select the reference frame in which the perturbations are physically characterized. We choose time-orthonormal coordinates (the synchronous gauge) as the most appropriate for the description of perturbations in a homogeneous and isotropic cosmological model. In this construction, we can imagine a set of observers, each attached to a comoving point, and each equipped with a clock synchronized relative to the neighboring observers. An event is labeled by three spatial coordinates x^α ($\alpha = 1, 2, 3$) corresponding to the position of the observer who passes through the event and the time $t = x^0$ displayed by the observer's clock. In this context, $\rho(\mathbf{x}, t)$ is the record of densities kept by the observer located at $\mathbf{x}$.

In the synchronous gauge, the line element describing a perturbed univers adopts the form

$$ds^2 = ds^2_{FRW} + h_{\alpha\beta} dx^\alpha dx^\beta, \tag{2.24}$$

where $\alpha, \beta = 1, 2, 3$, and ds^2_{FRW} is the FRW line element given by eq. (2.2). The relativistic treatment of gravitational instability involves the selection of a set of hypersurfaces upon which the perturbations are measured, the derivation of the background equations for the densities of the different species of matter contributing to the Friedmann equation which gives $a(t)$, and the derivation of the perturbed transport equations for all the fluid present (photons, baryons, cold dark matter, massless and massive neutrinos). In the case of a flat background metric, the formal solution turns out to be feasible, because perturba-

tion equations can be expanded in plane waves. This decomposition is a great simplification since perturbations are characterized by wavenumbers, and can be applied to open or close cosmologies provided the length scale is below the global curvature scale $k^{-1} \ll 3000\,(1-\Omega)^{1/2}h^{-1}$ Mpc (Bond 1989).

The relativistic treatment of gravitational instability outlined above is unavoidable when we deal with perturbations exceeding the Hubble length or streaming motions with relativistic velocities. Here, we will follow the linearized approximation, which assumes that perturbations in the metric are small $h_{\alpha\beta}h^{\alpha\beta} \ll 1$, and their sizes are always smaller than the horizon scale $\lambda_H \simeq 2t$. In this case the gravitational potential is weak enough to develop gravitational instability using Newtonian mechanics. If the mean free path between collisions of a particle is small, matter can be treated as an ideal fluid which satisfies the mass conservation equation

$$\left(\frac{\partial \rho}{\partial t}\right)_{\mathbf{r}} + \nabla_{\mathbf{r}} \cdot (\rho \mathbf{u}) = 0, \tag{2.25}$$

and the Euler equation of motion

$$\left(\frac{\partial \mathbf{u}}{\partial t}\right)_{\mathbf{r}} + (\mathbf{u} \cdot \nabla_{\mathbf{r}})\mathbf{u} = -\nabla_{\mathbf{r}}\Phi, \tag{2.26}$$

where Φ is the gravitational potential that verifies Poisson's equation

$$\nabla^2_{\mathbf{r}}\Phi = 4\pi G\rho. \tag{2.27}$$

$\mathbf{r}$ and $\mathbf{u}$ are respectively the position and velocity of a fluid element measured in an inertial frame.

In an expanding univers it is better suited to use comoving coordinates $\mathbf{x} = \mathbf{r}/a(t)$ instead of the inertial coodinate system. In the new reference frame the velocity field can be written as

$$\mathbf{u} = H\mathbf{r} + \mathbf{v}(\mathbf{x}, t), \tag{2.28}$$

where $\mathbf{v}$ is the peculiar velocity relative to the velocity imprinted by the general expansion. At this level, it is convenient to introduce the density contrast δ

that informs about the fractional departure of the mass density from the mean value around a point $\mathbf{x}$ at a given epoch

$$\delta(\mathbf{x},t) = \frac{\rho(\mathbf{x},t) - \rho_b(t)}{\rho_b(t)}, \tag{2.29}$$

where $\rho_b(t)$ is mean background density at a time t. As noted above, little inhomogeinities in the matter distribution cause variations in the gravitational potential. To distinguish between these perturbations and the mean gravitational potential, generated by a homogeneous distribution of matter, we will use the greek letter ϕ to denote the first and the capital greek letter Φ to denote the second.

With the change of position variables to comoving coordinates, the time derivative at fixed $\mathbf{r}$, and the gradient along the $\mathbf{r}$ direction at a fixed t have respectively the form

$$\left(\frac{\partial}{\partial t}\right)_{\mathbf{r}} = \left(\frac{\partial}{\partial t}\right)_{\mathbf{x}} - \frac{\dot{a}}{a}\mathbf{x}\cdot\nabla_{\mathbf{x}}, \qquad \nabla_{\mathbf{r}} = \frac{1}{a}\nabla_{\mathbf{x}}. \tag{2.30}$$

Applying these tranformations to equations (2.25)–(2.27) and after some algebra, we are led to the analog equations in the comoving frame expressed in terms of the density contrast, the peculiar velocity and the perturbed part of the gravitational potential

$$\frac{\partial(a\mathbf{v})}{\partial t} + (\mathbf{v}\cdot\nabla_{\mathbf{x}})\mathbf{v} = -\frac{1}{\rho}\nabla_{\mathbf{x}}P - \nabla_{\mathbf{x}}\phi, \tag{2.31}$$

$$\frac{\partial\rho}{\partial t} + 3\frac{\dot{a}}{a}\rho + \frac{1}{a}\nabla_{\mathbf{x}}(\rho\mathbf{v}) = 0, \tag{2.32}$$

$$\nabla^2_{\mathbf{x}}\phi = 4\pi G a^2(\rho - \rho_b) = 4\pi G a^2\rho_b\delta, \tag{2.33}$$

We can compute δ and $\mathbf{v}$ in linear perturbation theory by considering only small amplitude perturbations in the mass density, which leads to small streaming motions and small values of the gravitational potential ϕ. This is equivalent to expand perturbatively the density field, the velocity field, and the gravitational potential in equations (2.25)–(2.27), cut at first order the expansion,

and work out the equations containing only first order terms. The result of these operations leads to the following expressions

$$\frac{\partial \delta}{\partial t} + \frac{1}{a}\nabla_{\mathbf{x}} \cdot \mathbf{v} = 0, \tag{2.34}$$

$$\frac{\partial \mathbf{v}}{\partial t} + \frac{\dot{a}}{a}\mathbf{v} + \frac{1}{a}\nabla_{\mathbf{x}}\phi = -\frac{1}{\rho a}\nabla_{\mathbf{x}} P, \tag{2.35}$$

$$\nabla^2_{\mathbf{x}}\phi = 4\pi G a^2 \rho_b \delta, \tag{2.36}$$

for the continuity, Euler and Poisson equations respectively.

2.2.1 Pressureless Fluids

Let us start considering an expanding ideal fluid with negligible pressure, e.g., the univers in the matter dominated era. In this case the linearized equations describe the evolution of small density perturbations under the exclusive action of gravity.

Perturbation Growth in an Einstein-de Sitter univers

We obtain a second-order differential equation for the time evolution of density contrast by eliminating the peculiar velocity from equations (2.34) and (2.35), and using Poisson's equation

$$\ddot{\delta} + 2\frac{\dot{a}}{a}\dot{\delta} - 4\pi G \rho_b \delta = 0, \tag{2.37}$$

In the Einstein-de Sitter model ($\Lambda = 0$, $\Omega = 1$) the scale factor increases as $a(t) \propto t^{2/3}$, and the background density decreases as $\rho_b(t) \equiv \rho_{cr} \propto t^{-2}$. Therefore, equation (2.37) can be rewritten as

$$\ddot{\delta} + \frac{4}{3t}\dot{\delta} - \frac{2}{3t^2}\delta = 0 \tag{2.38}$$

This second-order diferential equation admits two solutions: a growing mode, proportional to $t^{2/3}$ ($\propto a$), and a decaying mode, proportional to t^{-1}. For perturbations with amplitude $\delta = \delta_i$ at an initial time t_i that begin to grow from rest [$\dot{\delta}(t_i) = 0$], the solution is a linear combination of increasing and decreasing modes

$$\delta(t) = \delta_i \left[\frac{3}{5} \left(\frac{t}{t_i} \right)^{\frac{2}{3}} + \frac{2}{5} \left(\frac{t}{t_i} \right)^{-1} \right], \tag{2.39}$$

From this equation we see that the growing mode contributes 60% to the density contrast at the initial time, whereas the decaying mode contributes 40 %. Due to the monotonous amplitude decrement as the time proceeds, the decaying mode goes to zero asymptotically. Because it does not actually play any role in structure formation, we hereafter deal only with the growing mode.

Perturbation Growth in Open and Close Models

Here we will follow the development done by Sahni & Coles (1995) to calculate the growing solution in a general cosmological model. These authors note that the decaying mode is always proportional to the Hubble parameter. On the other hand, the Wronskian of equation (2.37), defined as $W(t) = \dot{D}_+ D_- - \dot{D}_- D_+$ (being D_+, D_- the growing and decaying mode respectively), is proportional to a^{-2}. Once the decaying mode is known, and given the previous relation between the two modes, it is possible to find a differential equation for the growing one. Taking into account the Wronskian definition, we can write

$$\frac{W(t)}{D_-^2(t)} = \frac{d}{dt} \left(\frac{D_+(t)}{D_-(t)} \right). \tag{2.40}$$

Isolating $D_+(t)$ and integrating over t we have

$$\begin{aligned} D_+(t) &= D_-(t) \int^t W(t') D_-^{-2}(t') dt' = H(t) \int^t \frac{dt'}{a^2(t') H^2(t')}, \\ D_+(a) &= H(a) \int^a \frac{da}{(Ha)^3}. \end{aligned} \tag{2.41}$$

It is preferable to use the redshift z instead of the scale factor as the integration variable. Given the relation between both variables and the expression for $H(z)$

$$\begin{aligned} a(z) &= a_0(1+z)^{-1}, \\ H(z) &= H_0(1+z)(1+\Omega_0 z)^{\frac{1}{2}}, \end{aligned} \tag{2.42}$$

equation (2.41) turns into

$$D_+(z) = (a_0 H_0)^{-2}(1+z)(1+\Omega_0 z)^{\frac{1}{2}} \int_z^\infty \frac{dz'}{(1+z')^2(1+\Omega_0 z')^{3/2}}. \tag{2.43}$$

The integral of (2.43) admits an analytical solution that leads to

$$D_+(z) = \frac{1+2\Omega_0+3\Omega_0 z}{|1-\Omega_0|^2} + 3\Omega_0 \frac{(1+z)(1+\Omega_0 z)^{\frac{1}{2}}}{|1-\Omega_0|^{\frac{5}{2}}} f(\Omega_0, z), \tag{2.44}$$

where

$$\begin{aligned} f(\Omega_0, z) &= -\frac{1}{2}\log\left[\frac{(1+\Omega_0 z)^{\frac{1}{2}} + (1-\Omega_0)^{\frac{1}{2}}}{(1+\Omega_0 z)^{\frac{1}{2}} - (1-\Omega_0)^{\frac{1}{2}}}\right], \\ f(\Omega_0, z) &= \arctan\left[\frac{1+\Omega_0 z}{\Omega_0 - 1}\right]^{\frac{1}{2}}, \end{aligned} \tag{2.45}$$

for the cases $\Omega_0 < 1$ and $\Omega_0 > 1$, respectively. In the simpler case where $\Omega_0 = 1$, we have

$$D_+(z) \propto (1+z)^{-1} \tag{2.46}$$

We focus our attention on open comological models. In this case a good fit of the increasing mode solution is given by

$$D_+(z) \simeq \left(1+\frac{3}{2}\Omega_0\right)\left(1+\frac{3}{2}\Omega_0+\frac{5}{2}\Omega_0 z\right)^{-1}. \tag{2.47}$$

From this equation we find that for redshifts much greater than Ω_0^{-1} the growing mode is proportional to z^{-1}, whereas for redshifts much lesser than Ω_0^{-1} the growing mode becomes constant. This behavior is well understood in the context of the expansion history in an open model. At early epochs the scale factor always increases as $a(t) \propto t^{2/3}$ regardless of the value of the density parameter, and thus, it is expected that the growing mode resembles to that

of a flat univers. To see this, substitute the second line of equation (2.42), giving the variation of the Hubble parameter in terms of the redshift, in the definition of the density parameter (equation [2.10]). The result is

$$\frac{\Omega(z) = \Omega_0(1+z)}{1+\Omega_0 z.} \tag{2.48}$$

Then, at high redshifts the density always approaches the critical value. However, at low redshifts ($z \ll \Omega_0$) the expansion rate is experiencing an acceleration, owing to the increasing dominance of the curvature term in the equations of motion (2.3), causing the density perturbations to freeze out.

Perturbation Growth in Models with Cosmological Constant

We follow the same strategy than as in the previous case, but taking into account that the dynamics of the univers is now affected by the presence of a cosmological constant. As before, the decaying mode is proportional to $H(a)$, and the growing mode is given by equation (2.41). For a spatially flat univers ($\Omega_0 + \Omega_\Lambda = 1$)

$$H(a) \propto a^{-\frac{3}{2}} \left(1 + \frac{\Omega_0}{\Omega_\Lambda}\right)^{\frac{1}{2}}, \tag{2.49}$$

and the integration of equation (2.41) leads to

$$D_+(a) = C\,\frac{5}{6}\mathcal{B}_x\left(\frac{5}{6}, \frac{2}{3}\right)\left(\frac{\Omega_0}{\Omega_\Lambda}\right)^{\frac{1}{3}}\left[1 + \frac{\Omega_m}{\Omega_\Lambda a^3}\right]^{\frac{1}{2}}, \tag{2.50}$$

where

$$x = \frac{\Omega_\Lambda a^3}{\Omega_0 + \Omega_\Lambda a^3}, \tag{2.51}$$

C is an arbitrary constant, and $\mathcal{B}_x(\alpha, \beta)$ is the incomplete Beta function.

In models with cosmological constant, the expansion rate passes through two distinct stages. As the density of matter decreases ($\rho_m \propto a^{-3}$) the expansion rate growth experiences a deceleration, which leads to an almost constant scale factor with time. This happens when the repulsive force, driven by

the cosmological constant, and the gravitational attraction, driven by matter, cancels out. During this epoch density perturbations grow increasingly faster approaching the exponential Jeans rate, characteristic of a non-expanding universe. At later times, when the dynamics is completely dominated by the cosmological constant, the scale factor begins to grow again and tends to the value $a(t) = \exp(\sqrt{\Lambda/3}\,t)$. The acceleration in the expansion rate keeps the perturbation amplitude from growing. From equation (2.50), we see that the growing mode becomes a constant for $z \gg z_\Lambda = (\Omega_\Lambda/\Omega_0)^{1/3} - 1$.

Perturbation Growth in Models with Two Components

Let us consider the univers filled with presureless matter and radiation, the first component contributing with ρ_m and the second one contributing with ρ_r to the total density. In the case of a flat cosmology, and assuming that the radiation component is not perturbed [5], the resulting equations are

$$\ddot{\delta} + 2\left(\frac{\dot{a}}{a}\right)\dot{\delta} - 4\pi G\rho_b\delta = 0,$$

$$\left(\frac{\dot{a}}{a}\right)^2 = \frac{8\pi G}{3}(\rho_m + \rho_r) = \frac{8\pi G}{3}\rho_{tot}. \tag{2.52}$$

After changing the time variable to $\tau = \rho_m/\rho_r \propto a(t)$, the second-order differential equation can be rewritten as

$$\frac{d^2\delta}{d\tau^2} + \frac{(2+3\tau)}{2\tau(1+\tau)}\frac{d\delta}{d\tau} - \frac{3}{2\tau(1+\tau)}\delta = 0. \tag{2.53}$$

The growing solution of this equation is $D_+(\tau) \propto 1 + 3\tau/2$. We find that for $\tau \ll 1$ the growing mode becomes constant , so fluctuations do not grow. This behavior results from the existence of radiation which dominates the dynamics at early times causing the scale factor to evolve as $t^{1/2}$. As the time goes on, its contribution to the total energy density diminishes rapidly, and thus the matter takes its place as the preeminent component. Since the scale factor increases

[5] Primordial adiabatic perturbations affects radiation as well as matter. However, this simplification leads to the correct qualitative result

as $t^{3/2}$ during the matter dominated era, it is clear that the expansion rate experiences an acceleration throughout the transition. Therefore, the growth of density perturbations is suppressed as long as $\rho_r \gg \rho_m$.

Peculiar Velocities

To see how perturbations in the Hubble flow evolve with time, we only need to consider the linearized continuity equation with $P = 0$, Poisson's equation, and the solution of the second-order differential equation governing the density contrast growth. Since the growing mode is the dominant part of the general solution of equation (2.37), we are allowed to write $\delta(\mathbf{x}, t) = A(\mathbf{x})D_+(t)$. Substituting this result in equation (2.34) we have

$$\nabla_{\mathbf{x}} \cdot \mathbf{v} = -a\frac{\partial \delta}{\partial t} = -a\delta\frac{\dot{D}_+}{D_+} = -a\delta H f, \tag{2.54}$$

where the dimensionless velocity factor is

$$f = \frac{1}{H}\frac{\dot{D}_+}{D_+} = \frac{d\log\delta}{d\log a} \simeq \Omega_0^{0.6} + \frac{\Omega_\Lambda}{70}\left(\Lambda + \frac{\Omega_0}{2}\right). \tag{2.55}$$

Using Poisson's equation to isolate the density contrast, equation (2.54) writes

$$\nabla_{\mathbf{x}} \cdot \mathbf{v} = -\nabla_{\mathbf{x}}\left(\frac{Hf}{4\pi G a}\nabla_{\mathbf{x}}\phi\right), \tag{2.56}$$

and the integration of which leads to

$$\mathbf{v} = -\frac{2f}{3\Omega H a}\nabla_{\mathbf{x}}\phi + \frac{\text{const}}{a(t)}. \tag{2.57}$$

The linearized equations show that the peculiar velocity field associated with the growing mode can be exclusively expressed in terms of a velocity potential (i.e., the flow is irrotational) $\mathbf{v} = -\nabla_{\mathbf{x}}\phi_v/a$. In this case

$$\phi_v = \frac{2f}{3\Omega H}\phi. \tag{2.58}$$

This interesting property of the velocity field has been applied to several cosmological topics such as analytical approximations to the non-linear regime (Zel'dovich 1970) or reconstruction techniques devised to obtain the density field by measuring peculiar velocities (Bertschinger and Dekel 1989; Dekel, Bertschinger and Faber 1990; Dekel et al. 1993).

The presence of gravitational forces gives rise to an acceleration field of magnitude $\mathbf{g} = -\nabla_x \phi / a$. Taking the constant of integration equal to zero in equation (2.57), we get

$$\mathbf{v} = \frac{2f}{3\Omega H}\,\mathbf{g}. \tag{2.59}$$

This means that the peculiar velocity is parallel to the acceleration. In the Einstein-de Sitter model, with negligible cosmological constant and density parameter equal to unity, we have $f = 1$ and $H = 3/2\,t^{-1}$. Then the peculiar velocity field adopts the simple form $\mathbf{v} = \mathbf{g}\,t$. In the absence of a gravitational field ($\phi = 0$), the linearized Euler equation for presureless fluids writes

$$\frac{\partial \mathbf{v}}{\partial t} + \frac{\dot{a}}{a}\mathbf{v} = \frac{1}{a}\frac{\partial (a\mathbf{v})}{\partial t} = 0, \tag{2.60}$$

and any initial peculiar velocity decays as $a^{-1}(t)$.

2.2.2 Pressure Effects

So far we have consider the simple case of a presureless fluid. However, there are scales, at given epochs, on which pressure cannot be neglected. Then , the next step is to see what happens on these scales by introducing the pressure term in the linearized equations. Assuming that the pressure is just only a function of the density, and remembering that the sound speed is defined as $c_s = (dP/d\rho)^{1/2}$, the pressure force in an expanding fluid writes

$$\mathbf{F} = -\frac{1}{a}\nabla_{\mathbf{x}} P = -\frac{dP}{d\rho}\frac{\nabla_{\mathbf{x}}\rho}{a} = -c_s^2 \rho_b \frac{\nabla_{\mathbf{x}}\delta}{a}. \tag{2.61}$$

Coming back to the linearized equations, the substitution of the former result in the Euler equation (2.35) leads to

$$\frac{\partial \mathbf{v}}{\partial t} + \frac{\dot{a}}{a}\mathbf{v} + \frac{1}{a}\nabla_{\mathbf{x}}\phi = -\frac{c_s^2}{a}\nabla_{\mathbf{x}}\delta. \tag{2.62}$$

Following the same steps as in the presureless case, we arrive at the perturbation equation

$$\frac{\partial^2\delta}{\partial t^2} + 2\frac{\dot{a}}{a}\frac{\partial\delta}{\partial t} - \left(\frac{v_s}{a}\right)^2 \nabla_{\mathbf{x}}{}^2\delta - 4\pi G\rho_b\delta = 0. \tag{2.63}$$

It is convenient to expand the density contrast in Fourier series

$$\delta = \sum_k \delta_k \exp(-i\mathbf{k}\cdot\mathbf{x}), \tag{2.64}$$

where $k \equiv |\mathbf{k}| = 2\pi a/\lambda$ is the comoving wavenumber. Then the amplitude $\delta_k(t)$ associated with the wavenumber k satisfies the second-order differential equation

$$\ddot{\delta}_k + 2H\dot{\delta}_k + \omega_k^2\delta_k = 0. \tag{2.65}$$

This is the damped oscillator equation with a damped factor equal to $2H$ and a proper frequency

$$\omega_k^2 = \left(\frac{kc_s}{a}\right)^2 - 4\pi G\rho, \tag{2.66}$$

According to equation (2.65), density perturbations are damped owing to the expansion of the univers as long as the frequency ω_k^2 remains positive. When it becomes negative we have to abandon the damped oscillator interpretation and reconsider the solutions for a presureless fluid. The limiting case is given by the condition $\omega_k^2 = 0$, which defines the so-called *Jeans length*

$$\lambda_J = c_s\left(\frac{\pi}{G\rho}\right)^{\frac{1}{2}}. \tag{2.67}$$

On scales $\lambda > \lambda_J$ perturbations do not feel the influence of pressure and keep on growing as in a presureless fluid, whereas on scales $\lambda < \lambda_J$ pressure gradients force perturbations to oscillate as acoustic waves with steadily decreasing amplitude. This behavior can also be discussed in terms of characteristic times.

From equation (2.67), we see that, for a Jeans length, the characteristic time of gravitational growth ($\sim \sqrt{G\rho_b}$) is comparable to the crossing time of pressure waves ($\sim \lambda_J/c_s$). On scales larger than the Jeans scale, the crossing time is longer than the gravitational growth time for the density contrast. Therefore, pressure effects can be neglected. On scales smaller than the Jeans scale, the opposite trend is true, and the density contrast behaves as a damped oscillator.

From equation (2.67), it follows that the Jeans length is very sensitive to the sound speed within the fluid. During the radiation dominated era, electrons are tightly coupled to radiation via Thomson scattering in such a way that we are allowed to consider the mixture as a single fluid with an adiabatic speed of sound

$$c_s = \frac{1}{\sqrt{3}} \left(\frac{3\rho_m}{4\rho_\gamma} + 1 \right)^{-1/2} . \tag{2.68}$$

Taking into account that $\rho_r \gg \rho_m$ and $\rho_r \propto t^{-2}$, then the Jeans length is proportional to t. In other words, during radiation dominated epoch the Jeans length scales with cosmological horizon. During recombinaton, the coupling between electrons and radiation breaks down, and pressure becomes supported by neutral hydrogen atoms instead of radiation. This change in the physical properties of the fluid is responsible for an abrupt decrease in the value of the sound speed. If the mass associated with Jeans length at recombination is $M_J \simeq 9 \times 10^{16} (\Omega h^2)^{-2} M_\odot$ (the same order than that of superclusters of galaxies), the corresponding value after recombination drops to $M_J \simeq 1.3 \times 10^5 (\Omega h^2)^{-\frac{1}{2}} M_\odot$, which is comparable to the mass of a globular cluster.

Just before recombination, another phenomenon start playing a relevant role on the evolution of density perturbations. As recombination approaches, the mean free path of photons increases due to the progressive weakening of the coupling between matter and radiation. As a result, photons are able to escape from the potential wells created by overdensities, and carry with them still tightly coupled electrons. This free-streaming causes an effective damping of perturbations in the photon-baryon mixture on scales smaller than a characteristic length known as the *Silk length*. The associated Silk mass at recombination is $M_s \simeq 1.3 \times 10^{12} (\Omega h^2)^{-3/2} M_\odot$ similar to that of a galaxy.

2.3 The Spherical Collapse Model

In this section we will discuss the simplest class of non-linear approach: the spherical collapse model. It assumes a univers spherically symmetric about one point filled with presureless matter that behaves as an ideal fluid. This means that, in the real density field, any tidal effect of neighbouring perturbations upon the evolution of the perturbation, and any deviation from sphericity of the potential well due to the distribution of matter inside the volume element are neglected. The model also suposes that the density profile of the perturbation is monotonously decreasing in order to avoid shell crossing and, hence, ensure mass conservation inside evolving spherical shells. Under these simplifying assumptions an exact analytical treatment of the non-linear stage of gravitational instability is possible.

2.3.1 Energy Balance and Maximum Expansion Radius

We suppose that at an initial time t_i the spherical density inhomogeneity centered on a point $\mathbf{r}$ is moving with the general expansion, and is not affected by peculiar velocities. Consider a spherical shell of initial radius R_i around $\mathbf{r}$ containing a mass [6] $M = \rho_b(1+\delta_i)(4/3)\pi R_i^3$, where δ_i is the initial overdensity, and ρ_b is the density of the background. At early times the expansion of the shell is virtually indistinguishable from that of the rest of the Universe so that the velocity of the shell relative to the center is $\dot{R}_i = H_i R_i$, being H_i the Hubble parameter at an initial time. Thus, the kinetic energy per unit mass

[6] We assume that the shell has a flat density profile

$$\rho(r) = \rho_b\,(1+\delta_i) \quad \text{for } r \leq R_i,$$

$$\rho(r) = \rho_b \qquad\qquad \text{for } r > R_i.$$

with δ_i the real mean density contrast interior to the shell of radius R_i. Notice that the collapse dynamics is governed by the interior mean density, indeed.

at a distance R_i from the center is $K_i = H_i^2 R_i^2/2$, and the potencial energy per unit mass can be expressed as

$$U_i = -GM/R_i = -\frac{4\pi G}{3H_i^2}\rho_b(1+\delta_i)H_i^2 R_i^2 = -\Omega_i K_i. \tag{2.69}$$

Conservation of energy guarantees that the sum of the kinetic and potential energies is a constant. In particular, at the initial time we have

$$E = K_i + U_i = K_i\Omega_i[\Omega_i^{-1} - (1+\delta_i)]. \tag{2.70}$$

The requirement for a shell to be gravitationally bounded is that its total energy must be negative. In this case, the shell keeps on expanding until it reaches a maximum radius, turns around and begins to collapse. According to equation (2.70), the condition ensuring $E < 0$ is $1 + \delta_i > \Omega_i^{-1}$. Taking into account that the initial time t_i corresponds to a given redshift z, the former condition can be rewritten as

$$\delta(z) > \Omega^{-1}(z) - 1 = \frac{1-\Omega_0}{\Omega_0(1+z)}. \tag{2.71}$$

In an open univers, where $\Omega_0 < 1$, if the initial density contrast is less than a critical value, the energy is positive and the shell never stops expanding. For flat and closed cosmological models, with $\Omega_0 = 1$ and $\Omega_0 > 1$ respectively, any infinitesimal positive initial density perturbation gives rise to collapsed objects.

For gravitationally bound shells, it is straightforward to relate the maximum expansion radius to its initial values R_i, and δ_i [equivalently $R(z)$ and $\delta(z)$]. Owing to the monotonous decreasing density profile of the spherical perturbation, a shell with a given radius does not cross with other shells, so the mass contained remains constant with time. On the other hand, the shell velocity at turnaround is $\dot{R}|_{ta} = 0$. Then, only potential energy contributes to the total energy at turnaround

$$E = U_{ta} = -\frac{GM}{R_{ta}} = -\frac{R_i}{R_{ta}}K_i\Omega_i(1+\delta_i). \tag{2.72}$$

Equating this equation and (2.70) we obtain the relation

$$\frac{R_{ta}}{R_i} = \frac{1+\delta_i}{\delta_i - (\Omega_i^{-1} - 1)} \equiv [1+\delta(z)]\left[\delta(z) - \frac{1-\Omega_0}{\Omega_0(1+z)}\right]^{-1}. \tag{2.73}$$

2.3.2 Motion of a Mass Shell

The radius $R(t)$ of a spherical shell comprising mass M satifies the equation of motion

$$\frac{dr^2}{d^2t} = -\frac{GM}{r^2}. \tag{2.74}$$

Its first integral leads to the energy equation

$$\left(\frac{dr}{dt}\right) = 2\frac{GM}{r} + 2C, \tag{2.75}$$

where the constat of integration $2C$ is just the total energy. Taking $C < 0$ ($C > 0$) we recover the case of a gravitationally bounded (unbounded) spherical shell. The solution of equations (2.74) and (2.75) can be expressed in a parametric form

$$R = A(1-\cos\theta) \qquad t = B(\theta - \sin\theta) \tag{2.76}$$

for the case $C < 0$, and

$$R = A(\cosh\theta - 1) \qquad t = B(\sinh\theta - \theta) \tag{2.77}$$

for the case $C > 0$. The constants A and B are not idependent, but related trough $A^3 = GMB^2$. As we have noted above, the dynamical evolution of an spherical mass shell is similar to that of the whole universe. In fact, the corresponding parametric solution for a close univers is (see Peebles 1980)

$$R_b = A_b(1-\cos\mu) \qquad t = B_b(\mu - \sin\mu) \tag{2.78}$$

and for an open univers

$$R_b = A_b(\cosh\mu - 1) \qquad t = B_b(\sinh\mu - \mu) \tag{2.79}$$

If we assume that $a(t) = R_b(t)$, then the spherical portion of the univers contains the same mass as in the shell, and the constrain between A_b and B_b just writes $A_b^3 = GMB_b^2$.

At this point we are able to compute the density contrast in each mass shell. Since mass is conserved we get, using $M = 4\pi R^3\rho/3$ and eq. (2.76),

$$\rho(t) = \frac{3M}{4\pi A^3(1-\cos\theta)^3}. \tag{2.80}$$

In a spatially flat matter dominated Universe the background density scales as

$$\rho_b(t) = \frac{1}{6\pi G t^2} = \frac{1}{6\pi G B^2(\theta-\sin\theta)^2}. \tag{2.81}$$

So, from the definition of the density contrast in terms of the ratio $\rho(t)/\rho_b(t)$, and using equations (2.80) and (2.81), we have

$$\delta(\theta) \equiv \frac{\rho(t)}{\rho_b(t)} - 1 = \frac{9}{2}\frac{(\theta-\sin\theta)^2}{(1-\cos\theta)^3} - 1, \tag{2.82}$$

for gravitationally bounded density perturbations, and

$$\delta(\theta) = \frac{9}{2}\frac{(\theta-\sinh\theta)^2}{(\cosh\theta-1)^3} - 1 \tag{2.83}$$

for unbounded density fluctuations.

Constants A and B can be expressed in terms of the maximum expansion radius and the time at which it is reached. According to equation (2.76), maximum expansion occurs for $\theta = \pi$. Then, for this specific value of the developing angle, constants A and B are

$$A = R_{ta}/2, \qquad B = t_{ta}/\pi. \tag{2.84}$$

However, these relations are only valid for gravitationally bounded shells. More general expressions can be achieved using initial quantities instead of "turnaround" quantities. This is achieved by applying equation (2.73), the

constrain $A^3 = GMB^2$ and expressing the constant mass M in terms of R_i and ρ_i. The final result is

$$\begin{aligned} A &= \left(\frac{R_i}{2}\right) \frac{1+\delta_i}{\delta_i - (\Omega_i^{-1}-1)} \\ B &= \frac{1+\delta_i}{2H_i\Omega_i^{1/2}[\delta_i - (\Omega_i^{-1}-1)]^{3/2}}. \end{aligned} \tag{2.85}$$

Bearing in mind that initial conditions are set in an early epoch, it is reasonable to assume $\delta_i \ll 1$. Then, in a flat cosmological model equation (2.85) becomes, Universe,

$$A \simeq \frac{R_i}{2\delta_i}, \qquad B \simeq \frac{3}{4} t_i \delta_i^{-3/2}. \tag{2.86}$$

From equations (2.82) and (2.86) we recover the density contrast limit for small θ (or small t):

$$\lim_{\theta \to 0} \delta(\theta) \simeq \frac{3\theta^2}{20} \simeq \frac{3}{20}\left(\frac{6t}{B}\right)^{2/3} = \frac{3}{5}\delta_i \left(\frac{t}{t_i}\right)^{2/3}, \tag{2.87}$$

indicating that only 3/5th of the initial amplitude is in the growing mode. In view of equation (2.87) the critical condition (2.71) turns into $\delta_i > 3(\Omega_i^{-1}-1)/5$.

2.3.3 Turnaround and Collapse

For bounded shells the spherical model provides us with a variety of relations between quantities computed at turnaround ($\theta = \pi$) and at collapse ($\theta = \pi$) times. We consider a flat background cosmology with negligible cosmological constant. From equation (2.76) we have that the collapse time t_{coll} is twice the turnaround time t_{ta}. From equation (2.82) we find that $\delta(\theta = \pi) \simeq 4.6$ at the maximum expansion radius, whereas at collapse the overdensity tends to infinity due to the fact that the radius becomes zero. In fact $\delta_{coll} \to \infty$ is never achieved since exact spherical collapse breaks down as the density perturbation starts the collapse. Physical processes, such as shell crossing and rebounding, and the subsequent violent relaxation, ensures that the system reaches virial equilibrium at a finite density. The typical radius of the virialized

perturbation can be estimated by means of energetic arguments. At the instant of turnaround, only the potential energy contributes to the total energy of the spherical shell. After relaxation, the system satisfies the virial theorem, i.e., $2K = |W|$. Energy conservation leads to

$$U(R = R_{ta}) = E = U(R = R_{vir})/2, \tag{2.88}$$

being $U(R) = -GM/R$. Since the shell mass is conserved along the process, then the final virial radius R_{vir} is twice the turnaround radius R_{ta}. This result assumes that the uniform density profile is preserved during the relaxation process. But virialized objects exhibit the characteristic King profile instead of a flat one. In this case the the final potential energy does not take the same form than that the turnaround epoch, and consequently relation $2R_{vir} = R_{ta}$ does not hold. Then, for realistic density profiles the following calculations should be taken as raw estimations. Bearing in mind this warning, let us compute the typical overdensity of a virialized object $\delta_{vir} = \rho_{vir}/\bar{\rho}_{vir} - 1$ where $\bar{\rho}_{vir}$ is the background density at the epoch of virialization. From the previous results, we know that

$$\rho_{vir} = 8\rho_{ta} = 8\bar{\rho}_{ta}(4.6 + 1) \tag{2.89}$$

Taking into account that the background density scales as t^{-2}, and assuming that $t_{vir} \simeq t_{coll} \simeq 2t_{ta}$ then $\delta_{vir} = 8\ 5.6\ 4\ -1 = 178.2$. From here, it is easy to calculate the density of the relaxed system in terms of the present mean density and the collapse redshift z_{vir}

$$\rho_{vir} \simeq 179.2(1 + z_{vir})^3\rho_0. \tag{2.90}$$

Sometimes it is interesting to know extrapolated values of the density contrast assuming that the perturbation always evolves in the linear regime. This is equivalent to consider the limit of equation (2.82) for small values of the developing angle θ (small t). Remember that we have set initial conditions at an early epoch; in this way the linear behavior of the perturbation is ensured. So, the extension of the limit (2.87), only valid for times close to the initial one, to any epoch gives the wanted extrapolation. Equations (2.76) and (2.86)

bring this limit to

$$\delta_L(\theta) \simeq \frac{3}{5}\left(\frac{3}{4}\right)^{\frac{2}{3}}(\theta - \sin\theta)^{\frac{2}{3}}. \tag{2.91}$$

In particular, $\delta_L(\pi) \simeq 1.063$ for the linear density contrast at turnaround, and $\delta_L(2\pi) \simeq 1.686$ at recollapse. In an Einstein-de Sitter univers, perturbations in the linear regime grow as the scale factor $[a(z) \propto (1+z)^{-1}]$. Then, known the linear density contrast of a given spherical perturbation, the corresponding true redshifts at which the perturbation reached the maximum expansion and collapsed are, respectively,

$$\begin{aligned} 1 + z_{ta} &\simeq \frac{\delta_L}{1.063} \\ 1 + z_{coll} &\simeq \frac{\delta_L}{1.686}. \end{aligned} \tag{2.92}$$

But the spherical collapse model is founded on strong assumptions. It can only be applied to a very limited range of astrophysical problems. The most and better studied one is the spherical infall of matter onto an initial overdensity (Fillmore & Goldreich 1984, Bertschinger 1985). Nonetheless, the model is far from giving a trustful description of the collapse of protogalaxies or protoclusters, since, as proved by Lin, Mestel & Shu (1965), departures from spherical simmetry get amplified once the almost spherical density perturbation starts collapsing. During this stage the perturbation develops non-radial motions which invalidates the applicability of the spherical model. However, this phenomenon can be incorporated to the analysis by modeling the collapsing perturbation as a homogeneous ellipsoid of ideal fluid with negligible pressure. Classical studies on the motion of homogeneous spheroids, neglecting the tidal field of surrounding matter, show that collapse occurs along the minor axis, at a faster rate than that of an equivalent spherical overdensity, while the other axes tend to contract or expand in finite magnitudes, so the perturbation finally reachs a pancake configuration.

2.4 Statistics of Relaxed Objects

The most interesting processes giving rise to the present cosmic structure take place during the non-linear stage of the evolution of density perturbation. A detailed theory explaining how objects form and cluster would allows us to compare between quantities of the observed univers (e.g., number density of quasars, damped Lyman-α clouds, and galaxy clusters at different redshifts) and predictions in specific scenarios of structure formation. Nonetheless, this task is not an easy one because the exact treatment of perturbation growth in the non-linear regime requires the use of huge numerical simulations. Moreover, these complex calculations are not completely satisfactory due mainly to the excessive cost in CPU time and limitations in the avalaible dynamical range.

The spherical collapse model allows us to relate linear density perturbations to relaxed objects in a more or less simple way. In this section we will go one step beyond, and will show how to obtain statistics of highly non-linear structures from the linear density field through the use of this simple model. In particular, we will deal with the multiplicity or mass function, which informs about the number density of relaxed objects with mass in an infinitesimal range at a given epoch and, therefore, gives some clues about clustering history of objects. But some kind of statistical description is required before undertaking this topic.

2.4.1 Statistics of Primordial Density Fluctuations

The primordial density field $\delta(\mathbf{x})$ can be mathematically described as a homogeneous and isotropic three-dimensional scalar Gaussian random field, as long as perturbation amplitude remains small. There are physical and statistical arguments which support the Gaussianity assumption. The physical argument relies on inflation. According to this theory, small amplitude curvature perturbations generated by quantum fluctuations in the inflationary phase are very likely to be Gaussian. The statistical argument is based on the *central limit*

theorem, which states that the superposition of a large number of independent random variables (all drawn from the same distribution) gives rise to a new random variable whose probability distribution is Gaussian. We have seen that the density field $\delta(\mathbf{x})$ can be written as an infinite sum with coeficients $\delta(\mathbf{k})$, which are statistically independent in the linear regime and come from the same distribution. Furthermore, the phases between the different modes are suposed to be random and uniformly distributed from 0 to 2π, unless density fluctuations arise from gravitational fall into topological defects such us cosmic strings.

For statical purposes, it is convenient to express the density field in the Fourier space by using the Fourier tranform

$$\delta(\mathbf{x}) = \frac{1}{(2\pi)^3} \int d^3\mathbf{k}\, \delta(\mathbf{k})\, e^{-i\mathbf{k}\cdot\mathbf{x}}, \tag{2.93}$$

which has inverse

$$\delta(\mathbf{k}) = \int d^3\mathbf{x}\, \delta(\mathbf{x})\, e^{i\mathbf{k}\cdot\mathbf{x}}. \tag{2.94}$$

Remember that, in k-space, the Dirac delta function admits the following form

$$\delta^D(\mathbf{k}) = \frac{1}{(2\pi)^3} \int d^3\mathbf{x}\, e^{\pm i\mathbf{k}\cdot\mathbf{x}}. \tag{2.95}$$

The most relevant quantity in the statistical description of the density field is the two-point correlation function or autocovariance function defined as the volume average of the product of the function $\delta(\mathbf{x})$ evaluated at points $\mathbf{x}_1$ and $\mathbf{x}_2 = \mathbf{x}_1 + \mathbf{r}$ [7]

$$\langle \delta(\mathbf{x}_1)\delta(\mathbf{x}_2) \rangle = \xi(|\mathbf{x}_1 - \mathbf{x}_2|) = \xi(r), \tag{2.96}$$

where we have used the fact that the field is homogeneous and isotropic (i.e., invariant under translations and rotations), which means that the covariance function only depends on the relative distance between points. Developing

[7] Since random Gaussian processes are ergodic, volume averages are equivalent to ensemble averages. Hereafter, angular brackets mean averages over a large number of realizations.

equation(2.96) in the k-space and taking into account the reality of $\delta(\mathbf{x})$, we have

$$\xi(r) = \langle \delta(\mathbf{x}_1)\delta(\mathbf{x}_2) \rangle = \langle \int \frac{d^3\mathbf{k}_1}{(2\pi)^3} \delta(\mathbf{k}_1)\, e^{-i\mathbf{k}_1\cdot\mathbf{x}_1} \int \frac{d^3\mathbf{k}_2}{(2\pi)^3} \delta(\mathbf{k}_2)\, e^{-i\mathbf{k}_2\cdot\mathbf{x}_2} \rangle =$$
$$\int\int \frac{d^3\mathbf{k}_1}{(2\pi)^3} \frac{d^3\mathbf{k}_2}{(2\pi)^3} \langle \delta(\mathbf{k}_1)\, \delta^*(\mathbf{k}_2) \rangle e^{-i\mathbf{k}_1\cdot\mathbf{x}_1}\, e^{i\mathbf{k}_2\cdot\mathbf{x}_2} =$$
$$\int \frac{d^3\mathbf{k}}{(2\pi)^3} P(k)\, e^{-i\mathbf{k}\cdot(\mathbf{x}_1-\mathbf{x}_2)}, \qquad (2.97)$$

where $P(k)$ is the power spectrum, defined as [8]

$$P(k)\, \delta^D(\mathbf{k}_1 - \mathbf{k}_2) = \langle (\delta(\mathbf{k}_1)\, \delta^*(\mathbf{k}_2) \rangle, \qquad (2.98)$$

The Dirac delta function is introduced because modes of different spatial frequency are statistically independent (and thus have vanishing covariance) in a homogeneous univers. On the other hand, isotropy implies that the power espectrum should depend on the modul of $\mathbf{k}$ and not on its direction. When the condition $\mathbf{k}_1 = \mathbf{k}_2$ is enforced, we obtain the expression $P(k) = \langle |\delta(k)|^2 \rangle$ sometimes used as a definition of the power espectrum. The relevance of the two-point correlation function, or its Fourier transform the power spectrum, comes from the fact that, in Gaussian processes, it is the only quantity required to fully characterize the random field.

Many physical properties of the primordial density field can be related to the power spectrum. For example, the mean square density fluctuation is defined as the average $\langle \delta(\mathbf{x})\, \delta(\mathbf{x}) \rangle$, so from equations (2.96) and (2.98) we get

$$\langle \left(\frac{\delta\rho}{\rho} \right)^2 \rangle = \langle \delta(\mathbf{x})\, \delta(\mathbf{x}) \rangle = \frac{1}{2\pi^2} \int_0^\infty dk\, k^2 P(k). \qquad (2.99)$$

In hierarchical scenarios of structure formation the linear density field contains perturbations on all scales. If we are interested in singling out a given scale the

[8] This expression is equivalent to

$$P(k)\, \delta^D(\mathbf{k}_1 + \mathbf{k}_2) = \langle (\delta(\mathbf{k}_1)\, \delta(\mathbf{k}_2) \rangle$$

usual procedure is to smooth the density field using a spherically symmetric window with the appropriate size. The filtering operation brings equation (2.99) to

$$\langle\left(\frac{\delta\rho}{\rho}\right)^2\rangle_R \equiv \sigma_0^2(R) = \frac{1}{2\pi^2}\int_0^\infty dk\, k^2 W^2(kR) P(k), \qquad (2.100)$$

where $W(kR)$ is the Fourier transform of the filter function used to smooth the density field in real space. It tends to unity for small values of the argument, and falls off rapidly beyond the value $k_c \sim 1/R$ suppressing the contribution to the filtered density field from modes of wavelength smaller than the size of the smoothing function. The most used filters are the top hat or spherical, the gaussian and the sharp k-space, which have the following form in the real and Fourier space

top hat

$$\begin{aligned} W(r;R_T) &= \left(\frac{4\pi}{3}R_{TH}^3\right)^{-1}\theta\left(1-\frac{r}{R_{TH}}\right) \\ W(k;R_T) &= 3\,\frac{\sin(kR_T)-kR_T\cos(kR_T)}{(kR_T)^3}; \end{aligned} \qquad (2.101)$$

Gaussian

$$\begin{aligned} W(r;R_G) &= \frac{1}{(2\pi)^{3/2}R_G^3}\exp\left(-\frac{r^2}{2R_G^2}\right) \\ W(k;R_G) &= \exp\left(-\frac{k^2R_G^2}{2}\right) \end{aligned} \qquad (2.102)$$

Sharp k-space

$$\begin{aligned} W(k;R_T) &= \frac{\sin(r/R_S)-r/R_S\cos(r/R_S)}{2\pi^2r^3} \\ W(r;R_T) &= \theta(1-kR_S), \end{aligned} \qquad (2.103)$$

where $\theta(x)$ is the Heavyside step function. The rms fluctuation can be interpreted as the zero-order spectral moment. It is straightforward to extend the

definition (2.100) to include moments of higher order

$$\sigma_j^2(R) = \frac{1}{2\pi^2}\int_0^\infty dk k^{2(j+1)} W^2(kR) P(k). \tag{2.104}$$

Quantities such as the mean square velocity smoothed on a scale R and the mean square gravitational potential fluctuation can be calculated by using the linearized continuity equation and Poisson's equation expressed in the Fourier space. The contribution of this quantities, along with the mass fluctuation, per logarithmic interval of wavenumber is

$$\begin{aligned}
\frac{d\sigma^2}{d\log k} &= 4\pi k^3 P(k); \\
\frac{d\sigma_v^2}{d\log k} &= 4\pi (aHf)^2 k P(k); \\
\frac{d\sigma_\phi^2}{d\log k} &= 4\pi \left(\frac{3}{2}\Omega_0 H^2 a^2\right)^2 \frac{P(k)}{k}.
\end{aligned} \tag{2.105}$$

In order to complete this statistical description, we should specify the fluctuation spectrum. Inflationary theories predict an scale-invariant power spectrum with a power-law form

$$P(k) = A\, k^n, \tag{2.106}$$

usually with index $n = 1$. This special case, known as the *Harrison-Zel'dovich power spectrum*, results also from assuming that density fluctuations on any scale enters the horizon with the same amplitude. Unfortunately, the shape of the primordial spectrum is not conserved even in the linear regime because, after horizon entry, the grow of density perturbations is affected by collisional processes (see § 2.2.2). The so-called *transfer function* is introduced to account for the changes in the primordial power spectrum,

$$P(k, t_f) = T^2(k, t_f)\, P(k, t_i) \tag{2.107}$$

When perturbation evolution is only driven by gravity, the transfer function adopts the simple form $T(k, t_f) \propto D_+(k, t_f)$). Transfer functions depend on the

matter content of the univers and the values of the cosmological parameters. If the dynamics of the univers is driven by weak interacting massive particles which left the relativistic regime at a very later epoch, then we should apply the Hot Dark Matter (HDM) transfer function, which get rid of power on small and intermediate scales. If the matter content of the univers is dominated by weak interacting massive particles non-relativistic in all epochs of interest, then we should a apply the Cold Dark Matter (CDM) transfer function, which gently bends the primordial power-law power spectrum from $n = 1$ on large scales to $n \approx -3$ on small scales. Expressions of these tranfer functions are given in Appendix G of BBKS.

The primordial amplitude A is usually determined empirically. The first attempts were based on galaxy counts on scales large enough to ensure linear regime. One approach uses the statistics J_3, which is the integral of the two-point correlation function $\xi(r)$ times r^2. In terms of the power spectrum J_3 becomes

$$J_3(R) \equiv \int_0^R \xi(r) r^2 dr = \frac{4\pi}{3} R^3 \int_0^\infty dk\, k^2 W^2(kR) P(k). \tag{2.108}$$

The variance of galaxy counts-in-cells is easily related to the power spectrum by means of equation (2.100). Measures seem to indicate that perturbations on scales of $8h^{-1}$ Mpc are currently entering the non-linear regime. However, this result assumes that galaxies trace the mass, and there is no evidence that this has to be true. It is believed that fluctuations in galaxy counts can be proportional to mass perturbations

$$\left(\frac{\delta N}{N}\right) = b \left(\frac{\delta \rho}{\rho}\right), \tag{2.109}$$

with the bias factor b likely dependent on the scale. Taking into account this proportionality, the normalization condition writes

$$\sigma_0 (8\, h^{-1} \mathrm{Mpc})_{t_0} = b^{-1} \tag{2.110}$$

Another method to normalize the primordial amplitude of the fluctuation spectrum is based on the level of the CMBR anisotropies. It can be shown

(see e.g. Sahni & Coles 1995) that the quadrupole moment, which appears after the expansion of temperature fluctuations in spherical harmonics, can be expressed in terms of the primordial power spectrum. The measure of the quadrupole moment by the DMR aboard COBE has allowed the use of this theoretical relation to obtain a reliable spectrum normalization.

2.4.2 The Press & Schechter Formalism

At this point we have the necessary tools to present a method capable of retrieving an analytical mass function of relaxed objects in terms of properties of the initial density field. The derivation is basically founded on the linear extrapolation, for the growing mode, of the growth of density fluctuations with limit given by the spherical collapse. This method was originally devised by PS and, therefore, is commonly referred as the PS formalism. As usual, all the scales and densities will be henceforth expressed in comoving coordinates. To turn comoving lengths into physical ones, we should multiply by the scale factor $a(t)$.

According to the spherical model, the collapse time for a shell of radius R around the center, located at $\mathbf{r}$, of a spherically symmetric, outwards decreasing (to avoid shell crossing), linear density fluctuation at t_i only depends on the mean value of δ inside it. More exactly, the value of the average density contrast for collapse at t in an Einstein-de Sitter universe is $\delta_c(t) = \delta_{c0}\, a(t_i)/a(t)$ with $\delta_{c0} = 1.686$. Of course, the collapse of the shell of radius R represents the appearance, at t, of a virialized object of mass equal to $4\pi/3\,\rho_0 R^3$ to 0th order in δ_c[9]. This therefore suggests that anypoint in the real density field at t_i smoothed with a top hat filter of scale R with density contrast *above* a positive linear threshold δ_c should tend to collect matter so to reach, at a time t related to δ_c through the previous expression, a mass M *larger than* $4\pi/3\,\rho_0 R^3$. Since we are dealing with a Gaussian density field, the probability that a given point

[9]Since the mean density within the spherical perturbation is $\rho = \rho_0(1+\delta_c)$, then the actual mass contained inside a radius R is $M(R) = 4\pi/3\,\rho_0(1+\delta_c)\,R^3$.

has density contrast above some critical value δ_c when the field is smoothed on the scale R adopts the simple form

$$\begin{aligned} P(\delta > \delta_c, R) &= \frac{1}{\sqrt{2\pi}\sigma_0(R)} \int_{\delta_c}^{\infty} d\delta \exp\left[-\frac{\delta^2}{2\sigma_0^2(R)}\right] \\ &\equiv \frac{1}{2}\mathrm{erfc}\left[\frac{\delta_c}{\sqrt{2}\sigma_0(R)}\right] \end{aligned} \tag{2.111}$$

where $\sigma_0(R)$ is the linear rms fluctuation on scale R given by equation(2.100). According to the PS formalism, this probability can also be interpreted as the probability that a given point has ever been embedded in a collapsed object on scales greater than R. This assumes that if a point has a density contrast exceeding δ_c on a given scale, then it will reach the value δ_c when filtered on some larger scale and will be computed as a distinct object of the larger scale. In other words, it assumes that the only objects which exist at epoch t are those that have just collapsed. But, what happens to underdense regions which seems to contain half of the univers matter? PS argued that the matter of underdense regions was efficiently accreted by overdense regions, and therefore, the correct probability was obtained by adding a factor 2.

The probability $P(\delta > \delta_c, R)$ gives the volume fraction occupied by points with overdensity above the threshold δ_c when the density field is smoothed on scale R with a top hat window. Consequently, by differentiating this probability over M one should obtain the volume fraction contributing at t with objects of mass between M and $M + dM$, and by dividing the result by M/ρ_0 to the number density of such objects

$$\begin{aligned} N(M,t)\,dM &= 2\,\frac{\rho_0}{M}\left|\frac{\partial P(\delta > \delta_c, R)}{\partial R}\right|\frac{dR}{dM}\,dM \\ &= \sqrt{\frac{2}{9\pi}}\,\frac{\rho_0}{M^2}\,\frac{\delta_c}{\sigma_0}\left|\frac{d\ln\sigma_0}{d\ln R}\right| bigg|\,\exp\left[-\frac{\delta_c^2}{2\sigma_0^2}\right]\,dM. \end{aligned} \tag{2.112}$$

Since every particle in the universe must be at any time t within some virialized object with the appropriate mass, then the mass function has to

verify the normalization condition

$$\int_0^\infty dM\, M\, N(M) = \rho_0. \tag{2.113}$$

The factor 2 in the right-hand member of equation (2.112) is the one added to account for the underdense regions and, in fact, leads to a mass function correctly normalized.

Another quantity closely related to the mass function is the mass fraction contained in objects of mass M

$$\begin{aligned} f(M)dM &= \frac{M}{\rho_0} N(M)dM \\ &= \frac{1}{M}\sqrt{\frac{2}{9\pi}}\,\frac{\delta_c}{\sigma_0}\left|\frac{d\ln\sigma_0}{d\ln R}\right| \exp\left[-\frac{\delta_c^2}{2\sigma_0^2}\right] dM \end{aligned} \tag{2.114}$$

For a power-law power spectrum $P(k) \propto k^n$ and the top hat filter, the rms fluctuation on scale R is $\sigma_0(R) \propto R^{-(n+3)/2}$, or in terms of the mass $\sigma_0(M) \propto M^{-(n+3)/6}$. Let us define the characteristic mass M_* as the mass for which the rms fluctuation is equal to the threshold value $\sigma_0(M_*) = \delta_c$ or $\delta_c = M_*^{-(n+3)/6}$. In this case the mass function and the mass fraction of objects in an infinitesimal interval of the variable M/M_* have the respective forms

$$\begin{aligned} N\left(\frac{M}{M_*}\right) &= \sqrt{\frac{2}{\pi}}\,\frac{n+3}{6}\,\frac{\rho_0}{M_*}\left(\frac{M}{M_*}\right)^{\frac{n}{6}-\frac{3}{2}} \exp\left[-\frac{1}{2}\left(\frac{M}{M_*}\right)^{\frac{n+3}{3}}\right] \\ f\left(\frac{M}{M_*}\right) &= \sqrt{\frac{2}{\pi}}\,\frac{n+3}{6}\left(\frac{M}{M_*}\right)^{\frac{n}{6}-\frac{1}{2}} \exp\left[-\frac{1}{2}\left(\frac{M}{M_*}\right)^{\frac{n+3}{3}}\right] \end{aligned} \tag{2.115}$$

Notice that for a scale invariant power spectrum the mass fraction when expressed in terms of the variable M/M_* is time invariant, as it is expected in self-similar models of structure evolution.

But the PS mass function is not fully satisfactory. The origin of the "fudge factor two" is unclear and the disappearance of objects of any given mass swallowed by previously collapsed ones owing to cloud-in-cloud configurations is not accounted for. In addition, the real density field is not spherically

symmetric and outwards decreasing around any point. As a consequence, the growth of density fluctuations leaving the linear regime deviates from spherical collapse and involves complicated non-local, nonlinear, dynamics. Therefore, it is by no means obvious that the PS prescription can provide a good description of the formation of bound virialized objects. In particular, small changes in those aspects the most strongly connected with the spherical collapse model might be suitable. This leads to the following questions. What is the filtering window that better reproduces the clustering of objects? What is the mass to be associated with the filtering scale R? What overdensity does really correspond to the collapse time t? Finally, there is no reason for every point above the threshold overdensity to tend to accrete matter. This is expected to happen rather onto density maxima or "peaks" (Doroshkevich 1970; Kaiser 1984; Doroshkevich & Shandarin 1978; Peacock & Heavens 1985; Bardeen et al. 1986, herein BBKS; Bernardeau 1994).

Yet, the PS mass function gives very good fits to the "empirical" mass function inferred from N-body simulations (Nolthenius & White 1987; Efstathiou et al. 1988; Efstathiou & Rees 1988; Carlberg & Couchman 1989; White et al. 1993; Bahcall & Cen 1993; Lacey & Cole 1994). For this reason numerous authors have tried to properly justify it by introducing slight modifications if necessary. The origin of the fudge factor two and the cloud-in-cloud problem have been solved by Bond et al. (1991) by means of the powerful "excursion set formalism" and the use of the k-sharp window (see § 2.3.3 for a detailed discussion). Jedamzik (1994) got rid of the cloud-in-cloud problem by only considering isolated regions, defined as those regions lying above the threshold on a given scale, and lying below the threshold for any larger scale. He obtained a correctly normalized mass function that seems to agree much better with mass distributions derived from N-body simulations than the PS one. The effects of the departure from spherical collapse have also been studied. Monaco (1994) used the Lagrangian equations of motion of a cold and irrotational fluid in single stream regime, and characterized non-spherical perturbations by means of the shear determined non-locally by all the matter field. But all these improvements only apply to the PS original prescription dealing with undefined regions above the threshold overdensity, while there is

no satisfactory derivation of the theoretical mass function for peaks as seeds of virialized objects. Furthermore, none of the former studies has supplied a well justified relation between the window used to filter the density field and the mass of the collapsed object, or the one between the critical overdensity and the time of collapse. We will return to these open questions in Chapter 4.

2.4.3 The Excursion Set Formalism

The PS formalism applies only to hierarchical scenarios where structure evolves in time from small to large scales under the action of gravity. Therefore, the filtering of the primordial density field is fundamental to single out the scales of the future objects. This is done by convolving the linear field with a spherically symmetric smoothing function $W(r, R)$ on resolution scale R

$$\delta(\mathbf{r}, R) = \int d^3\mathbf{r}'\, W(\mathbf{r} - \mathbf{r}')\, \delta(\mathbf{r}, 0) \tag{2.116}$$

$$\delta(\mathbf{k}, R) = W(kR)\, \delta(\mathbf{k}, 0) \tag{2.117}$$

where the second equation comes from applying the Fourier transform to both sides of the first one. The other key element in the PS formalism is the critical overdensity which controls the collapse time. The regions of the linear density that lies above the threshold when the field is smoothed on a scale R are known as *excursion regions*, and the set including all the excursion regions is named the *excursion set*. So the PS method is basically founded on the determination of excursion sets.

Instead of considering the filtered density field $\delta(\mathbf{r}, R)$, let us focus our attention on what happens to a fixed point when the smoothing radius is varied. For physically interesting power spectra and window functions, the rms fluctuation $\sigma_0(R)$ vanishes asymptotically as the smoothing radius R tends to infinity. This behavior reflects the fact that, for a infinite radius, the density field around the point is averaged over the whole univers. For finite radii, the function $\delta(\mathbf{r}, R)$ is expected to vary randomly owing to the contributions from overdense and underdense regions to the averaged density field. So, equation

(2.116) can be interpreted as the equation of a trajectory $\delta(R)$, and the plot of this function is known as the δ–R diagram. (Examples of this trajectories can be found in Figure 3 of BCEK). Statistical properties of the trajectories are obtained by averaging over different realizations of the linear density field.

For the case of a k-sharp window, the trajectory is a Brownian random walk because the transition from one filter to a smaller one is obtained by adding statistically independent random field. The most interesting consequence of this is that Brownian trajectories can be described by means of a simple diffusion equation when the scale R is expressed in terms of the variance $\sigma_0^2(R) \equiv S$, known in this context as the resolution,

$$\frac{\partial Q}{\partial S} = \frac{1}{2}\frac{\partial^2 Q}{\partial \delta^2}, \tag{2.118}$$

where $Q(\delta, S)$ is the number density of trajectories at resolution S in the interval δ to $\delta + d\delta$. All the trajectories begin at the point (0,0) in the δ–S diagram and difusse away as the resolution increases.

In the framework of the excursion set formalism, the cloud-in-cloud problem that affects the PS mass function is solved in an ellegant way. Let us consider the trajectory $\delta(R)$ for a generic point. It may happen that for a given scale the trajectory upcrosses the threshold δ_c, so the point belong to an object of mass, let us say, M_1, and for a greater scale the trajectory crosses through the threshold again, so the point is included in another distinct object of mass $M_2 > M_1$. This situation can be avoided by selecting the maximum scale for which the trajectory $\delta(R)$ crosses through the line $\delta = \delta_c(t)$. In this way, regions which are above the threshold when averaged over this scale will be below the threshold when averaged on larger scales. In terms of the diffusion equation, this is equivalent to put an absorber barrier at $\delta = \delta_c(t)$ which absorbs trajectories as they try to cross through it. The probability that a trajectory is absorbed by the barrier in the interval S to $S + dS$ must be equal to the reduction in the number of surviving trajectories below the barrier

$$f_S(S, \delta_c) = -\frac{\partial}{\partial S}\int_{-\infty}^{\delta_c} Q(\delta, S)d\delta = -\left[\frac{1}{2}\frac{\partial Q}{\partial \delta}\right]_{-\infty}^{\delta_c} \tag{2.119}$$

$f_S(S,\delta_c)$ is the probability that a trajectory crosses through the threshold in the interval S to $S+dS$, that is, the probability that a point is within an object of scale in the interval S to $S+dS$ or, equivalently, the mass fraction in objects of mass M associated with resolutions in the interval S to $S+dS$. Chandrasekhar (1943) found that the difussion equation with the absorbing boundary condition admits a unique solution

$$Q(\delta,S,\delta_c)=\frac{1}{\sqrt{2\pi}\,S}\left\{\exp\left(-\frac{\delta^2}{2S}\right)-\exp\left[-\frac{(\delta-2\delta_c)^2}{2S}\right]\right\}d\delta. \qquad (2.120)$$

Substituting this expression in equation (2.119) we get

$$f_S(S,\delta_c)\,dS=\frac{\delta_c}{\sqrt{2\pi}\,S^{3/2}}\exp\left(-\frac{\delta_c^2}{2S}\right)dS. \qquad (2.121)$$

which becomes the PS mass fraction once the variable $S\equiv\sigma_0^2(R)$ is expressed in terms of the mass. Note that equation (2.121) naturally includes the factor 2, since the absorbing barrier solution takes into account underdense regions at resolution S which exceed the threshold at a lower resolution.

Other interesting quantity that can be derived in this context is the conditional probability that an object of mass M_1 in the interval M_1 to M_1+dM_1 at a time t_1 ends up in an object of mass M_2 at time $t_2>t_1$. In terms of Brownian trajectories this is equivalent to place two absorbing barriers at $\delta_{c1}=\delta_c(t_1)$ and $\delta_{c2}=\delta_c(t_2)$ $(\delta_{c1}>\delta_{c2})$ and calculate the density of trajectories crossing through the line δ_{c1} knowing that previously they have crossed trough δ_{c2}. This is the same situation as before, but with the source of trajectories moved from the origin to the point (S_2,δ_{c2})

$$f_{S1}(S_1,\delta_{c1}|S_2,\delta_{c2})\,dS_1=\frac{\delta_{c1}-\delta_{c2}}{\sqrt{2\pi}(S_1-S_2)^{3/2}}\exp\left[-\frac{(\delta_{c1}-\delta_{c2})^2}{2(S_1-S_2)}\right]dS_1, \qquad (2.122)$$

where $S_1\equiv\sigma_0(R_1)$ and $S_2\equiv\sigma_0(R_2)$ By manipulating this equation, we can calculate the probability that a object of mass M_1 at time t_1 has merged to form an object of mass between M_2 and M_2+dM_2 at time t_2

$$f_{S1}(S_2,\delta_{c2}|S_1,\delta_{c1})\,dS_2 \;=\; \frac{f_{S1}(S_1,\delta_{c1}|S_2,\delta_{c2})\,dS_1\,f_{S2}(S_2,\delta_{c2})\,dS_2}{f_{S1}(S_1,\delta_{c1})}\,dS_1$$

$$= \sqrt{\frac{1}{2\pi}} \left[\frac{S_1}{S_2(S_1 - S_2)}\right]^{3/2} \frac{\delta_{c2}(\delta_{c1} - \delta_{c2})}{\delta_{c1}}$$
$$\times \exp\left[\frac{-(\delta_{c2}S_1 - \delta_{c1}S_2)^2}{2S_1S_2(S_1 - S_2)}\right] dS_2 \qquad (2.123)$$

This conditional multiplicity function was used by Lacey & Cole (1993) to derive quantities related to the gravitational clustering of objects, such as the merger rate, the survival time, and the formation time.

It is noteworthy to mention that this simple derivation is only valid for the k-sharp window. For the top hat and Gaussian windows the trajectories build up by adding correlated random fields, so the difussion representation does not work, and the mass function has to be derived numerically by using Monte Carlo simulations.

3

STATISTICS OF PEAKS IN 3D GAUSSIAN FIELDS

The PS formalism considers any positive perturbation as the seed of some object at a given epoch. These overdense regions evolve linearly until their density contrast reachs a value about unity and then experience a collapse analog to that of a perfect spherical, isolated inhomogeneity. This picture implies a rapid transition from linear to non-linear regime and a good correspondence between overdense regions and final objects. In other words, in the PS formalism, any point with density contrast above a critical value when the density field is smoothed on a specific scale is able to give rise to a collapsed object with the appropriate mass at t. This means that, somehow, points have to efficiently accrete the surrounding matter in order to achieve the mass corresponding to the filtering radius at the appropriate collapse time.

However, this view is not accurate enough. Numerical simulations claim that only the most overdense regions in the linear density field end up in collapsed objects at any given epoch (BCEK). This result suggests that a perturbation does not evolve as fast as to avoid the interactions induced by other neighboring perturbations. Thus, points of the smoothed density field do not

fulfill the requirements demanded by the simple collapse picture on which the PS formalism is based. Fortunately, there is a physically better motivated candidate as seeds of present objects. Maxima of the density field (peaks) are supposed to be efficient accretion sites, less influenced by the surrounding distribution of matter. Furthermore, high amplitude peaks have rounded shapes, and it has been proved (Bernardeau 1994) that for steep power-law power spectra ($n < -1$) and moderate heights ($\nu \equiv \delta/\sigma_0 \geq 2$) the non-linear evolution of these peaks is well described by the spherical collapse. Therefore, it is highly convenient to develop a formalism capable of giving the mass function (and possibly other quantities related to the gravitational clustering) of relaxed objects by dealing with maxima of the linear density field. We put off this topic until Chapter 4, and focus here our attention on the characterization of peaks.

The statistics of peaks in Gaussian random fields has been developed in a series of papers (Doroshkevich, & Shandarin 1976, Peacock, & Heavens 1985, BBKS Couchman 1987, Heavens, & Peacock 1988, Coles 1989) and in the classical textbook by Adler (1981). Here we will review the general theory concerning the derivation of number densities, and will present some extensions to the classical calculations.

3.1 Basic Theory

Along this chapter we will consider a homogeneous and isotropic Gaussian random field $\delta(\mathbf{r})$ characterized by a power spectrum $P(k)$. If the random field describes the primordial density field, then the power spectrum gives information about the distribution of density perturbations as a function of the scale. Since we are interested in those cosmogonical scenarios which lead to a hierarchical gravitational clustering, the corresponding spectra have power on all scales. In order to pick out a specific one, the density filed has to be mathematically filtered with a smoothing function. The additional dependence on scale should be always born in mind, although sometimes it will not be

explicitly specified (for the sake of notation).

3.1.1 The Joint Probability Function

In § 2.3.2, we have used the fact that the density field is a random Gaussian field to calculate the probablity of finding a point above a threshold when the field is smoothed on a given scale (equation [2.111]). In that case, the probability density writes

$$P(\delta)\,d\delta = \frac{1}{\sqrt{2\pi}\,\sigma_0}\exp\left(\frac{\delta^2}{2\sigma_0^2}\right)\,d\delta. \tag{3.1}$$

The extension of the distribution probability function to two points separated by a distance r requires the use of the covariance function $\xi(r)$, because the values of the density field at different points are not statistically independent. Then the probability that one of the points has density contrast in the interval δ_1 to $\delta_1 + d\delta_1$, and the other point has density contrast in the interval δ_2 to $\delta_2 + d\delta_2$ is

$$P(\delta_1,\delta_2)\,d\delta_1 d\delta_2 = \frac{1}{2\pi\sigma_0^2}\frac{1}{\sqrt{1-w^2(r)}}\exp\left[-\frac{\delta_1^2+\delta_2^2-2w(r)\delta_1\delta_2}{2\sigma_0^2[1-w^2(r)]}\right]\,d\delta_1 d\delta_2 \tag{3.2}$$

where $w(r) = \xi(r)/\sigma_0^2$ is the scaled correlation function. Notice that if the points were not correlated [$\xi(r) = 0$] the above probability would be simply equal to the product $P(\delta_1)\,P(\delta_2)$. It is easy to generalize the former Gaussian joint probability distribution for m points

$$P(\delta_1,...,\delta_m)\prod_i^m d\delta_i = \frac{\exp(-Q)}{[(2\pi)^m\det(\mathbf{M})]^{1/2}}\prod_i^m d\delta_i \tag{3.3}$$

$$Q \equiv \frac{1}{2}\sum_{ij}^m \delta_i(\mathbf{M}^{-1})_{ij}\delta_j \tag{3.4}$$

where we have taken the means of random variables $\langle\delta_i\rangle = 0$. In this case, only the covariance matrix $M_{ij} \equiv \langle\delta_i\delta_j\rangle = \xi(r_{ij})$ is required to specify the

distribution. Since the successive derivatives of a random Gaussian field are Gaussian random fields, expression (3.4) for the joint probability function not only holds for the values of the density field at different points, but also for values of its derivatives.

3.1.2 The maximum constraint

The characterization of maxima for one-dimensional functions reduces to find those points with null first derivative and negative second derivative. In the case of a Gaussian random field, we need the joint probability function for the value of the field δ, and its first $\delta' \equiv \eta$, and second $\delta'' \equiv \zeta$ derivatives at a given point. By enforcing $\eta = 0$, and $\zeta < 0$,the integration over these variables in the appropriate domains leads to the probability of finding a maximum at the point with density contrast in the interval δ to $\delta + d\delta$. However, this procedure cannot be applied because the set comprising those points with $\eta = 0$ has null measure, so the corresponding probability seems to be zero. Fortunately, it is possible to substitute $d\eta$ for $|\zeta| dx$ [1], being x the spatial coordinate, because, owing to ergodicity, the integral over x is equivalent to the integral over the probability distribution. In this way, the measure problem is avoided and a peak number density, instead of a probability, is achieved once we divide by dx.

In three-dimensional Gaussian random fields (as the one depicting the density field), the strategy to follow for characterizing peaks is the same than in one dimension, but now taking into account that first cartesian derivatives of the field involve three components, $\eta_i = \nabla_i \delta$, (one for each possible direction), and second derivatives $\zeta_{ij} = \nabla_i \nabla_j \delta$ make up a symmetric 3×3 matrix with six independent components. Therefore, the probability of having a maximum

[1] The Taylor expansion of the first derivative of the field in the neiborghood of a maximum located at x_p writes

$$\eta(x) \approx \zeta(x_p)(x - x_p).$$

at a given point with density contrast in the range from δ to $\delta + d\delta$ is

$$p_{pk}(\delta)\, d\delta = d\delta \int d^3\eta d^6\zeta P(\delta, \boldsymbol{\eta} = \mathbf{0}, \zeta), \tag{3.5}$$

integrated over the domain for which the second derivatives are negative. To overcome the problem of null measure sets, we turn the ensemble average into a volume average. The Jacobian of the transformation is just $J = \det \zeta$, then the probability (3.5) becomes

$$p_{pk}(\delta)\, d\delta = d\delta\, d^3r \int d^6\zeta |\det \zeta| P(\delta, \boldsymbol{\eta} = \mathbf{0}, \zeta). \tag{3.6}$$

By dividing both sides by the volume element d^3r we obtain the number density of peaks per infinitesimal range of height[2]. Owing to the homogeneity and isotropy of the Gaussian field, the probability (number density) of peaks does not depend on the position. For simplicity, we will hereafter evaluate the joint probability functions at $\mathbf{r} = \mathbf{0}$.

The expression (3.6) can also be derived considering a point process. In this case the number density of of points p selected to be maxima of the field $\delta(\mathbf{r})$ is

$$n_{pk} = \sum_p \delta^{(3)}(\mathbf{r} - \mathbf{r}_p) \tag{3.7}$$

where $\delta^{(3)}$ is the three-dimensional Dirac delta function. The following step is to express this point process in terms of the random field and its derivatives. To do so, let us expand the field and its gradient in Taylor series around the maximum located at $\mathbf{r}_p$

$$\begin{aligned} \delta(\mathbf{r}) &\approx \delta(\mathbf{r}_p) + \frac{1}{2}\sum_{ij} \zeta_{ij}(r - r_p)_i(r - r_p)_j, \\ \eta_i(\mathbf{r}) &\approx \sum_j \zeta_{ij}(r - r_p)_j. \end{aligned} \tag{3.8}$$

If the matrix ζ is non-singular then we can write

$$\begin{aligned} \mathbf{r} - \mathbf{r}_p &\approx \zeta^{-1}(\mathbf{r}_p)\eta(\mathbf{r}), \\ \delta^{(3)}(\mathbf{r} - \mathbf{r}_p) &= |\det \zeta(\mathbf{r}_p)| \delta^{(3)}[\eta(\mathbf{r})]. \end{aligned} \tag{3.9}$$

[2]In peak statistics jargon, the density contrast is also referred as the peak "height".

Notice that the δ-function picks out all of the points satisfying $\boldsymbol{\eta}(\mathbf{r})= \mathbf{0}$. By the moment, only we can obtain the number density of extrema

$$n_{ext} = |\det \zeta(r_p)|\delta^{(3)}[\boldsymbol{\eta}(\mathbf{r})] \tag{3.10}$$

In practice, only the ensemble average of expression (3.10) can be calculated. This average involves the joint probability function $P(\delta, \boldsymbol{\eta}, \zeta)$ evaluated at $\mathbf{r} = \mathbf{0}$. Integrating over the domain where ζ is negative we get the number density of peaks with height in the interval δ to $\delta + d\delta$

$$\langle n_{pk}(\delta)\rangle d\delta = d\delta \int d^6\zeta |\det \zeta| P(\delta, \boldsymbol{\eta} = \mathbf{0}, \zeta). \tag{3.11}$$

3.2 The Number Density of Peaks

3.2.1 Evaluating the Maximum Constraint

The notation used in this chapter follows the one introduced by BBKS. Therefore, $\mathcal{N}_{pk}(\nu)d\nu$, with $\nu = \delta/\sigma_0(R)$, denotes the number density of peaks per infinitesimal range of height, and $n_{pk}(\nu_c)$ denotes the number density of peaks with height above the value ν_c. Both quantities also depend on the scale R, which works as a parameter. Sometimes we will include it as an argument, to explicitly stress the dependence.

In order to evaluate the joint probability function $P(\delta, \boldsymbol{\eta}, \zeta)$, we need the correlations between the different fields. Even though correlations between variables are strictly convolution products, owing to ergodicity, they can be also calculated as ensemble averages over different realizations of the field. Therefore, it is convenient to perform these calculations in the Fourier space, in which the smoothed field $\delta(\mathbf{r}, R)$, its gradient $\eta_i(\mathbf{r}, R)$, and its second-order cartesian derivatives $\zeta_{ij}(\mathbf{r}, R)$ have the form

$$\delta(\mathbf{r}, R) = \frac{1}{(2\pi)^3} \int d^3\mathbf{k}\, \delta(\mathbf{k})\, W(kR) e^{-i\mathbf{k}\cdot\mathbf{r}},$$

$$\eta_i(\mathbf{r},R) = \frac{1}{(2\pi)^3}\int d^3\mathbf{k}\,(-ik_i)\delta(\mathbf{k})\,W(kR)e^{-i\mathbf{k}\cdot\mathbf{r}}, \qquad (3.12)$$
$$\zeta_{ij}(\mathbf{r},R) = \frac{1}{(2\pi)^3}\int d^3\mathbf{k}\,(-k_ik_j)\,\delta(\mathbf{k})\,W(kR)e^{-i\mathbf{k}\cdot\mathbf{r}}.$$

In order to simplify the notation, we will not show explicitly the dependence on the point and scale in the field variables. From the definitions of the power spectrum (equation [2.98]) and the spectral momenta (equation [2.104]), it can be shown that

$$\begin{aligned} &\langle\delta\,\delta\rangle = \sigma_0^2, && \langle\eta_i\,\eta_j\rangle = \frac{\sigma_1^2}{3}\delta_{ij}, \\ &\langle\delta\,\eta_i\rangle = 0, && \langle\eta_i,\zeta_{jk}\rangle = 0, \\ &\langle\delta\,\zeta_{ij}\rangle = -\frac{\sigma_1^2}{3}\delta_{ij}, && \langle\zeta_{ij}\,\zeta_{kl}\rangle = \frac{\sigma_2^2}{15}(\delta_{ij}\delta_{kl}+\delta_{ik}\delta_{jl}+\delta_{il}\delta_{jk}). \end{aligned} \qquad (3.13)$$

The covariance matrix $\mathbf{M}$ has dimension 10 since it includes correlations between the field, its three first derivatives and its six independent second derivatives. It is almost diagonal apart from one 3×3 box involving the second-order derivatives. We label them ζ_A, where subscript A ranging from 1 to 6 refers to $ij = 11, 22, 33, 12, 13, 23$. The Gaussian joint probability P does not depend on the form of the variables chosen to characterize the random field. By using variables x, y, and z, defined as

$$\sigma_2 x = -\nabla^2\delta = -(\zeta_1+\zeta_2+\zeta_3), \quad \sigma_2 y = -\frac{1}{2}(\zeta_1-\zeta_3),$$
$$\sigma_2 z = -\frac{1}{2}(\zeta_1-2\zeta_2+\zeta_3), \qquad (3.14)$$

instead of ζ_1, ζ_2, and ζ_3 we achieve a diagonal covariance matrix. If we also introduce the variable $\nu = \delta/\sigma_0$ the corresponding non-zero correlations adopt the simple form

$$\langle\nu^2\rangle = 1, \quad \langle x^2\rangle = 1, \quad \langle\nu\,x\rangle = \gamma, \quad \langle y^2\rangle = \frac{1}{15}, \quad \langle z^2\rangle = \frac{1}{5}, \qquad (3.15)$$

where $\gamma = \sigma_1^2/(\sigma_0\sigma_2)$ is a measure of the bandwith of the power spectrum. Once we have the covariance matrix $\mathbf{M}$ we are able to calculate the quadratic

form Q

$$2Q = \nu^2 + \frac{(x - x_*)^2}{1 - \gamma^2} + 15\, y^2 + 5\, z^2 + 3\, \frac{\boldsymbol{\eta} \cdot \boldsymbol{\eta}}{\sigma_1^2} + \sum_{A=4}^{6} \frac{15 \zeta_A^2}{\sigma_2^2}, \tag{3.16}$$

with $x_* = \gamma\, \nu$.

Other relevant step aimed to simplify calculations consists of selecting a suitable reference frame. This procedure is always allowed because the correlations given by (3.15) are independent of this choice. Since the matrix ζ_{ij} is symmetric, then we can find a rotation which diagonalizes it: $\mathrm{diag}(\lambda_1, \lambda_2, \lambda_3) = -R\, \zeta\, R^\dagger$, where λ_i $(i = 1, 2, 3)$ are the eigenvalues of the matrix $-\zeta_{ij}$, and R and $R^\dagger$ are the rotation matrix and its transpose repectively. We can select the principal axes along the direction of the eigenvalues λ_i; thus $\zeta_A = -\lambda_A$ $(A = 1, 2, 3)$. In this way, we have used up three degrees of freedom. The other avalaible three permits to fix the orientation of the orthonormal eigenvectors of the matrix by means of the Euler angles α_1, α_2, α_3.

All these choices introduce changes in the volume element associated to the space defined by the second-order derivatives

$$\prod_{A=1}^{6} d\zeta_A = |(\lambda_1 - \lambda_2)(\lambda_2 - \lambda_3)(\lambda_1 - \lambda_3)|\, d\lambda_1\, d\lambda_2\, d\lambda_3\, \frac{d\Omega_{S^3}}{6},$$

$$d\Omega_{S^3} = \sin\alpha_2\, d\alpha_2\, d\alpha_1\, d\alpha_3, \tag{3.17}$$

$$\prod_{A=1}^{3} d\lambda_A = \frac{2}{3}\sigma_2^3\, dx\, dy\, dz. \tag{3.18}$$

$d\Omega_{S^3}$ is the volume element on the surface of the three-sphere. Since the whole space is avalaible (there is no constraint on the Euler angles), then its integration yields $2\pi^2$. The factor 6 dividing arises because the eigenvalues are not ordered. In the new variables, the joint probability function becomes

$$P(\nu, \boldsymbol{\eta}, x, y, z)\, d\nu d^3\eta\, dx\, dy\, dz = F |2y\, (y^2 - z^2)| e^{-Q} d\nu\, dx\, dy\, dz\, \frac{d^3\eta}{\sigma_0^3},$$

$$F = \frac{15^{5/2}}{32\pi^3}\, \frac{\sigma_0^3}{\sigma_1^3\, (1 - \gamma^2)^{1/2}}. \tag{3.19}$$

To make sure that matrix ζ_{ij} is negative definite we order the eigenvalues just as

$$\lambda_1 \geq \lambda_2 \geq \lambda_3, \tag{3.20}$$

and impose $\lambda_3 > 0$. In this case we have to drop the factor $1/6$ in the first of equations (3.17). The eigenvalue ordering causes the variables x, y, and z to be constrained in such a way that the integration only picks out positive values for the λ's. The solution of the inequation system leads to two different domains

$$\begin{aligned} &0 < x, \quad 0 \leq y \leq \frac{x}{4}, \quad -y \leq z \leq y \\ &0 < x, \quad \frac{x}{4} \leq y \leq \frac{x}{2}, \quad 3y - x \leq z \leq y \end{aligned} \tag{3.21}$$

The peak density for maxima of height ν_0 is given by the average

$$\mathcal{N}_{pk}(\nu_0)\, d\nu = \langle |\lambda_1\lambda_2\lambda_3| \theta(\lambda_3)\delta^{(3)}(\eta)\delta(\nu - \nu_0)\rangle d\nu \tag{3.22}$$

which involves the integration of the joint probability function over the variables η_i and λ_i (or x, y, z) taking into account the corresponding constraints. It is valuable to consider the number density of peaks with parameters ν and x [3]per infinitesimal range. This is done by introducing additional δ-functions in equation (3.22). The result is

$$\mathcal{N}_{pk}(\nu, x)\, d\nu\, dx = \frac{e^{-\nu^2/2}}{(2\pi)^2 R_*^3} \frac{f(x)}{[2\pi\,(1-\gamma^2)]^{1/2}} \exp\left[-\frac{(x - x_*)^2}{2(1-\gamma^2)}\right] d\nu\, dx \tag{3.23}$$

where $R_* = \sqrt{3}\,\sigma_1/\sigma_2$ is a measure of the characteristic coherence length of the field, and $f(x)$ contains the outcome of integrating the joint probability function over the variables z and y

$$\begin{aligned} f(x) \;&=\; \left(\frac{x^3 - 3x}{2}\right)\left\{\operatorname{erf}\left[x\sqrt{\frac{5}{2}}\right] + \operatorname{erf}\left[\frac{x}{2}\sqrt{\frac{5}{2}}\right]\right\} \\ &+\; \sqrt{\frac{2}{5\pi}}\left[\left(\frac{31x^2}{4} + \frac{8}{5}\right) e^{-5x^2/8} + \left(\frac{x^2}{2} - \frac{8}{5}\right) e^{-5x^2/2}\right]. \end{aligned} \tag{3.24}$$

[3]Notice that in this case we cannot strictly say that these points are peaks since the variable x can be positive or negative. We think of peaks because we bear in mind that $x > 0$.

Taking into account the asymptotic behavior of $f(x)$ for the limits $x \to 0$ and $x \to \infty$, this function can be reasonably approximated by

$$f_{app}(x) = \frac{x^8}{13.2\,(1+5x^2/8)} \qquad \text{for } x < 1.5,$$

$$f_{app}(x) = x^3 - 3x + \frac{4.08}{x^2} \qquad \text{for } x \geq 1.5.$$

Finally, the integration over the variable x ($x > 0$) leads to the number density of peaks with height in the interval ν to $\nu + d\nu$

$$\mathcal{N}_{pk}(\nu)\,d\nu = \frac{e^{-\nu^2/2}}{(2\pi)^2 R_*^3}\,G(\gamma, x_*)\,d\nu \tag{3.25}$$

where the numerical function

$$G(\gamma, x_*) = \frac{1}{[2\pi\,(1-\gamma^2)]^{1/2}} \int_0^\infty dx\, f(x)\, \exp\left[-\frac{(x-x_*)^2}{2(1-\gamma^2)}\right], \tag{3.26}$$

has been accurately fitted by BBKS (see their equations [4.4] and [4.5]) in the range $0.3 < \gamma < 0.7$ and $x_* > 1$.

In the peak model framework, it is assumed that collapsed objects arise from peaks of the smoothed density field with height above a specific threshold. Thus, we can compute the number density of these objects by integrating the differential density (3.25) over the variable ν constrained in the interval (ν_c, ∞)

$$n_{pk}(\nu_c) = \int_{\nu_c}^\infty \mathcal{N}_{pk}(\nu)\,d\nu. \tag{3.27}$$

3.2.2 The conditional number density

In hierarchical scenarios the evolution of density fluctuations on a given scale can be altered by the presence of fluctuations on larger scales. The most notable example is the forementioned cloud-in-cloud problem. Furthermore, we

observe regions of the space almost devoided of galaxies (voids), and regions with galaxy density greater than that of the background. This effect can be easily interpreted in the peak model framework. Since present objects are supposed to arise from peaks of the density field above a global critical height, the presence of a background field is able to boost the object formation in those sites where the background density is higher than the average (due to the decrement of the local threshold) and supress it in those sites where the background density is lower than the average (because the local threshold is increased). In practice, the peak and the background fields are generated by smoothing the same random density field $\delta(\mathbf{r})$ on two different scales that we denote R_s and R_b respectively. Instead of writing explicitly the scale dependence, we will use subscripts s and b to refer to quantities concerning the peak and the background fields.

To quantify this effect we need the number density of peaks on backgrounds with a specific height. We begin with the calculation of the conditional probability $P(\nu_b|\nu_s, x)\, d\nu_b$, which gives the probability that the background field has height $\nu_b = \delta_b/\sigma_{0b}$ in an infinitesimal range subject to the constraint that there is a peak with $\nu_s = \delta_s/\sigma_{0s}$ and scaled Laplacian x [4]. According to BBKS, conditional probabilities involving Gaussian variables adopt a Gaussian form with mean equal to

$$\langle Y_B \otimes Y_A \rangle \langle Y_A \otimes Y_A \rangle^{-1} Y_A^{\dagger} \tag{3.28}$$

and dispersion equal to

$$\langle Y_B \otimes Y_B \rangle - \langle Y_B \otimes Y_A \rangle \langle Y_A \otimes Y_A \rangle^{-1} \langle Y_A \otimes Y_B \rangle \tag{3.29}$$

The angular brackets indicate ensemble averages. The tensor product notation $Y_B \otimes Y_A$ just builds a $m \times n$ matrix out of the vectors Y_B, of dimension m, and Y_A, of dimension n. In this particular case we have $Y_B = \nu_b$ and $Y_A = (\nu_s, x)$. We have already found the correlation between the peak variables $\langle \nu\, x \rangle = \gamma$. The other non-vanishing correlations appearing in the calculations are

$$\langle \nu_b^2 \rangle = 1, \quad \langle \nu_b \nu_s \rangle = \frac{\sigma_{0h}^2}{\sigma_{0s}\sigma_{0b}} \equiv \epsilon, \quad \langle \nu_b\, x \rangle = \frac{\sigma_{1h}^2}{\sigma_{2s}\sigma_{0b}} = \gamma_s \epsilon r_1, \tag{3.30}$$

[4] It is not necessary to introduce more variables to characterize the peak because the background variable ν_b does not correlate with y, z, and ζ_A, $A = 4, 5, 6$.

with the cross-momenta defined as

$$\sigma_{jh}^2 = \int_0^\infty \frac{dk\, k^{2j+1}}{2\pi^2} P(k)\, W(kR_s).\, W(kR_b) \tag{3.31}$$

The parameters ϵ and $r_1 = \sigma_{1h}^2\, \sigma_{0s}^2/(\sigma_{0h}^2\, \sigma_{1s}^2)$ accounts for the correlations between the peak and the background fields resulting from the fact that both are obtained by smoothing the same random field on two different scales. For physically interesting power spectra an filtering functions, this kind of correlations decreases asymptotically to zero as the background smoothing radius increases. For instance, a power-law power spectrum filtered with a Gaussian window leads to

$$\epsilon = \left(\frac{R_s R_b}{R_h^2}\right)^{(n+3)/2} \to \left(\frac{2R_s}{R_b}\right)^{(n+3)/2}, \quad r_1 = \left(\frac{R_s}{R_h}\right)^2 \to 2\left(\frac{R_s}{R_b}\right)^2, \tag{3.32}$$

where $R_h^2 = (R_b^2 + R_s^2)/2$. The limits hold for $R_b \gg R_s$.

Finally the wanted conditional probability can be written as

$$P(\nu_b|\nu_s, x)\, d\nu_b = \frac{1}{\sqrt{2\pi}\,\Delta\nu_b} \exp\left[-\frac{(\nu_b - \bar{\nu}_b)^2}{2(\Delta\nu_b)^2}\right] d\nu_b, \tag{3.33}$$

with mean $\bar{\nu}_b$ and dispersion $\Delta\nu_b$ given respectively by

$$\begin{aligned} \bar{\nu}_b &= \frac{\epsilon^2}{1-\gamma_s^2}[\nu_s(1-\gamma_s^2 r_1) - \gamma_s x(1-r_1)], \\ \Delta\nu_b^2 &= 1 - \frac{\epsilon^2}{1-\gamma_s^2}(1 - 2\gamma_s^2 r_1 + \gamma_s^2 r_1^2). \end{aligned} \tag{3.34}$$

The second step consist of calculating the joint density of points with height ν_b when the field is smoothed on scale R_b, and height ν_s and scaled Laplacian x when it is filtered on scale R_s. This quantity is easily derived from the differential number density $\mathcal{N}_{pk}(\nu_s, x)$ (see equation[3.23]) and the conditional probability $P(\nu_b|\nu_s, x)$

$$\mathcal{N}_{pk}(\nu_b, \nu_s, x)\, d\nu_b d\nu_s dx = \mathcal{N}_{pk}(\nu_s, x)\, d\nu_s dx\, P(\nu_b|\nu_s, x)\, d\nu_b. \tag{3.35}$$

By integrating this expression over x, with the constraint $x > 0$, we make sure that the points with height ν_s are peaks

$$\begin{aligned} \mathcal{N}_{pk}(\nu_b,\nu_s)\,d\nu_b\,d\nu_s &= d\nu_b\,d\nu_s \int_0^\infty dx\,\mathcal{N}_{pk}(\nu_s,x)\,P(\nu_b|\nu_s,x) \\ &= \frac{G(\tilde{\gamma},\tilde{x}_*)}{(2\pi)^2\,R_{*s}^3}\exp\left[-\frac{(\nu_s-\epsilon\nu_b)^2}{2(1-\epsilon^2)}\right]\frac{e^{-\nu_b^2/2}d\nu_b\,d\nu_s}{\sqrt{2\pi\,(1-\epsilon^2)}}. \end{aligned} \tag{3.36}$$

The tilde variables $\tilde{\gamma}$, $\tilde{x}_* = \tilde{\gamma}\,\tilde{\nu}$ have been introduced to express the integral in a closed form

$$\tilde{\gamma}^2 = \gamma_s^2\left[1+\epsilon^2\,\frac{(1-r_1)^2}{1-\epsilon^2}\right], \quad \tilde{\nu} = \frac{\gamma_s}{\tilde{\gamma}}\left(\frac{1-r_1}{1-\epsilon^2}\right)\left[\nu_s\left(\frac{1-\epsilon^2 r_1}{1-r_1}\right)-\epsilon\nu_b\right]. \tag{3.37}$$

The conditional number density $\mathcal{N}_{pk}(\nu_s|\nu_b)\,d\nu_s$ of peaks with height in the interval ν_s to $\nu_s + d\nu_s$ in backgrounds with height ν_b is derived by dividing the joint density $\mathcal{N}_{pk}(\nu_b,\nu_s)$ by the probability of finding a background. Taking into account that this probability is Gaussian the wanted conditional number density just writes

$$\begin{aligned} \mathcal{N}_{pk}(\nu_s|\nu_b)\,d\nu_s &\equiv \frac{\mathcal{N}_{pk}(\nu_b,\nu_s)}{P(\nu_b)}d\nu_s \\ &= \frac{G(\tilde{\gamma},\tilde{x}_*)}{(2\pi)^2\,R_{*s}^3\sqrt{1-\epsilon^2}}\exp\left[-\frac{(\nu_s-\epsilon\nu_b)^2}{2(1-\epsilon^2)}\right]d\nu_s \end{aligned} \tag{3.38}$$

If we are interested in the density of peaks exceeding a given threshold at a point where the background field has height ν_b, we have to integrate the above expression over ν_s with the constraint $\nu_s > \nu_c$

$$n_{pk}(\nu_c|\nu_b) = \int_{\nu_c}^\infty \mathcal{N}_{pk}(\nu|\nu_b)\,d\nu. \tag{3.39}$$

Finally, the effect produced by a background field on the peak population can be quantified by means of the *enhancement factor*, which is defined as the ratio

$$E(\nu_b) = \frac{n_{pk}(\nu_c|\nu_b)}{n_{pk}(\nu_c)}. \tag{3.40}$$

3.3 Extensions of BBKS Theory

3.3.1 Disappearing Peaks

So far we have dealt with points which are peaks on a specific scale, but what happens to a given peak when the random Gaussian field is smoothed on a slightly different scale? One possiblity is that this peak disappears because any of the maximum constraints is not fulfilled on the new scale. With the help of the tools presented in the preceding sections we plan to characterize the disappearing peaks and calculate the corresponding number density.

From the Taylor series expansion of the gradient of the density contrast smoothed on scale R, η, around the location $\mathbf{r}_p$ of a neighboring peak we have (to first order in $|\mathbf{r} - \mathbf{r}_p|$)

$$\eta_i(\mathbf{r}) \approx -\lambda_i(r - r_p)_i, \tag{3.41}$$

with $\lambda_i > 0$ the eigenvalues of the second order cartesian derivative tensor ζ_{ij} changed of sign. Since there is at most one peak in the neighborhood of any point the density of peaks around $\mathbf{r}$ is

$$\delta^{(3)}(\mathbf{r} - \mathbf{r}_p) = |\lambda_1\lambda_2\lambda_3|\delta^{(3)}[\eta(\mathbf{r})]. \tag{3.42}$$

But η_i and λ_i are random Gaussian variables. So the typical density of peaks on scale R around an arbitrary point $\mathbf{r}$ is given by the mean

$$\langle\delta^{(3)}(\mathbf{r} - \mathbf{r}_p)\rangle = \langle|\lambda_1\lambda_2\lambda_3|\delta^{(3)}[\eta(\mathbf{r})]|\rangle \tag{3.43}$$

for the joint probability of the random variables involved, with λ_i strictly positive. This is the scheme we have followed for obtaining the density $\mathcal{N}_{pk}(\nu, R)$ $d\nu$ of peaks with scaled density contrast ν in an infinitesimal range.

Let us consider a peak at $\mathbf{r}_p$ on scale R. When the Gaussian random field is smoothed on scale $R + \Delta R$, with ΔR positive and arbitrarily small, the point $\mathbf{r}_p$ may not be a peak, but it can be found one in the neighborhood of

$\mathbf{r}_p$. In fact, it can be proved that there cannot be more than one peak on scale $R + \Delta R$ in the neighborhood of any point which was a peak on scale R. Let us assume that there are two peaks located at $\mathbf{r}_{p'_1}$ and $\mathbf{r}_{p'_2}$ on scale $R + \Delta R$ with $|\mathbf{r}_p - \mathbf{r}_{p'_j}| \leq O(\Delta R)$, $j = 1, 2$. Expanding the gradient around the point $\mathbf{r}_p$ and scale R, and bearing in mind that there is a peak at $\mathbf{r}_p$ on scale R, we are led to the following expressions for each point

$$\begin{aligned} 0 &= \partial_R \eta_i \Delta R - \lambda_i \Delta r_{p'_1 i}, \\ 0 &= \partial_R \eta_i \Delta R - \lambda_i \Delta r_{p'_2 i}. \end{aligned} \tag{3.44}$$

Therefore, both peaks must be the same to first order in ΔR. According to this result, we will say that a peak at $\mathbf{r}_p$ on scale R disappears in reaching the scale $R + \Delta R$ provided only this is the first scale larger than R with no peak in the neighborhood $|\mathbf{r} - \mathbf{r}_p| \leq O(\Delta R)$ of the former peak (see § 4.2.1 for the exact justification of this statement). From the Taylor series expansion of $\boldsymbol{\eta}$ at the nearest point $\mathbf{r}_{p'}$ with $\boldsymbol{\eta} = 0$ on scale $R + \Delta R$ around the peak $\mathbf{r}_p$ on scale R we have

$$(r_{p'} - r_p)_i \approx \frac{\partial_R \eta_i}{\lambda_i} \Delta R. \tag{3.45}$$

Thus, on the new scale $R+\Delta R$ there is some peak in the neighborhood $|\mathbf{r}-\mathbf{r}_p| \leq O(\Delta R)$ of the old peak on scale R provided only that all λ_i are of order unity (this also guarantees that all λ_i are positive at $\mathbf{r}_{p'}$ on scale $R + \Delta R$). Strictly, some λ_i could be of order ΔR or smaller, if the corresponding $\partial_R \eta_i$ were too. But the probability for this to happen is negligible as compared to the more general preceding case. Therefore, for that condition to be broken for the first time at $R+\Delta R$, some eigenvector λ_i must become of order ΔR or, equivalently, must vanish at $R \pm \Delta R$.

Consequently, the density of peaks on scale R at an arbitrary point $\mathbf{r}$ disappearing at R' in the neighborhood of R, with $R' > R$, is given by the mean $\langle \delta^{(3)}(\mathbf{r} - \mathbf{r}_p) \rangle$, with all eigenvalues λ_i positive, as in BBKS, *and* the smallest one satisfying the relation

$$R' - R \approx \frac{\lambda_i}{|\partial_R \lambda_i|}. \tag{3.46}$$

But condition (3.46) implies, at the same time, that the smallest eigenvalue λ_i also vanishes in the neighborhood of $\mathbf{r}_p$ on scale R. Thus, in neglecting second order terms in equation (3.41) the term in that component λ_i must be neglected, too. Accordingly, were we interested in calculating the density of peaks disappearing at R' in the neighborhood of R, we should take for that component of $\mathbf{r} - \mathbf{r}_p$ the relation

$$(r - r_p)_i \approx \frac{\partial_R \eta_i - \partial_R \eta_i(\mathbf{r})}{\partial_R \lambda_i}, \tag{3.47}$$

instead of (3.41). So, $\langle \delta^{(3)}(\mathbf{r}-\mathbf{r}_p) \rangle$ will involve now the mean for this component i of the values of $\partial_R \eta_i$ on scale R at both points $\mathbf{r}$, and $\mathbf{r}_p$.

To perform this calculation it is convenient to use the scaled variables ν, x, y, and z (see their definition in § 2.2.1), and the new variables $X = \sigma_2^{-1} \partial_R(\sigma_2 x)$, $Y = \sigma_2^{-1} \partial_R(\sigma_2 y)$, and $Z = \sigma_2^{-1} \partial_R(\sigma_2 z)$. For simplicity of the notation we will also write I_i for $\partial_R \eta_i$. For a Gaussian window the non-null correlations involving the new variables are (see equation [3.14] for the rest)

$$\begin{gathered}
\langle X^2 \rangle = \frac{\sigma_4^2}{\sigma_2^2} R^2 \qquad \langle Y^2 \rangle = \frac{1}{15} \frac{\sigma_4^2}{\sigma_2^2} R^2 \qquad \langle Z^2 \rangle = \frac{1}{5} \frac{\sigma_4^2}{\sigma_2^2} R^2 \\
\langle x\, X \rangle = -\frac{\sigma_3^2}{\sigma_2^2} R \qquad \langle y\, Y \rangle = -\frac{1}{15} \frac{\sigma_3^2}{\sigma_2^2} R \qquad \langle z\, Z \rangle = -\frac{1}{5} \frac{\sigma_3^2}{\sigma_2^2} R \\
\langle \nu\, X \rangle = -\frac{\sigma_2}{\sigma_0} R \qquad \langle \eta_i\, \mathrm{I}_i \rangle = -\frac{\sigma_2^2}{3} R \qquad \langle \mathrm{I}_i^2 \rangle = \frac{\sigma_3^2}{3} R^2,
\end{gathered} \tag{3.48}$$

and $\langle \zeta_A^2 \rangle = \sigma_2^2/15$, $A = 4, 5, 6$ ($A = 1, 2, 3, 4, 5, 6$ stand for $ij = 11, 22, 33, 23, 13, 12$), while they all have null mean. The covariance matrix $\mathbf{M}$ associated to variables ν, x, X, y, Y, z, Z, η_1, I_1, η_2, I_2, η_3, I_3, ζ_4, ζ_5, ζ_6 is therefore nearly diagonal. The only non-null components, apart from those concerning ζ_A for $A = 4, 5, 6$, are in small 2×2 boxes, for each couple of variables denoted by the same small and capital (roman or greek) letter, except for one 3×3 box for variables ν, x, and X, all of them along the diagonal. Thus we can readily calculate the square root of the determinant of the covariance matrix $\mathbf{M}$ and its associate quadratic form Q entering in the expression of the joint probability

function for these Gaussian random variables. The result is

$$\sqrt{\det \mathbf{M}} = \frac{(\sigma_1\sigma_2\sigma_3\, D\, R)^3}{3^{11/2}\, 5^{7/2}} (1-\gamma^2)^{1/2} (1-\Gamma^2)^{1/2} (1-\gamma_2^2)^{3/2}, \tag{3.49}$$

and

$$\begin{aligned} 2Q &= \nu^2 + \frac{3}{\sigma_1^2}\left[\boldsymbol{\eta}^2 + \frac{\sigma_1^2}{\sigma_3^2}\frac{(\mathbf{I}-\mathbf{I}_*)^2}{R^2(1-\gamma_2^2)}\right] + \frac{(x-x_*)^2}{1-\gamma^2} + \frac{(X-X_*)^2}{(1-\Gamma^2)\, D^2} \\ &+ 15\left[y^2 + \frac{(Y-Y_*)^2}{D^2}\right] + 5\left[z^2 + \frac{(Z-Z_*)^2}{D^2}\right] + \frac{15}{\sigma_2^2}\sum_{A=4}^{6}\zeta_A^2, \end{aligned} \tag{3.50}$$

with

$$\begin{aligned} X_* &\equiv -\left[x - \Delta x\,(1-\gamma_2^2)\right]\frac{\sigma_3^2}{\sigma_2^2}\, R \\ Y_* &\equiv -y\,\frac{\sigma_3^2}{\sigma_2^2}\, R, \\ Z_* &\equiv -z\,\frac{\sigma_3^2}{\sigma_2^2}\, R, \\ \mathrm{I}_{i*} &\equiv -\eta_i\,\frac{\sigma_2^2}{\sigma_1^2}\, R, \end{aligned} \tag{3.51}$$

being $\sigma_i(R)$ the ith order spectral momenta, and $D \equiv (1-\gamma_3^2)^{1/2}\sigma_4/\sigma_2\, R$, $\Gamma \equiv \gamma_1\gamma_3(1-\gamma_2^2)/[(1-\gamma_1^2)(1-\gamma_3^2)]^{1/2}$, $\Delta x \equiv x - (x-x_*)(1-\gamma^2)^{-1}$, with $\gamma_1 = \sigma_1^2/(\sigma_0\,\sigma_2) \equiv \gamma$, $\gamma_2 = \sigma_2^2/(\sigma_1\,\sigma_3)$, $\gamma_3 = \sigma_3^2/(\sigma_2\,\sigma_4)$.

Now we can take advantage of the fact that the covariance matrix $\mathbf{M}$ does not depend on the orientation of the coordinate axes, and assume them orientated along the orthonormal eigenvectors of tensor $-\zeta_{ij}$. This makes $\lambda_i \equiv -\zeta_i \equiv -\zeta_{ii}$ to write in terms of x, y, and z, the other three degrees of freedom, associated to the null components ζ_A for $A = 4, 5, 6$, being absorbed in the values of the Euler angles fixing the triad orientation. So, making use of the relation

$$dx\, dy\, dz \prod_{A=4}^{6} d\zeta_A = |(\lambda_1-\lambda_2)(\lambda_2-\lambda_3)(\lambda_1-\lambda_3)|\, dx\, dy\, dz\, \frac{d\Omega_{S^3}}{6}, \tag{3.52}$$

where $d\Omega_{S^3}$ is the volume element on the surface of the three-sphere S^3 we can integrate the joint probability function P over the Euler angles. This reduces the initial set of variables by three. Notice that, once the coordinate axes are fixed, there is no more freedom left, and we cannot further assume the eigenvectors of the tensor ζ_{ij} on scale $R + \Delta R$ also well orientated. So $\partial_R \lambda_i$ introduce, in principle, the whole set of 6 independent variables $\partial_R \zeta_A$. Fortunately, the different orientation of the triads of eigenvectors of tensors ζ_{ij} on scales R and $R + \Delta R$ is very small because arising from the small increment ΔR, and by neglecting second order terms in ΔR we have that the same expressions for λ_i as linear combinations of x, y, and z, are also valid for $\partial_R \lambda_i$ in terms of X, Y, and Z. So we do not actually need to introduce the variables $\partial_R \zeta_A$ for $A = 4, 5, 6$.

For simplicity in the calculations we will require that λ_2 be the smallest eigenvalue, and $\lambda_1 \geq \lambda_3$. With this ordering (making the factor 6 dividing the left hand side of equation [3.52] unnecessary; see BBKS) to guarantee that all λ_i are positive we must simply require $\lambda_2 > 0$. So after the integration over the Euler angles (the integral over Ω_{S^3} giving $2\pi^2$) the joint probability for the remaining variables subject to the above ordering conditions writes

$$P(\nu, x, y, z, X, Y, Z, \boldsymbol{\eta}, \mathbf{I})\, d\nu\, dx\, dy\, dz\, dX\, dY\, dZ\, d^3\eta\, d^3\mathbf{I} = \frac{1}{(2\pi)^6 R_*^3} \frac{\sigma_1^3}{\sigma_2^3} \frac{3^7\, 5^{7/2}}{2\sigma_2^3}$$
$$\times \frac{|(\lambda_1 - \lambda_2)(\lambda_2 - \lambda_3)(\lambda_1 - \lambda_3)|\, \exp(-Q)}{(1-\gamma^2)^{1/2}\,(1-\Gamma^2)^{1/2}\,(1-\gamma_2^2)^{3/2}}\, d\nu\, dx\, dy\, dz \frac{dX\, dY\, dZ}{D^3} \frac{d^3\eta}{\sigma_1^3} \frac{d^3\mathbf{I}}{(\sigma_3 R)^3}. \tag{3.53}$$

It is also convenient to transform the variables z and Z to $z' \equiv 3\lambda_2/\sigma_2 = x - 2z$ and $Z' \equiv 3\partial_R \lambda_2/\sigma_2 = X - 2Z$. This is readily achieved through the relation

$$P(..., z', ..., Z')\, ...dz'...dZ' = \langle \delta(z' - x + 2z)\, \delta(Z' - X + 2Z) \rangle\, ...dz'...dZ', \tag{3.54}$$

with the mean in angular brackets for the joint probability (3.53). Finally, taking into account relations (3.46) and (3.47) both for $i = 2$, and (3.41) for the two remaining components we are led to the fact that the mean density of peaks on scale R disappearing within the next dR, with variables ν, x, y, z', X, Y, Z'

taking values $\nu_0, x_0, y_0, z'_0, X_0, Y_0, Z'_0$ in infinitesimal ranges is

$$\mathcal{N}^{dis}_{pk}(\nu_0, x_0, y_0, z'_0, X_0, Y_0, Z'_0, R)\, d\nu\, dy\, dz'\, dX\, dY\, dZ'\, dR = \langle 3^{-1}\sigma_2\, |Z'| \times\delta[\mathrm{I}_2 - \mathrm{I}_2(\mathbf{r})]|\lambda_1\lambda_3|\, \delta(\eta_1)\, \delta(\eta_3)\, \delta(\Delta R - z'/|Z'|)\, \theta(z')\, \delta(\nu_0 - \nu)\delta(x - x_0) \times\delta(y - y_0)\delta(z' - z'_0)\delta(X - X_0)\delta(Y - Y_0)\delta(Z' - Z'_0)\rangle\, d\nu\, dy\, dz'\, dX\, dY\, dZ'\, dR, \tag{3.55}$$

with θ the Heaviside unit function, $\lambda_1 = \sigma_2(x + 2y - z'/3)/2$, and $\lambda_3 = \sigma_2(x - 2y - z'/3)/2$, and with the mean in angular brackets for the joint probability (3.54) (subject to the above ordering conditions) times the probability of finding I_2 at $\mathbf{r}$ (subject to no constraint, in particular, on $\eta_2(\mathbf{r})$). Strictly, since $\mathbf{r}_p$ is a peak instead of the joint probability (3.54) we should use the conditional joint probability given that η_2 is null at this point. But this makes no difference at all in the final probability function.

After dropping the subindexes 0 and performing the averages over $\boldsymbol{\eta}$, $\mathbf{I}$, and $\mathrm{I}_2(\mathbf{r}_p)$, we arrive to the following expression

$$\mathcal{N}^{dis}_{pk}(\nu, x, y, z', X, Y, Z', R)\, d\nu\, dx\, dy\, dz'\, dX\, dY\, dZ'\, dR = \frac{3^{5/2}\, 5^{7/2}}{2^{5/2}\, (2\pi)^{9/2}\, R_*^3\, D^3\, R} \times\frac{\sigma_1}{\sigma_3}\frac{\delta(z' - |Z'|\Delta R)\, Z'^2\, |F(x, y, z')|\, \chi\, \exp(-\tilde{Q})}{(1 - \gamma^2)^{1/2}\, (1 - \Gamma^2)^{1/2}\, (1 - \gamma_2^2)^{1/2}} d\nu\, dx\, dy\, dz'\, dX\, dY\, dZ'\, dR, \tag{3.56}$$

where

$$2\tilde{Q} = \nu^2 + \frac{(x - x_*)^2}{1 - \gamma^2} + \frac{(X - X_*)^2}{(1 - \Gamma^2)\, D^2} + 15\left[y^2 + \frac{(Y - Y_*)^2}{D^2}\right] + \frac{5}{4}\left[(z' - x)^2 + \frac{(Z' - Z'_*)^2}{D^2}\right], \tag{3.57}$$

with $Z'_* \equiv X - 2Z_* = X - (x - z')\,(\sigma_3^2/\sigma_2^2)\, R$, the function $F(x, y, z')$ defined as $y[y^2 - (x - z')^2/4][(3x - z')^2/4 - 9y^2]$, and χ equal to 1 if the constraints in the x, y, z' domain are satisfied, and 0 otherwise. In this concern, such constraints are equivalent to $0 \leq z',\, z' \leq x$, and $0 \leq y \leq (x - z')/2$.

The integrals over Y and z' can be readily performed. Then, neglecting higher order terms in ΔR, and rearranging terms we obtain

$$\mathcal{N}_{pk}^{dis}(\nu,x,R)\,d\nu\,dx\,dR = \frac{3^2\,5^3}{2^{5/2}\,(2\pi)^4\,R_*^3\,D^2\,R}\,\frac{\sigma_1}{\sigma_3}\,\frac{e^{-\nu^2/2}}{(1-\gamma^2)^{1/2}}\,d\nu$$
$$\times\frac{e^{-5x^2/8}\,e^{-\frac{(x-x_*)^2}{2(1-\gamma^2)}}}{(1-\Gamma^2)^{1/2}\,(1-\gamma_2^2)^{1/2}}\,dx\,dR\int_0^{x/2}dy\,e^{-15y^2/2}\,y\left(y^2-\frac{x^2}{4}\right)^2$$
$$\times\int_{-\infty}^{\infty}dZ'\,Z'^2\int_{-\infty}^{\infty}dX\,e^{-\frac{5(Z'-Z'_*)^2}{8D^2}}\,e^{-\frac{(X-X_*)^2}{2(1-\Gamma^2)D^2}}. \qquad (3.58)$$

for $x>0$. And after integration over X, Z', and y we are finally led to

$$\mathcal{N}_{pk}^{dis}(\nu,x,R)\,d\nu\,dx\,dR = \frac{(1-\gamma_2^2)^{3/2}}{\gamma_2}\,\mathcal{N}_{pk}(\nu,x,R)\,d\nu\,dx$$
$$\times\ (\tau+\Delta^2 x)\,g(x)\,f(x)\,\frac{\sigma_3^2}{\sigma_2^2}\,R\,dR, \qquad (3.59)$$

with $\mathcal{N}_{pk}(\nu,x,R)\,d\nu\,dx$ the analog normal density of peaks given in equation (3.23),

$$g(x)\,f(x)=\frac{6}{\sqrt{5\pi}}\left\{e^{-5x^2/8}\left[1-\frac{15}{8}\,x^2+\frac{1}{2}\left(\frac{15}{8}\,x^2\right)^2\right]-e^{-5x^2/2}\right\}, \qquad (3.60)$$

and $\tau\equiv[(1-5\Gamma^2/9)/(5\Gamma^2/9)]/[(1-\gamma^2)/\gamma^2]$.

Finally, integrating over x, we obtain the density of peaks with height ν (on scale R) in an infinitesimal range which disappear in the next dR,

$$\mathcal{N}_{pk}^{dis}(\nu,R)\,d\nu\,dR=\mathcal{N}_{pk}(\nu,R)\,d\nu\,\mathcal{K}^{dis}(\boldsymbol{\gamma},x_*)\,\frac{\sigma_3^2}{\sigma_2^2}\,R\,dR, \qquad (3.61)$$

with

$$\mathcal{K}^{dis}(\boldsymbol{\gamma},x_*)=\frac{(1-\gamma_2^2)^{3/2}}{\gamma_2}<(\tau+\Delta^2 x)\,g(x)>, \qquad (3.62)$$

where the angulars brackets denote now the mean defined as

$$<h(x)>=\frac{\int_0^\infty dx\,h(x)\,f(x)\exp\left[-\frac{(x-x_*)^2}{2(1-\gamma^2)}\right]}{\int_0^\infty dx\,f(x)\exp\left[-\frac{(x-x_*)^2}{2(1-\gamma^2)}\right]} \qquad (3.63)$$

According to equation (3.61), we see that the density of peaks wich disappears in a neighborhood ΔR from R is of order ΔR greater than the expression (3.25), which does not include this contribution. Indeed, in performing the average (3.43) for all components, disappearing peaks with the smallest λ_i of order ΔR yield a null contribution. In other words, these densities only include those peaks robust enough for their continuity to be guaranteed in a range of scales around R.

3.3.2 Densities of Peaks with Specific Values of Random Variables

In next Chapters we will be concerned with densities of peaks with values of different random Gaussian variables with null mean, v_i ($i = 0, 1, ..., n$ with n arbitrarily large), in infinitesimal ranges. All these densities can be inferred from the density of peaks with $v_0 = \nu$ and $v_1 = x$ on scale R in infinitesimal ranges $\mathcal{N}_{pk}(\nu, x, R)\, d\nu\, dx$ (see equation [3.23]). One must simply apply the recursive relation

$$\begin{aligned} \mathcal{N}_{pk}(v_0, v_1, ..., v_n, R)\, dv_0\, dv_1 ...dv_n &= \mathcal{N}_{pk}(v_0, v_1, ..., v_{n-1}, R)\, dv_0\, dv_1, ...dv_{n-1} \\ &\times \mathcal{P}(v_n, R|v_0, v_1, ..., v_{n-1}, R)\, dv_n, \end{aligned} \quad (3.64)$$

with $\mathcal{P}(w, R|v_0, v_1, ..., v_{n-1}, R)\, dw$ the conditional probability of finding the value of w in an infinitesimal range given that $v_0, v_1, ..., v_{n-1}$ take some given values. As we have seen in § 2.2.3 this conditional probability adopts a Gaussian form

$$P(w, R|v_0, v_1, ..., v_{n-1}, R)\, dw = \frac{1}{\sqrt{2\pi}\,\sigma_w} \exp\left[-\frac{(w - \bar{w})^2}{2\,\sigma_w^2}\right] dw, \quad (3.65)$$

with

$$\begin{aligned} \bar{w} &= \mathbf{M}_{wv}\, \mathbf{M}_{vv}^{-1}\, \mathbf{V}^{\dagger} \\ \sigma_w^2 &= < w^2 > - \mathbf{M}_{wv}\, \mathbf{M}_{vv}^{-1}\, \mathbf{M}_{wv}^{\dagger}, \end{aligned} \quad (3.66)$$

where $\mathbf{M}_{wv}$ and $\mathbf{M}_{vv}$ are the $1 \times n$ and the $n \times n$ correlation matrixes of w with v_i, $\langle w\, v_i \rangle$, and v_i with themselves, $\langle v_i\, v_j \rangle$, respectively, $\mathbf{V}$ stands for the $1 \times n$ matrix of components v_i, and $\dagger$ denotes transpose. Note that the conditional probability (3.65) refers to points in general, the positive value of x guaranteeing by itself that they can be peaks. Indeed, the null values of the three components of $\boldsymbol{\eta}$ in peaks make them be possible to ignore in practice. From equation (3.65) it is clear that if v_n does not correlate with any of the previous variables v_i the conditional probability $P(v_n, R|v_0, v_1, ..., v_{n-1}, R)\, dv_n$ is simply equal to the Gaussian probability $P(v_n, R)\, dv_n$ of finding v_n on scale R in some infinitesimal range. Thus, the only densities of peaks with non trivial distributions of the variables involved are those for variables correlating with ν (or δ) and x on scale R, or any other explicit variable correlating with them.

Let us consider the series of variables $v_0 = \nu$, $v_1 = x$, and

$$v_i = \frac{1}{\sigma_{2i}\, R^{i-1}}\, \partial_R [\sigma_{2(i-1)}\, R^{i-2}\, v_{i-1}] \tag{3.67}$$

($i \geq 2$), involving all order scale derivatives of the density contrast. The correlations among them take, for the Gaussian window, the general form,

$$\langle v_i\, v_j \rangle (-1)^{i+j+\delta_{0i}+\delta_{0j}}\, \frac{\sigma_{i+j}^2}{\sigma_{2i}\, \sigma_{2j}} \tag{3.68}$$

($i, j \geq 0$), with δ_{ij} the Krönecker delta. We must remark that, although the notation used in equations (3.64) to (3.68) presumes all variables defined on scale R, they are also valid for variables defined on different scales. In particular, were any variable, say v_i, defined on another scale R', one would be led to just the same expression for the correlations as in equation (A11) but with σ_i and σ_{i+j} replaced by $\sigma_i' \equiv \sigma_i(R')$ and $\sigma_{i+j\,h} \equiv \sigma_{i+j}\left[\sqrt{0.5\,(R^2 + R'^2)}\right]$, respectively. This will be used in Appendix A. From equations (3.64) to (3.68) one can readily calculate the density function $\mathcal{N}_{pk}$ of peaks at a fixed scale R per infinitesimal ranges of ν, x, and any other set of the previous variables v_i ($i \geq 2$).

Moreover, following the same scheme starting from the conditional density analogous to the normal density in equation (3.23) but for peaks subject to

any given constraint (e.g., a background of height ν_b on scale R_b) one is led to the relation

$$\begin{aligned} \mathcal{N}_{pk}(v_0, ..., v_n, R|\nu_b, R_b)\, dv_0, ...dv_n &= \mathcal{N}_{pk}(v_0, ..., v_{n-1}, R|\nu_b, R_b)\, dv_0, ...dv_{n-1} \\ &\times \mathcal{P}(v_n, R|v_0, ..., v_{n-1}, R)\, dv_n. \end{aligned} \tag{3.69}$$

Thus, all the conditional densities can be derived from the one with values of ν and x in infinitesimal ranges

$$\begin{aligned} \mathcal{N}_{pk}(\nu, x, R|\nu_b, R_b)\, d\nu\, dx &= \frac{e^{-\nu^2/2}}{(2\pi)^2\, R_*^3} \frac{\exp\left[-\frac{(\nu-\epsilon\nu_b)^2}{2(1-\epsilon^2)}\right]}{\sqrt{2\pi\,(1-\epsilon^2)}} \frac{\exp\left[-\frac{(x-\tilde{x}_*)^2}{2(1-\tilde{\gamma}^2)}\right]}{\sqrt{2\pi\,(1-\tilde{\gamma}^2)}} \\ &\times f(x)\, d\nu\, dx. \end{aligned} \tag{3.70}$$

4

THE MASS FUNCTION IN THE PEAK MODEL

4.1 Introduction

The success of the PS mass function in matching the results of N-body simulations is the key proof for supporting its ability to properly describe the real gravitational clustering. Despite this fact, it is not well understood how present objects can arise from points of the smoothed density field, the contrast density of which exceeds a given value. Peaks are the best seeds of virialized objects we can think about right now, and certainly physically better motivated than the undefined volumes used in the PS prescription. Since there is no satisfactory derivation of the theoretical mass function in the peak model framework, it is valuable to make an effort to build a consistent one.

The first step consist of stablishing the conexion between peaks of the linear density field and collapsed objects. This is done by means of peak model ansatz, which states that objects at a time t emerge from peaks with density contrast equal to a fixed linear overdensity δ_c in the smoothed, on any scale R,

density field at the arbitrary initial time t_i. The critical overdensity is assumed to be a monotonous decreasing function of t, while the mass M of collapsing clouds associated with peaks is assumed to be a monotonous increasing function of R. (The collapsing cloud associated with a peak is simply the region surrounding the peak with total mass equal to that of the final virialized object at t.) Therefore, the evolution, with shifting density contrast, of the filtering scale of peaks at t_i is believed to trace the growth in time of the mass of objects. Of course, this is just an ansatz whose validity has to be assessed, a posteriori, by comparing the clustering model it yields with N-body simulations. Note, in particular, that peaks might be good seeds of virialized objects and the mass of their associated collapsing clouds not be just an increasing function of R (see, e.g., Bond 1988) or the time of collapse of such clouds not be just a decreasing function of the smoothed density contrast. These assumptions intended to constrain the freedom left by the unknown dynamics of the collapse of density fluctuations are, nonetheless, very reasonable. They are suggested by the spherical collapse model, approximation which is particularly well suited when dealing with peaks. On the other hand, they are much less restrictive than the specific relations $\delta_c(t)$ and $M(R)$ predicted by that simple model. So there is much room left for any actual departure from it. Finally, there is the extra freedom arising from the filter used, which can be different from the top hat one.

The direct extension of the PS prescription to the peak model suggests itself. The resulting mass function is (Colafrancesco, Lucchin, & Matarrese 1989; Peacock & Heavens 1990)

$$N(M,t)\,dM \;=\; A\,\frac{1}{M}\left|\frac{\partial[n_{pk}(\delta_c,R)\,M_{pk}(\delta_c,R)]}{\partial R}\right|\frac{dR}{dM}\,dM, \qquad (4.1)$$

where A is a normalization factor, $n_{pk}(\delta_c,R)$ is the number density of peaks with density contrast above the threshold δ_c in the density field smoothed on scale R, and $M_{pk}(\delta_c,R)$ is the average mass of objects emerging from these peaks (when divided by ρ, equal to the mean volume subtended by the corresponding collapsing clouds). Note that since peaks included in $n_{pk}(\delta_c,R)$ do not have, in general, density contrast equal to δ_c, the average mass of their collapsing clouds, $M_{pk}(\delta_c,R)$, will differ from $M(R)$. The above mentioned

problem with the normalization of the PS mass function and the cloud-in-cloud effect is reflected in the variety of expressions found in the literature for the factor A and the function $M_{pk}(\delta_c, R)$ in equation (4.1). A more serious problem, however, is that this equation states that the mass in objects emerging from peaks with density contrast upcrossing δ_c in the range of scales between R and $R+dR$ is equal to the variation from R to $R+dR$ of the mass associated with peaks with density contrast above δ_c. It is therefore implicitly assumed that 1) the total mass associated with peaks (with $\delta > 0$) is conserved with varying scale, and 2) the density contrast of peaks is a decreasing function of scale. Both points seem to follow, indeed, from the peak model ansatz. But this is actually not true. As shown below, point 2 crucially depends on the shape of the window used, while the frequent discontinuities in peak trajectories in the δ vs. R diagram yielded by mergers invalidate point 1 and, hence, equation (4.1) in any event.

Before we proceed further, one brief comment on the notation used throughout the paper is in order. Rather than the integrated density of peaks on scale R, $n_{pk}(\delta_c, R)$, appearing in equation (3) we will use the differential density of peaks on a fixed scale R with scaled density contrasts $\nu \equiv \delta/\sigma_0(R)$ in an infinitesimal range, $\mathcal{N}_{pk}(\nu, R)\, d\nu$. In addition, we will introduce the differential density of peaks with fixed density contrast δ on scales in an infinitesimal range, denoted by $N_{pk}(R, \delta)\, dR$. Caution must be made in not mixing up these two densities, as well as their respective conditional forms.

Thus, the only reliable strategy to derive the mass function of objects in the peak model framework is to directly count the density of peaks with density contrast δ_c in infinitesimal ranges of scale, $N_{pk}(R, \delta_c)\, dR$, and then transform it to the mass function of objects at the time t, $N(M,t)\, dM$, by using the appropriate $M(R)$ and $\delta_c(t)$ relations. Unfortunately, apart from the uncertainty about these latter two relations and the filter to be used, as well as the cloud-in-cloud effect which is always present, this strategy faces a new important drawback: the differential density of peaks is well-defined for a fixed filtering scale, not for a fixed density contrast. In other words, we only know the form of $\mathcal{N}_{pk}(\nu, R)\, d\nu$ while we need that of $N_{pk}(R, \delta)\, dR$. Bond

(1988) proposed the following "reasonable, although not rigurously derivable", expression for the scale function of peaks at fixed density contrast,

$$N_{pk}(R,\delta)\,dR = \mathcal{N}_{pk}(\nu,R)\,\frac{\partial\nu}{\partial R}\,dR, \tag{4.2}$$

with $\mathcal{N}_{pk}(\nu,R)$ calculated in BBKS. Soon after, this same author (Bond 1989; hereafter B89) attempted to formally derive the wanted scale function. The expression found, identical to that independently obtained by Appel & Jones (1990; hereafter AJ), recovers equation (4.2) as an approximate relation valid in the limit of rare events, i.e., for peaks with $\nu \gg 1$. But in these derivations it is assumed, for simplicity, that points which are peaks on a given scale keep on being peaks when the scale is changed, which is obviously not true in general. In changing the scale, the spatial location of peaks also changes. As a consequence, there is no obvious connection between peaks on different scales and, what is more important, between their respective density contrasts. More recently, Bond & Myers (1993a, 1993b) have proposed a new method, the so-called "peak patch formalism", to obtain the mass function of objects. This follows the correct strategy for peaks, the cloud-in-cloud effect is corrected for, and a more accurate collapse dynamics than the spherical model is used. However, this new method involves complex calculations including Monte Carlo simulations and, hence, does not provide us with any practical analytical or semianalytical expression for the mass function as wanted.

In the present paper we give a fully justified formal derivation of the theoretical mass function of objects relying just on the peak model ansatz. This derivation draws inspiration from (and, in fact, is very close to) those followed by B89 and AJ. The main differences are: 1) we do not assume that the spatial locations of peaks remain fixed when the scale is changed, but let them vary, and 2) we provide a consistent way to correct the resulting scale function for the nesting of collapsing clouds. These improvements as well as the determination of the only consistent filtering window and $M(R)$ and $\delta_c(t)$ relations to be used are possible thanks to the development, in § 4.2, of a new formalism, hereafter referred to as the "confluent system formalism" (see also Salvador-Solé & Manrique 1994), which is able to follow the filtering evolution of peaks. In § 4.3 we apply this formalism to derive the scale function of peaks

with fixed density contrast, and to correct it for the cloud-in-cloud effect. In § 4.4 we determine the form of the $M(R)$ and $\delta_c(t)$ relations which are consistent with the peak model for different power spectra of the density field in an Einstein-de Sitter universe. Finally, we derive, in § 4.5, the mass function of objects in these cosmogonies. Other important quantities connected with the detailed growth history of objects are calculated in the next Chapter.

4.2 The Confluent System Formalism

In gravitational clustering one can make the practical distinction between accretion and merger. Accretion is, by definition, a continuous and differentiable process in time. For any accreting object of given mass M another object of mass $M + dM$ can be found which subtends the former. In contrast, merger is a discontinuous event. There is a discrete gap ΔM in mass values in which no object subtending the matter of some given initial one can be found. This gap delimits the merging object whose mass evolution is being followed from the object resulting from the merger. According to the peak model ansatz enunciated above, peaks in the smoothed density field rearrange, with decreasing overdensity, essentially as objects do in time through accretion and mergers. Therefore, we can identify events analogous to accretion and merger in the filtering process in a very straightforward way by means of the correspondence between objects with increasing mass along the increasing time t and those peaks tracing them at t_i with decreasing density contrast δ when the filtering scale R is increased.

4.2.1 Filtering Accretion

A point which is a peak on scale R is not so, in general, on scale $R + \Delta R$, with ΔR positive and arbitrarily small. To guarantee that a peak on scale $R + \Delta R$ traces the same accreting object as the peak on the initial scale R

at the times corresponding to their respective density contrasts the separation between both points must be, at most, of the order of ΔR. In this manner, the collapsing cloud associated with the peak on scale $R + \Delta R$ will include the volume (mass) subtended by the collapsing cloud associated with the peak on scale R. Furthermore, this proximity condition is not only necessary for the identification of peaks on contiguous scales, but also sufficient. Indeed, as readily seen from the Taylor series expansion of the density gradient around a density maximum, there cannot be more than one peak on scale $R + \Delta R$ in the neighborhood of any point which was a peak on scale R. (See § 4.2.2 for the case that no identification is possible for a given peak of scale R.)

This identification allows us to draw a δ vs. R diagram similar to that obtained by Bond et al. (1991) in the excursion set formalism but for the fact that, in our diagram, each trajectory $\delta(R)$ is attached to one individual object or, what is the same, to *the changing peaks tracing it* in the filtering process instead of to one fixed point. To construct this diagram we must find all peaks on a given scale R in some arbitrary volume, increase the scale by ΔR, find the new peaks on the scale $R+\Delta R$, and identify each of them with one of the peaks on scale R, repeating the process from the largest scale reached at each step as many times as necessary. The continuous curves $\delta(R)$ determined by each series of identified peaks (disregarding their changing spatial location) represent the trajectories followed by peaks "evolving" through filtering accretion and trace the time evolution of the mass of bound virialized objects as they accrete matter.

The density contrast of an evolving peak on scale $R + \Delta R$ is, to first order in ΔR, simply given by $\delta + \partial_R \delta \, \Delta R$ in terms of the values of the random variables δ and $\partial_R \delta$ at the same evolving peak on scale R. To see this one must simply take the Taylor series expansion of the density contrast of the former peak around the position $\mathbf{r}$ and scale R of the latter and take into account that, according to our identification criterion, we have $O(|\Delta \mathbf{r}|^2) \leq O[(\Delta R)^2]$. Notice that there is, indeed, no first order term in $\Delta \mathbf{r}$ in that series expansion owing to the null density gradient in peaks. We therefore conclude that the total derivative $d\delta/dR$ of a peak trajectory in the δ vs. R diagram coincides

with the partial derivative $\partial_R\delta$ of the respective peak currently at (R, δ).

We are now ready to check the self-consistency of the peak model ansatz on which the previous natural identification criterion among peaks on different scales is based. As accreting objects evolve in time their mass obviously increases. But the mass is an increasing function of R, while the time a decreasing function of the density contrast. Consequently, peaks on scale $R+\Delta R$ must, for consistency, have smaller density contrast than those identified with them on scale R or, equivalently, the total derivative $d\delta/dR$ of peak trajectories must be negative. Let us see whether this is really satisfied.

By writting the scale derivative of the density contrast smoothed with any spherical window $W(r^2/R^2)$ of scale R, $\delta(\mathbf{r}, R)$, in terms of the Fourier transform of the unfiltered field, $\delta(\mathbf{k}, 0)$, we have

$$\partial_R\delta(\mathbf{r}, R) = -\frac{R}{(2\pi)^3}\int_{-\infty}^{\infty} d^3k\, k^2\, \delta(\mathbf{k}, 0)\, J(k^2R^2)\, \exp(-i\mathbf{kr}), \tag{4.3}$$

with $J(k^2R^2)$ equal to $-2\,[\partial W(k^2R^2)/\partial(k^2R^2)]$ and $W(k^2R^2)$ the Fourier transform of the smoothing window. Relation (5) can be rewritten in the form

$$\partial_R\delta(\mathbf{r}, R) = R\,\nabla^2[\delta(\mathbf{r}, 0) * J(r^2/R^2)], \tag{4.4}$$

with $J(r^2/R^2)$ the inverse Fourier transform of $J(k^2R^2)$ and $*$ denoting the convolution product. For a Gaussian window, i.e., $W(r^2/R^2) \equiv \exp[-r^2/(2R^2)]$, we have $J(k^2R^2) = W(k^2R^2)$ and equation (4.3) leads to the equality $\partial_R\delta(\mathbf{r}, R) = R\,\nabla^2\delta(\mathbf{r}, R)$. This implies that $\partial_R\delta(\mathbf{r}, R)$ and, consequently, $d\delta/dR$ are automatically negative for peaks as needed. However, for any other window $J(k^2R^2)$ is different from $W(k^2R^2)$ and the sign of $\nabla^2[\delta(\mathbf{r}, 0) * J(r^2/R^2)]$ is not determined by that of $\nabla^2[\delta(\mathbf{r}, R)]$, but depends on the particular density distribution around each point $\mathbf{r}$. Thus, condition $d\delta/dR = \partial_R\delta(\mathbf{r}, R) < 0$ is not guaranteed for every peak. We are therefore led to the conclusion that the shape of the window used is crucial for the self-consistency of the peak model ansatz: only the Gaussian window is able to recover such a fundamental property of gravitational clustering as the systematic growth, by accretion, of the mass of objects in any realistic density field. This might explain the good behavior of the Gaussian window in N-body simulations of structure formation

from peaks (Mellot, Pellman, & Shandarin 1993; see also Katz, Quinn, & Gelb 1993). It is interesting to note that the characteristics of the density distribution in the real universe causing the departure from spherical collapse also make the peak model ansatz inconsistent with the filtering by means of a top hat window. If such a density field were spherically symmetric and outwards decreasing around $\mathbf{r}$, then the condition $\partial_R \delta(\mathbf{r}, R) < 0$ would be clearly fulfilled by the top hat window (and many others depending on the particular density profile). However, in the real universe, the Gaussian window is the only one that guarantees this condition. Herafter, we adopt this particular filter.

4.2.2 Filtering Mergers

As a peak evolves through filtering accretion the volume of its associated collapsing cloud increases. Provided there is full coverage of space by collapsing clouds associated with peaks of fixed overdensity, that volume increase makes peaks progressively become located inside the collapsing clouds of others with identical density contrast but larger filtering scale. This is but the well-known cloud-in-cloud effect which must be corrected for if we want the scale function of peaks at a fixed overdensity to reflect the mass function of virialized objects at the corresponding time. Notice that, the non-nested peaks that remain at each fixed overdensity will provide the exact coverage of space since just those causing the excessive coverage of space at any δ have been removed. Hereafter, we focus on the filtering evolution of non-nested peaks, as efficient tracers of virialized objects.

The nesting-corrected δ vs. R diagram contains a set of continuous peak trajectories suddenly truncated when their respective evolving peaks become located inside the collapsing cloud associated with any other peak with identical density contrast but a larger filtering scale. Since the volume (mass) of the collapsing cloud associated with an accreting peak which becomes nested is covered by that of the host peak, we can think about the former as evolving into the latter (becoming part of it) through a discrete horizontal jump in the nesting-corrected δ vs. R diagram. Such discrete jumps among peak trajecto-

ries towards larger scales along the line of fixed density contrast reflect discrete mass increases, at a fixed time, of the virialized objects they trace. Therefore, the nesting of, until then, non-nested peak trajectories can be naturally identified with mergers. Notice that the key assumption in this identification has been that collapsing clouds associated with non-nested peaks of given fixed density contrast yield the exact coverage of space. This is ensured by the peak model ansatz itself: an incomplete (or excessive) coverage of space by collapsing clouds associated with non-nested peaks is not allowed because this would overestimate (underestimate) the density of objects at the corresponding t inferred from counting their respective seeds. Thus, our identification of filtering mergers also directly follows from the peak model ansatz.

But, apart from becoming nested, peak trajectories in the nesting-corrected δ vs. R diagram can also disappear or appear. This is due to the fact that, as pointed out in § 4.2.1, the identification among peaks on different scales is not always possible. An infinitesimal increase in R can make a continuous peak trajectory disappear (there is no peak on scale $R + \Delta R$ in the close neighborhood of the peak on scale R) or a new continuous peak trajectory appear (there is no peak on scale R in the close neighborhood of the peak on scale $R + \Delta R$). When a peak appears without being nested (otherwise the event would go unnoticed in the nesting-corrected δ vs. R diagram) some peaks with identical density contrast and smaller scale automatically become nested into it. These filtering events therefore trace the *formation* of new virialized objects from the merger of smaller ones. However, when a peak disappears before becoming nested (otherwise we could ignore the event) the volume (mass) associated with it will be necessarily covered by that of collapsing clouds associated with other peaks with identical density contrast and *smaller* scale. This will produce the split of the former peak into the latter ones. N-body simulations also find sporadic splits in the *gravitational evolution of peaks* (van de Weygaert & Babul 1993). However, gravitational splits of peaks take place prior to collapse, while filtering splits of peaks refer to virialized objects. Thus, this latter kind of filtering events has no natural counterpart in the gravitational evolution of virialized objects. Moreover, these are not the only unrealistic events we can find in the filtering evolution of peaks. Nested peaks can also leave their host

clouds yielding, in this manner, a different kind of split of peak trajectories. Thus, in contrast with virialized objects which tend to progressively cluster with each other without exception, peaks tend to come together as we diminish the critical overdensity but they also sporadically split into pieces. This reflects the limitations of the peak model to provide an exact description of the growth history of individual objects. Yet, we are not concerned with the detailed evolution of *individual* objects, but rather in the *statistical* description of the clustering process they follow. In fact, for the confluent system formalism to provide an acceptable clustering model we only need that both the net amount of peaks becoming nested (after substraction of those leaving their host clouds) and the net amount of peaks appearing as the result of mergers (after substraction of those disappearing and breaking into small pieces) are positive at any location of the nesting-corrected δ vs. R diagram. In the present paper, we focus on obtaining the scale function of non-nested peaks at a fixed density contrast. In Chapter 5, we calculate those net amounts and show the statistical validity of the confluence system formalism, at least for density fields leading to hierarchical clustering, i.e., those with σ_0 a decreasing function of R.

4.2.3 The Confluent System Diagram

The nesting-corrected δ vs. R diagram of such a hierarchical clustering looks like the idealized one plotted in Figure 1. To avoid crowding we have drawn just a few trajectories to illustrate the general behavior of the diagram one would obtain from a fair sample volume of the universe. As can be seen, this diagram differs from the analogous one obtained in the excursion set formalism (BCEK) in three main aspects: 1) all trajectories have the same monotonous trend of decreasing density contrast with increasing scale, 2) they all have a finite continuous extent limited by mergers, and 3) the number of trajectories decreases with increasing filtering scale. Mergers reduce, indeed, the total number of surviving peaks. At $R = 0$ we have a large, usually infinite, number of trajectories, while for R tending to infinity we end up with just one trajectory approaching to $\delta = 0$. This is the reason why we call this diagram the confluent

system of peak trajectories. From Figure 4.1 it is apparent that the variation in the density of peaks above δ_c between scales R and $R + \Delta R$ is not equal to the density of peaks upcrossing the δ_c line in this range of scales nor is the mass of the collapsing clouds associated with them. Large horizontal skips along the R axis direction caused by mergers also contribute to this variation, which invalidates equation (3). Note also that, owing to these horizontal skips, there are peaks missing on every scale R making the integral of the *average mass* of collapsing clouds associated with peaks *at a fixed scale* be different from the mean density of the universe.

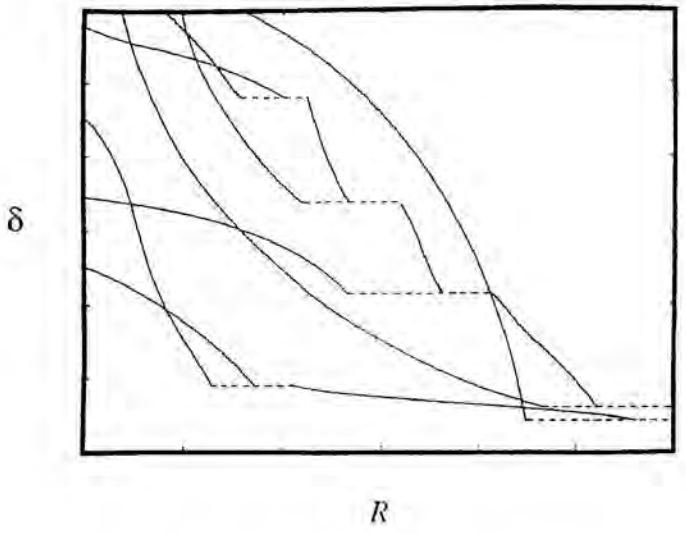

Figure 4.1: *Idealized confluent system of peak trajectories for a limited sample volume. In full line, the continuous filtering evolution of peaks tracing accretion by the corresponding virialized objects. In dashed lines, discontinuities tracing mergers of similarly massive objects.*

We want to stress that, as clearly stated at the begining of this section, the distinction between accretion and merger in gravitational as well as in filtering evolutions is a practical one *which makes only sense from the viewpoint of any particular evolving object or peak.* In particular, what is a merger for one object can be either a merger or an accretion process for any other object partaking

of the same event. This is shown in Figure 4.1. Peaks *resulting* from mergers can be either evolving through continuous accretion or forming depending on whether or not they can be identified with peaks at an infinitesimally larger δ. This reflects a well-known fact in gravitational clustering: if some object is massive enough relative to any other merger partner its relaxed state is not essentially altered by the event and one can keep on identifying it with the resulting object. Thus, from the viewpoint of such a massive object, the merger is a simple accretion. Conversely, from the viewpoint of the small accreted object which is destroyed in the event, the process is seen as a true merger of that object with a much more massive one. Of course, this latter phenomenon also has its counterpart in the filtering evolution of peaks: the exact coverage of space by collapsing clouds guarantees that the increase, with decreasing δ, of the volume (mass) of clouds associated with any accreting peak is made at the expense of the volume (mass) of the collapsing clouds associated with those peaks which become nested into it. (This alternate interpretation of accretion is not systematically represented, however, in Fig.4.1 since this would yield a continuous crowd of horizontal dashed lines starting from very small scales.) In other words, the analogy about mergers, accretion, and their interconnection, between gravitational and filtering evolutions is complete. It is important to note that the ambivalence of some processes of mass increase depending on the viewpoint of the particular object whose evolution is followed far from being a drawback of the confluent system formalism is at the base of its great potential. For example, in the excursion set formalism where there is no such ambivalence, accretion can only be treated as a series of mergers with very tiny objects (see, e.g., Lacey & Cole 1993). But, then, one cannot naturally distinguish such important events as the formation or the destruction of an object because there is no clear difference, from any viewpoint, between the mergers which characterize those notable events and all the mergers which constitute of the accretion process experienced by the object during its life. Thus, the possibility of following the mass increase of any given object by making the natural distinction between accretion and merger events is an important characteristic of the confluent system formalism with notable practical applications (see next Chapter).

4.3 The Scale Function

4.3.1 The Scale Function of Peaks with Fixed Density Contrast

To compute the density of peak trajectories upcrossing the δ_c line in infinitesimal ranges of scale we must calculate the density of peaks on scale R with density contrast larger than δ_c which *evolve* into peaks with density contrast equal to or lower than that value on scale $R + \Delta R$, with ΔR positive and arbitrarily small. That is, we must compute the density of peaks on scale R satisfying: $\delta_c < \delta$ and $\delta_c \geq \delta + d\delta/dR\,\Delta R$. From the results of § 4.2 we have that these two constraints can be expressed as

$$\delta_c < \delta \leq \delta_c - \nabla^2\delta\, R\,\Delta R. \tag{4.5}$$

This coincides with the procedure followed by B89 and AJ. The difference between both approaches is that, contrary to these authors, *we do not assume that points which are peaks on scale R keep on being peaks on scale $R + dR$.* We have just taken into account the identification criterion among peaks on different scales (with different locations, in general). This determines (see § 4.2) the density contrast of any peak at $R + \Delta R$ in terms of that of the peak at R identified with it and, hence, the condition for any *evolving peak* to cross the threshold δ_c.

Now, following § 3.2.1 step by step, we can readily calculate the mean density of peaks on scale R satisfying the constraint given by equation (4.5) by taking the mean for the joint probability function $P(\delta, \eta = 0, \zeta_A)$ of the full random density field of these peaks. Variables η_i and ζ_A (A =1, 2, 3, 4, 5, 6 stand for ij =11, 22, 33, 23, 13, 12, respectively) are the first and second order cartesian derivatives of the mass density field smoothed on scale R, respectively. To calculate that mean it is convenient to use the new variables $\nu \equiv \delta/\sigma_0$, $x \equiv -(\zeta_1 + \zeta_2 + \zeta_3)/\sigma_2$, $y \equiv -(\zeta_1 - \zeta_3)/(2\sigma_2)$, and $z \equiv -(\zeta_1 - 2\zeta_2 +$

$\zeta_3)/(2\sigma_2)$, with σ_j the jth spectral momentum

$$\sigma_j^2(R) = \int_0^\infty \frac{dk\, k^{2(j+1)}}{2\pi^2} P(k) \exp(-k^2 R^2), \tag{4.6}$$

where $P(k)$ is the power spectrum of the density field. The only difference with respect to the usual procedure is that we must include the extra factor $\delta(x - x_0)$ in the calculation of the mean density of peaks in order to obtain a function of the variables ν_0 and x_0 ($x_0 > 0$). This leads to

$$\mathcal{N}_{pk}(\nu, x, R)\, d\nu\, dx = \frac{\exp(-\nu^2/2)}{(2\pi)^2 R_*^3 [2\pi(1-\gamma^2)]^{1/2}} f(x) \exp\left[-\frac{(x-\gamma\nu)^2}{2(1-\gamma^2)}\right] d\nu\, dx \tag{4.7}$$

(dropping subindexes 0), with $f(x)$ the function given by equation [3.24], $\gamma \equiv \sigma_1^2/(\sigma_0\sigma_2)$, and $R_* \equiv \sqrt{3}\sigma_1/\sigma_2$. The density function of peaks satisfying condition (7) is therefore

$$N_{pk}(R, \delta_c) = \lim_{\Delta R \to 0} \frac{1}{\Delta R} \int_0^\infty dx \int_{\nu_c}^{\nu_c + [\sigma_2(R)/\sigma_0(R)]\, x\, R\, \Delta R} d\nu\, \mathcal{N}_{pk}(\nu, x, R), \tag{4.8}$$

with $\nu_c \equiv \delta_c/\sigma_0(R)$. By integrating over ν and x and dividing by ΔR we finally obtain at $\Delta R \to 0$

$$N_{pk}(R, \delta_c)\, dR = \frac{H(\gamma, x_*)}{(2\pi)^2 R_*^3} \exp\left(-\frac{\nu_c^2}{2}\right) \frac{\sigma_2(R)}{\sigma_0(R)} R\, dR, \tag{4.9}$$

with $x_* \equiv \gamma\nu_c$, and

$$H(\gamma, x_*) = \int_0^\infty x\, f(x) \frac{\exp\left[-\frac{(x-x_*)^2}{2(1-\gamma^2)}\right]}{[2\pi(1-\gamma^2)]^{1/2}} dx. \tag{4.10}$$

The scale function (4.9) coincides with that given by B89 and AJ (in the latter case, except for a factor two in the expression finally quoted). It is also similar to the expression given by equation (4.2) initially proposed by Bond (1988). Indeed, an alternate expression for equation (4.9) in terms of the density function $\mathcal{N}_{pk}(\nu_c, R)$ equal to the integral of $\mathcal{N}_{pk}(\nu_c, x, R)$ over the whole range of positive values of x is

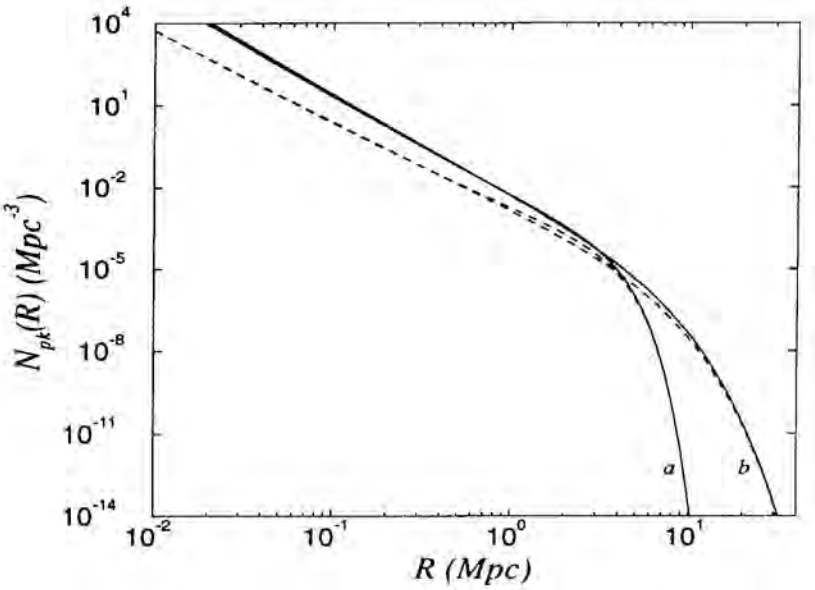

Figure 4.2: *Comparison between the scale function of peaks derived here (full line), and the one guessed by Bond (1989) (dashed line) corresponding to the present epoch in a univers with* $\Omega = 1$, $\Lambda = 0$, *and a density field endowed with CDM (a) or* $n = -2$ *power-law (b) power spectrum, normalized to the present rms density fluctuation inside a sphere of* $8h^{-1}$ *Mpc equal to* 0.67. *The value of the critical density* δ_{c0} *used for each power spectrum is the same as in Fig. 3.4.*

$$N_{pk}(R, \delta_c)\, dR = \mathcal{N}_{pk}(\nu_c, R)\, \frac{\sigma_2(R)}{\sigma_0(R)} < x > R\, dR, \tag{4.11}$$

with

$$< x > \equiv \frac{\int_0^\infty x\, f(x) \exp\left[-\dfrac{(x - x_*)^2}{2\,(1-\gamma^2)}\right] dx}{\int_0^\infty f(x) \exp\left[-\dfrac{(x - x_*)^2}{2\,(1-\gamma^2)}\right] dx}. \tag{4.12}$$

While, the relation

$$\frac{1}{\sigma_0}\frac{d\sigma_0}{dR} = -R\frac{\sigma_1^2}{\sigma_0^2} \tag{4.13}$$

valid for the Gaussian filtering allows us to write equation (4.2) in the form

$$N_{pk}(R,\delta_c)\,dR = \mathcal{N}_{pk}(\nu_c,R)\,\frac{\sigma_2(R)}{\sigma_0(R)}\,x_*\,R\,dR. \tag{4.14}$$

Equations (4.9) and (4.11) only differ by the effective scaled Laplacian x appearing in both expressions. As shown in 4.2, this difference is negligible at the large scale end when the approximation of rare events is valid. However, it introduces a notable deviation between the two functions at the small-scale end. For power-law power spectra, $P(k) \propto k^n$ $(-3 < n < 4)$, γ is constant, R_* is proportional to R, and the function H is constant for small R. Since σ_2/σ_0 is proportional to R^{-2} the logarithmic slope at small R of the scale function (4.9) or (4.11) is therefore equal to -4. As pointed out by A.J, such a steep slope makes the mass integral diverge for collapsing clouds with M proportional to R^3. (This is the same to say that there is a divergent coverage of space by such collapsing clouds). But we do not know the actual relation $M(R)$. Moreover, before applying the scale function (4.9) or (4.11) to objects we must correct it for the cloud-in-cloud effect.

4.3.2 Correction for the Cloud-in-Cloud Effect

To perform this correction we must first compute the density of peaks at fixed density contrast, subject to the condition of being located in some particular background. Following just the same reasoning as in § 3.1 but from the conditional density $\mathcal{N}_{pk}(x,\nu,R|\nu_b,R_b)\,dx\,d\nu$ given by equation() instead of the density $\mathcal{N}_{pk}(x,\nu,R)\,dx\,d\nu$ (equation [3.23]), one is led to the following density of peaks with density contrast δ_c on scales between R and $R+dR$ at points with density contrast δ_b on scales R_b

$$N_{pk}(R,\delta_c|R_b,\delta_b)\,dR = \frac{H(\tilde{\gamma},\tilde{x}_*)}{(2\pi)^2 R_*^3}\,\frac{\exp\left[-\dfrac{(\nu_c-\epsilon\nu_b)^2}{2(1-\epsilon^2)}\right]}{(1-\epsilon^2)^{1/2}}\,\frac{\sigma_2(R)}{\sigma_0(R)}\,R\,dR, \tag{4.15}$$

where $\tilde{x}_*$ is defined as $\tilde{\gamma}\tilde{\nu}$, with

$$\tilde{\gamma}^2 = \gamma^2\left[1 + \epsilon^2\frac{(1-r_1)^2}{1-\epsilon^2}\right], \qquad \tilde{\nu} = \frac{\gamma}{\tilde{\gamma}}\left(\frac{1-r_1}{1-\epsilon^2}\right)\left[\nu_c\left(\frac{1-\epsilon^2 r_1}{1-r_1}\right) - \epsilon\nu_b\right], \quad (4.16)$$

in terms of the spectral parameters $\epsilon \equiv \sigma_{0h}^2/(\sigma_0\sigma_{0b})$, and $r_1 \equiv \sigma_{1h}^2\sigma_0^2/(\sigma_{0h}^2\sigma_1^2)$, with $\sigma_{jh}(R, R_b)$ defined, for a Gaussian window, just as σ_j (equation [4.4]) but for the rms average scale $R_h \equiv [(R^2 + R_b^2)/2]^{1/2}$. The conditional density given in equation (17) can also be expressed as

$$N_{pk}(R, \delta_c|R_b, \delta_b)\, dR = \mathcal{N}_{pk}(\nu_c, R|\nu_b, R_b)\, \sigma_2(R) \widetilde{<x>}\, R\, dR, \quad (4.17)$$

in terms of the conditional density function $\mathcal{N}_{pk}(\nu, R|\nu_b, R_b)$ calculated in § 3.2.2 and the function $\widetilde{<x>}$ given by equation (4.12) now in terms of $\tilde{\gamma}$ and $\tilde{x}_*$ instead of γ and x_*.

We are now ready to obtain the master equation yielding the scale function of peaks at a fixed density contrast δ_c corrected for the cloud-in-cloud effect. The probability that a point is located inside the collapsing cloud associated with a non-nested peak of density contrast δ_c on some scale in the range between R_b and $R_b + dR_b$ is $\rho^{-1}\, M(R_b)\, N(R_b, \delta_c)\, dR_b$, where $\rho^{-1}\, M(R_b)$ is the volume of the collapsing cloud associated with the non-nested peak, and $N(R_b, \delta_c)\, dR_b$ is the unknown scale function of non-nested peaks. Given the meaning of the conditional density (19) we are led to the following relation

$$N(R, \delta_c) = N_{pk}(R, \delta_c) - \frac{1}{\rho}\int_R^\infty dR_b\, M(R_b)\, N(R_b, \delta_c)\, N_{pk}(R, \delta_c|R_b, \delta_c). \quad (4.18)$$

Equation (4.18) is a Volterra type integral equation of the second kind for the nesting-corrected scale function of peaks $N(R, \delta_c)$. According to the theory of integral equations, there exists a unique solution which can be obtained, numerically, by iteration from the initial approximate solution $N_{pk}(R, \delta_c)$ given by equation (4.9).

To correct the scale function of peaks for the nesting effect B89 used an exclusion factor which can be interpreted as the Poisson probability that, in a volume typically harboring one peak on scale R, there is no such peak located

in the volume fraction independently subtended by collapsing clouds associated with larger scale peaks. This correction is easier to implement than equation (4.18). However, it is only well justified in the framework of the excursion set formalism (Bond et al. 1991) dealing with the filtering evolution of fixed points. On the contrary, the correction given by equation (4.18) is fully consistent with the confluent system formalism. Moreover, it takes into account that the mean density of peaks on scale R located in the collapsing clouds of larger scale peaks *is different from the global mean density*, at the base of the N-point correlations among peaks neglected in B89's approximate expression.

But to solve equation (4.18) we must previously determine the function $M(R)$ in the kernel giving the mass of collapsing clouds associated with peaks at scales between R and $R + dR$. In the spherical collapse model $M(R)$ is equal to $4\pi/3\,\rho\,R^3$, that is, the mass subtended by a top hat window of scale R. But we know that this simple model does not apply. In a similar manner as the Gaussian window is better suited than the top hat one (§ 4.2), the right function $M(R)$ to use can notably deviate from that expression. On the other hand, to obtain the mass function $N(M,t)\,dM$ from the scale function $N(R,\delta_c)\,dR$ solution of equation (4.18), we also need the relation $\delta_c(t)$ which, for identical reasons, can notably deviate from the usual expression for the spherical collapse.

4.4 Dynamical Constraints on the $M(R)$ AND $\delta_c(t)$ Relations

4.4.1 The Mass vs. Scale Relation

In what follows, we will only consider the case of an Einstein-de Sitter universe ($\Omega = 1$, $\Lambda = 0$). If the density field is endowed with a power-law power spectrum there is no privileged time nor scale. So the scale function of peaks

at a fixed density contrast must be self-similar. This means that if we define, at any epoch, a characteristic length R_c from some arbitrarily fixed value of any physically distinguishable (although not privileged) quantity such as the amplitude of density fluctuations, through, say, $\sigma_0(R_c) = \delta_c$, then any quantity reporting to that characteristic length must be invariant in time. One of such quantities is the number of peaks inside the volume R_c^3 with density contrast $\sigma_0(R_c)$ (equal to δ_c) on scales R/R_c in an infinitesimal range. The density function of peaks with δ_c on scales in units of R_c is equal to R_c times the function $N_{pk}(R, \delta_c)$ given by equation (4.9). Thus, by multiplying this density by R_c^3 and writting all spectral moments involved in terms of R, R_c, and n we are led to

$$\mu_{pk}(R, \delta_c) = \frac{(n+5)^2 (n+3)^{\frac{1}{2}}}{12\sqrt{6}\,(2\pi)^2} H\left[\frac{n+3}{n+5}\left(\frac{R}{R_c}\right)^{\frac{n+3}{2}}\right]\left(\frac{R}{R_c}\right)^{-4} \exp\left[-\frac{1}{2}\left(\frac{R}{R_c}\right)^{n+3}\right]. \tag{4.19}$$

As can be seen, the right-hand side of equation (4.19) depends on R and δ_c just through the ratio R/R_c. Hence, μ_{pk} is time-invariant. Likewise, the number of *non-nested* peaks, $\mu(R, \delta_c)\, d(R/R_c)$, inside the same comoving volume with density contrast $\sigma_0(R_c)$ (or δ_c) on scales R/R_c in an infinitesimal range must also be invariant. From equation (4.18) we have

$$\mu(R, \delta_c) = \mu_{pk}(R/R_c) - \frac{1}{\rho}\int_{R/R_c}^{\infty} d(R_b/R_c)\, M(R_b)\, \mu(R_b/R_c)\, R_c\, N_{pk}(R, \delta_c | R_b, \delta_c). \tag{4.20}$$

By writting all spectral moments involved in the integrant on the right-hand side of equation (4.20) in terms of R, R_b, R_c, and n, we obtain a function of R/R_c and R_b/R_c times an extra factor R^{-3} or, equivalently, an extra factor R_c^3. Thus, $\mu(R, \delta_c)$ in equation (4.20) will be invariant as required *provided only that the mass $M(R_b)$ is proportional to R_b^3*. Indeed, by multiplying and dividing this integrant by R_c^3 we obtain a function of just R/R_c and R_b/R_c and, by integrating it, a function of R/R_c as μ_{pk}. We therefore arrive to the conclusion that the dynamical consistency of the scale function solution of equation (4.18) implies

$$M(R) = \rho\,(2\pi)^{3/2}\,[q\,R]^3, \tag{4.21}$$

with q an arbitrary constant likely dependent on the spectral index n. The natural volume subtended by a Gaussian window of scale R is $(2\pi)^{3/2} R^3$.

So the meaning of q in equation (4.21) is simply the ratio between the true Gaussian length of the collapsing cloud associated with a peak and the filtering scale used to find it. (In principle, the invariance of $\mu(R, \delta_c)$ would also hold if q were a function of R/R_c. But this more general dependence of q is not allowed because M can only depend on R, not on δ_c.) A third invariant function which is then also guaranteed is the mass fraction in objects with masses, in units of $M_c \equiv M(R_c)$, in an infinitesimal range. This is, by the way, the only invariant function one has in the usual PS approach. But from equation (??) we see that the function $M(R)$ cancels out in the explicit expression of this invariant. This is the reason why one cannot use a similar reasoning as above to constrain the form of $M(R)$ in that approach.

Equation (4.21) is only valid in the scale-free case. Nonetheless, every power spectrum can be approximated by a set of different power-laws in specific finite ranges of the scale. Thus, under the reasonable assumption that the dynamics of the collapse for a fluctuation of any given scale only depends (statistically) on the distribution of density fluctuations on similar scales, the form of $M(R)$ for non-power spectra will approximately follow equation (4.21). Some departure from that simple law cannot be avoided, for example, in the case of the CDM spectrum if the values of the constant q for the two power laws giving the asymptotic regimes at large and small scales are distinct. However, provided that the values of q for different spectral indexes n are not too different from each other, equation (4.21) will be a good approximation for some effective fixed value of q dependent, in general, on the particular non-power-law spectrum used. Let us adopt, hereafter, this simplifying assumption and check its validity a posteriori.

There is still another constraint on the function $M(R)$. The nesting-corrected scale function must satisfy the normalization condition

$$1 = \int_0^\infty \frac{M(R)}{\rho} N(R, \delta_c)\, dR. \tag{4.22}$$

Equation (4.22) expresses the fact that the collapsing clouds associated with non-nested peaks yield the exact coverage of space. (Remember that this is equivalent to ask for any particle in the universe to be, at the time t, inside

some virialized object with the appropriate mass.) Condition (4.22) should be automatically satisfied for any power-law spectrum. Indeed, as discussed at the end of § 4.3, collapsing clouds associated with peaks prior to the correction for the nesting effect yield, in this case, a divergent coverage of space. Hence, after correction for the nesting effect one should end up with the exact coverage. As a consequence, we expect the scale function $N(R, \delta_c)$ to be correctly normalized for whatever value of q. However, for non-power-law spectra, the coverage of space by collapsing clouds associated with uncorrected peaks may not diverge (for example, in the case of the CDM spectrum). Then, for any given value of δ_c there should be a unique effective value of q yielding the correct normalization. But M cannot depend on δ_c. We are therefore led to the following conclusion: if the (effective) value of q yielding the correct normalization is the same for every δ_c there will be a unique physically consistent solution of equation (4.18), while not, there will be no acceptable solution. It is worthwhile noting that, since the mass function given by equation (1) is always correctly normalized, the form of $M(R)$ in the PS approach, is not constrained by condition (4.22), either.

In summary, the existence of some consistent scale function $N(R, \delta_c)$ is only guaranteed in the scale-free case. Constant q is then a free parameter. For non-power-law spectra it is hard to tell a priori whether or not there is some consistent solution. But if there is, the effective value of parameter q is automatically fixed.

4.4.2 Overdensity vs. Collapse Time Relation

The previous arguments only concerned the scale function of peaks with fixed density contrast δ_c at t_i. Let us now turn to the corresponding mass function of objects at t. For this mass function to be well-defined, that is, independent of the arbitrary initial time t_i chosen, δ_c must be proportional to $a(t_i)$. Indeed, on changing t_i the values of the spectral parameters γ, σ_1/σ_2, and σ_2/σ_0 do not vary, the only variable affected being ν_c or, more exactly, σ_0 which appears dividing δ_c in the scale function (4.9) as well as in the conditional density of

peaks in the kernel of equation (4.18). Since σ_0 changes as $a(t_i)$ δ_c must also vary as $a(t_i)$ in order to balance that change. Therefore, the most general form for the critical overdensity vs. collapse time relation is

$$\delta_c(t) = \delta_{c0}(t)\,\frac{a(t_i)}{a(t)}. \tag{4.23}$$

For the scale-free case, any change in t_i and t determining the same cosmic expansion factor $a(t)/a(t_i)$ should go unnoticed. (There is no absolute reference to assess the shift produced in the normalization of the power spectrum, that is, in the value of σ_0.) Therefore, δ_{c0} in equation (4.23) must be constant and equation (4.23) reduces to the usual expression for the spherical collapse model except for the fact that the value of δ_{c0} can be different from 1.69 and possibly depend on the power index n. For non-power-law spectra, there is no obvious constraint on $\delta_{c0}(t)$. The spherical collapse model suggests that it should not be far from constant, but some slight departure is probable, just as for q in the function $M(R)$ discussed above. However, for identical reasons, we will assume that δ_{c0} is approximately equal to some effective constant value dependent, in general, on the particular non-power-law spectrum used, and check a posteriori the validity of this approximation.

A last comment is in order concerning the constants δ_{c0} and q. In the PS approach and a power-law spectrum, there is a degeneracy in their values. One can take any of them fixed according to the spherical collapse model and adjust the value of the other one by, for instance, fitting the mass function of virialized objects obtained from N-body simulations. This is due to the fact that the mass fraction in virialized objects, the only time-invariant function we have in this case, depends on q and δ_{c0} only through the characteristic mass $M_c = M(R_c)$ (see, e.g., Lacey & Cole 1994). As a consequence, every combination of the two parameters leading to the same value of M_c yields the same mass fraction or, equivalently, the same family of mass functions for different times. In contrast, there is no such degeneracy in the peak model framework. The mass fraction in objects depends on q and δ_{c0} not only through M_c, but also through q separately. Indeed, the mass $M(R_b)$ appearing in the invariant number of non-nested peaks inside the volume R_c^3 (equation 4.20])

depends only on q and the situation does not improve when that number is multiplied by $M(R)/(\rho\, R_c^3)$ in order to obtain the mass fraction in objects. The fact that, in the peak model, a change in q cannot be balanced by any change in δ_{c0} is not surprising since the parameter q controls by itself the importance of the nesting effect. Indeed, the value of q determines the invariant fraction of non-nested peaks, equal to the ratio of equations (4.20) and (4.19).

4.5 The Mass Function of Objects

The resulting mass function of objects in an Einstein-de Sitter universe is

$$N(M,t)\,dM \;=\; N(R,\delta_c)\,\frac{dR}{dM}\,dM, \tag{4.24}$$

with $N(R,\delta_c)$ given by equation (4.18), $M(R)$ by equation (4.19) for some unknown constant q, and $\delta_c(t)$ by equation (25) for δ_{c0} another unknown constant. Of course, the existence of any consistent solution is not yet guaranteed (see the end of § 4.4.1). Moreover, for any solution to be dynamically acceptable it must be close, for any value of t, to the PS mass function with top hat window and $\delta_{c0} = 1.69$ because this gives good fits to the mass function inferred from N-body simulations. The situation is specially critical in the case of non-power-law spectra because the similarity between both mass functions for different values of t is not trivial (they are not self-similar), and there is just the free parameter δ_{c0} to be adjusted.

For a given power spectrum and some arbitrary fixed values of t and t_i, we have solved equation (20) as indicated at the end of § 4.3 by choosing the value of q that satisfies, for each different value of δ_{c0} tried, the normalization condition (4.22). In the case of power-law spectra we find that the normalization condition (4.22) is satisfied by any value of q and δ_{c0}, as expected. (Varying δ_{c0} is equivalent, for a fixed value of t_i, to vary δ_c.) In the case of the CDM spectrum, the correct normalization is only obtained for one specific value of q for each δ_{c0} tried, also as expected. What is most remarkable is that this value

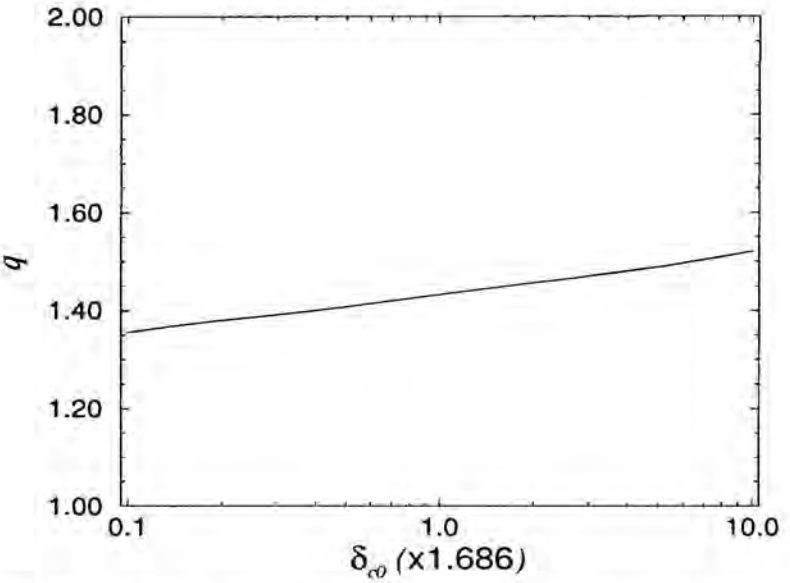

Figure 4.3: *Dependence on δ_{c0} of the parameter q for the CDM spectrum assuming the same mass vs. scale relation as found for power-law espectra.*

of q is quite insensitive to δ_{c0} just as needed for our simplifying assumption on the shape of $M(R)$ in that case to be acceptable. As shown in 4.3, q exhibits only a 10 % variation around the value 1.45 for values of δ_{c0} expanding along two decades.

It is worthwhile mentioning that the normalization condition (4.22) can be checked very accurately. Apart from numerical roundoff errors, there is a some uncertainty arising from the fact that to estimate the total mass integral we must extrapolate to $R = 0$ the scale function obtained down to some non-vanishing scale. In the case of power-law spectra, we cannot directly reach $R = 0$ because of the divergence there of the spectral moments. Yet, a log-log extrapolation gives an excellent approximation to the total mass integral which turns out to be correctly normalized up to an accuracy of 10^{-5}. In the case of the CDM spectrum, one cannot trust the scale function at small scales because of the poorly known shape of the power spectrum at very large k (all available analytic approximations are only valid up to some finite

wavenumber). Nonetheless, the total mass integral is essentially controlled, in this case, by the well-determined large-scale end of the scale function so that the result is also reliable. After trying with different analytic approximations for the CDM power spectrum, all with the expected k^{-3} asymptotical behavior, we can ascertain that the values of q satisfying the normalization condition for any given δ_{c0} are correct within 1 % of accuracy.

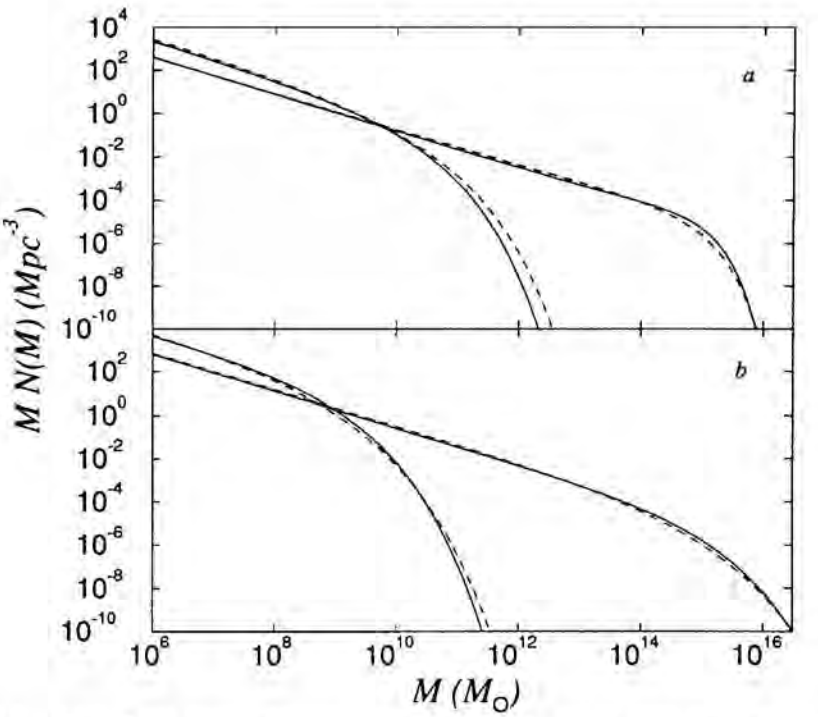

Figure 4.4: *The final mass functions specified in §4.5 (see text for the values of q and δ_{c0}) for the same spectra as in Fig. 2 (full lines) compared with PS original, correctly normalized, mass functions for top-hat filtering and $\delta_{c0} =$ 1.69 (dashed lines). In each panel we plot the solutions corresponding to two different epochs: the present time (curves reaching higher masses) and the time at which the cosmic scale factor was a tenth of its current value.*

In Figure 4.4 we plot, for the same power spectra as in Figure 2, the solutions obtained for the values of the parameters q (if free) and δ_{c0} which

give the best fit to the corresponding PS mass function. As can be seen, the similarity between both solutions in the CDM case for $\delta_{c0} \approx 6.4$ (and $q \approx 1.45$) is remarkable. This confirms that the relation $M(R)$ can be approximated, indeed, by equation (4.22). The similarity between both solutions also holds for any power-law spectrum tried. The solution plotted in Figure 4, corresponding to $n = -2$, is obtained for $\delta_{c0} \approx 8.4$ and $q \approx 1.45$. (Spectral indexes larger than -2 lead to values of q slightly smaller than 1.45. So the equality in the preceding two values of q is a mere coincidence.) Finally, Figure 4 also shows that these similarities hold for any value of t as required. Thus, the validity of our simplifying assumption that $\delta_{c0}(t)$ in equation (24) is approximately constant in the CDM case is also confirmed.

More accurate values for the constants q and δ_{c0} require the direct fitting of the mass function inferred from N-body simulations. In any event, there is little doubt on the marked departure of δ_{c0} from 1.69. This is not only caused by the departure from the spherical collapse, but mainly by the values of q found. These are large compared to the value of 0.64 yielding the same mass in objects for the Gaussian window as for the top hat one with identical scale R. But the collapse at the correct time of a large cloud requires (at least in the spherical collapse framework) a large value of the density contrast averaged just in the small central region. Hence, it is not surprising that large values of δ_{c0} are coupled to large values of q, while the values of both parameters cannot be reduced because there is no degeneracy in the confluence system formalism.

To conclude we want to stress that the present derivation of the mass function of objects relying just on the validity of the peak model ansatz has turned out to be an important test for this latter model. The fact that it has been possible to derive a fully consistent, well justified, and dynamically acceptable mass function gives strong support to the statistical validity of that simple model of structure formation provided, of course, the use of the appropriate window and $M(R)$ and $\delta_c(t)$ relations.

5

THE GROWTH HISTORY OF OBJECTS

5.1 Introduction

In the most studied scenario of structure formation via gravitational instability from a primordial random Gaussian field of density fluctuations, a first important step towards the construction of a clustering model was achieved by PS who derived a practical analytical estimate of the number density of objects of a given mass at any given epoch. This mass function was later on shown to agree with N-body simulations (see Manrique & Salvador-Solé 1995a, for references). But the mass function alone does not provide all the information required in many cosmological problems. The rates at which objects grow and the characteristic times of this process are also needed (e.g., Toth & Ostriker 1992; Richstone, Loeb, & Turner 1992; Kauffman, White & Guiderdoni 1993; Lacey & Cole 1993; González-Casado, Mamon, & Salvador-Solé 1994; Kauffman 1994; González-Casado et al. 1995). Richstone, Loeb, & Turner (1992) used the time evolution of the PS mass function to estimate the formation rate of objects of mass M at different epochs. However, this is not yet a very

accurate estimate since the time derivative of the mass function is equal to the rate at which objects reach mass M *minus the rate at which they leave this state*, both terms having comparable values.

Following the PS original prescription or a better sound version of it using the excursion set formalism, Bower (1991) and Bond et al. (1991), respectively, derived the mass function of objects of given mass at a given epoch subject to the condition of being part of another object with a larger mass at a later time. This conditional mass function was used by Lacey & Cole (1993; LCa; see also Kauffmann & White 1993) to infer self-consistent estimates of the instantaneous merger rate and the typical age and survival time of objects. Although this clustering model has been shown by Lacey & Cole 1994 (LCb) to agree with N-body simulations there is the formal caveat, as recognized by these authors, that the PS approach on which it is based is rather heuristic. In particular, the seeds of objects are rather fuzzy regions. (As a consequence, one cannot really count objects with a given mass but just calculate the probability that a given point is in a halo of that mass. This is at the base of a slight self-inconsistency in the analytical estimate of the formation time for power spectra with index $n > 0$; see LCa.) Furthermore, no natural distinction is made between merger and accretion. Indeed, the conditional mass function enables one to follow any instantaneous mass increase of objects, generically called "merger". Accretion does not play any role in this model. It is true that any merger with objects of mass below some *arbitrary* resolution can be interpreted as an accretion process. But this only enters in the graphical representation of the evolution of objects; an infinite resolution is used in all explicit calculations.

Although the interpretation that accretion is nothing but the merger of a massive object with a very tiny one is correct from the viewpoint of the tiny object, destroyed in the event, it is not from that of the massive one. Indeed, this does not account for the fact, characteristic of accretion as compared to a true merger, that the massive object *survives*, that is can be identified to the bound virialized object resulting from the capture of the tiny one. It can be argued that the fact that one given event can be regarded either as

accretion or as a true merger depending only on the particular object whose evolution is being followed reveals that the distinction between these two kinds of events is a mere convention. Yet, the possibility to achieve this convention *in a natural manner* is crucial for the idea itself of the "growth history of objects". This presumes, indeed, that the *mass increase* of a bound virialized object can be followed since its *formation* until its *destruction*. In other words, there must be some natural difference between "small" captures contributing to the (quasi-)continuous mass increase of objects, the so-called accretion, and "large" captures, called mergers, destroying and giving them rise. Since such a natural distinction is not made in the LCa model, it is not surprising that the formation, destruction and mass accretion rates, and the age and survival time of objects are strictly meaningless in this modeling. There is, instead, only one rather ambiguous "merger" rate, while these latter characteristic times are artificially and somewhat arbitrarily defined. For example, the formation time of an object of mass M at t is defined as the cosmic time at which some ancestror reaches for the first time a mass equal to $M/2$. Why half the mass and not any other fraction of it? (Note that for a fraction smaller than $1/2$, the adopted definition would not even guarantee that such a "main parent" keeps on being so at any later epoch.) What is more important, is the mass increase by a factor two of the "main parent" object quasi-continuous and peaceful or, on the contrary, is it rather concentrated on one single event at some particular moment?

Here we propose an alternate clustering model, based on the peak model ansatz, intended to avoid the main drawbaks of the previous model. In paper I, we presented the so-called confluent system formalism, able to follow the filtering evolution of peaks (see also Salvador-Solé & Manrique 1994). This formalism was applied to derive a mass function of objects fully justified within the peak model framework, which approximately recovers the PS mass function for appropriate values of two free parameters governing the dynamics of collapse. (A deeper insight into this model is also given in Salvador-Solé & Manrique (1995).) In the present paper, we apply this formalism to calculate the above mentioned rates and times characterizing the growth history of objects. The new clustering model is similar to that developed by LCa in the

sense that these quantities are derived from the statistics of the random density field at a fixed, arbitrary, epoch after recombination when fluctuations are still linear (and the growing factor only depends on time at all interesting scales) and Gaussian distributed, and the dynamics of collapse are approximated by the extrapolation of the linear theory (for the growing mode) according to the spherical model. However, the new model is physically better motivated since the assumed seeds of object are peaks instead of the fuzzy regions considered in the PS approach, and the natural distinction is made between merger and accretion. In § 5.2 we remind the basic lines of the confluent system formalism. In § 5.3 we derive the instantaneous formation, destruction, and mass accretion rates of objects. Their typical ages and survival times are calculated in § 5.4. Conclusions are drawn in § 5.5.

The notation used in this paper is the same as in paper I. Since many calculations are based on results obtained by Bardeen et al. (1986; BBKS) we have kept as close as possible to the notation introduced by these authors. The main difference comes from the fact that we deal with three different kinds of densities, while BBKS only dealt with one. Especial caution must be made in not mixing them up. Firstly, there are the normal and conditional density functions of peaks *at a fixed filtering scale* R per infinitesimal ranges of ν, i.e., the density contrast δ scaled to the rms value $\sigma_0(R)$, and other possible variables. These were already defined in BBKS and are denoted by a caligraphic capital n just as in that paper. A minor difference with the notation used in BBKS is that we specify the fixed value of the filtering scale R as one parameter. For example, we write $\mathcal{N}(\nu, R)\, d\nu$ instead of $\mathcal{N}(\nu)\, d\nu$. Second, there are the normal and conditional density functions of peaks *at a fixed density contrast* δ per infinitesimal ranges of the filtering scale R and other possible variables. These density functions, already introduced in paper I, are denoted by a roman capital n with the fixed value of δ as one parameter. We write, for example, $N(R, \delta)\, dR$. Finally, and this is a novelty, there are also density functions per infinitesimal ranges of both R and δ (or the corresponding mass M and time t, respectively) and any other extra variable. These are denoted by a capital n in boldface, for example, $\mathbf{N}(R, \delta)\, dR\, d\delta$. These different symbols, $\mathcal{N}$, N, and $\mathbf{N}$, are usually accompanyed by one superindex specifying

the characteristic property (if any) of the peaks involved and the subindex pk or no subindex at all depending on whether all peaks with that characteristic property are included or just those of them tracing bound virialized objects (see § 2), respectively. Hereafter, all quantities are comoving.

5.2 The Confluent System: Basic Results

According to the peak model ansatz, there is a correspondence between peaks of fixed linear overdensity in the filtered density field at some arbitrary initial epoch t_i and objects at the time t. The overdensity δ_c is assumed to be a decreasing function of the collapse time t and the filtering scale R, at least in the strict version of the model assumed here, an increasing function of the mass M of the resulting objects. This leads to the natural identification and distinction between each other of accretion and merger events *in the filtering process*. A peak on scale $R+\Delta R$, with ΔR positive and arbitrarily small, is the result of the evolution by accretion of a peak on scale R provided only that the volume (mass) subtended by the former is embedded within that subtended by the latter. (Strictly, we should talk about volumes subtended by "collapsing clouds associated to peaks", i.e., the regions surrounding each peak which enclose a total mass equal to that of the corresponding final object at t, rather than volumes subtended by "peaks". Likewise, we will say "nested peaks" instead of "peaks with nested associated collapsing clouds".) Whenever the identification between couples of peaks on contiguous scales is not possible, that is, whenever there is a discrete jump in scale between two consecutive embedded peaks, we are in the presence of a merger. It is important to mention that the filtering of the density field must be carried out with a Gaussian window for the density contrast δ of peaks to diminish with increasing filtering scale R as required by consistency with the growth in time of the mass of objects. Hereafter we assume this particular window.

When an object evolves by accretion its associated evolving peak traces a continuous and derivable trajectory $\delta(R)$ in the δ vs. R diagram. (We are as-

suming a continuous and infinitely derivable density field.) In contrast, when an object merges the evolving peak tracing it becomes nested on a larger scale peak with identical δ, which yields a discrete horizontal jump in scale of the associated peak trajectory in the δ vs. R diagram. Therefore, to compute the density of objects at t in an infinitesimal range of masses dM we must calculate the density of *non-nested* peaks with fixed value of δ appropriate to t on scales in the infinitesimal range dR corresponding to dM. This density, $N(R,\delta)\,dR$, can be obtained from the density of peaks satisfying identical constraints although disregarding whether they are nested or not, $N_{pk}(R,\delta)\,dR$, and the density of these same peaks subject to the condition of being located in a background with the same density contrast δ on a different filtering scale R', $N_{pk}(R,\delta|R',\delta')\,dR$. Indeed, these three quantities are related through (see eq. [A13])

$$N(R,\delta) = N_{pk}(R,\delta) - \int_R^\infty dR' \,\frac{M(R')}{\rho}\, N(R',\delta)\, N_{pk}(R,\delta|R',\delta). \qquad (5.1)$$

This is a Volterra type integral equation of the second kind for the unknown function $N(R,\delta)$ from the known ones $N_{pk}(R,\delta)$ and $N_{pk}(R,\delta|R',\delta)$, respectively equal to $\mathcal{N}_{pk}(\nu,R) < x > \sigma_2\, R/\sigma_0$ and $\mathcal{N}_{pk}(\nu,R|\nu',R') < \widetilde{x} > \sigma_2\, R/\sigma_0$ in terms of the normal and conditional density functions of peaks at a fixed scale R per infinitesimal range of $\nu = \delta/\sigma_0$, calculated in § 3.2, σ_i are the i-th order spectral moments, which only depend on R, and $< x >$ and $< \widetilde{x} >$ are some averages of $x \equiv -(\sigma_2\, R)^{-1}\partial_R\delta$, which depend on R and δ as well as on R' and δ' in the latter case, defined in § 4.3. The mass function of objects at t is then simply given by

$$N(M,t) = N(R,\delta_c)\left(\frac{dM}{dR}\right)^{-1}, \qquad (5.2)$$

with the dependence on R and t on the right hand side respectively given by the same function $M(R)$ appearing in the kernel of equation (5.1) and the relation $\delta_c(t) = \delta$ between the density contrast at t_i and the collapse time t. As shown in paper I, very general consistency arguments allows one to determine the shape of these two relations as

$$M(R) = (2\pi)^{3/2}\,\rho\,(q\,R)^3, \qquad (5.3)$$

with q a constant equal to ~ 1.45 for both the CDM and the $n = -2$ power-law spectra (in the power law case, the larger n, the smaller q), and the relation

$$\delta_c(t) = \delta_{c0} \frac{a(t_i)}{a(t)} = \delta_{c0} \left(\frac{t_i}{t} \right)^{2/3} \tag{5.4}$$

with a the cosmic scale factor and δ_{c0} a constant equal to ~ 6.4 and 8.4 for the CDM and the $n = -2$ power-law power spectra. Strictly, equations (5.3) and (5.4) are only valid for the scale-free case, i.e., a power-law spectrum and an Einstein-de Sitter universe ($\Omega = 1$, $\Lambda = 0$). However, as shown in Chapter 4 they are also good effective relations for other power spectra such as the CDM one. Furthermore, following the same strategy as in LCa, it should be possible to extend the applicability of the model to the cases $\Omega \neq 1$ and/or $\Lambda \neq 0$. The values of parameters q and δ_{c0} quoted above correspond to those giving acceptable fits to the original PS mass function (i.e., for top hat window and a critical threshold equal to 1.686) for the same cosmogonies. This tends to priviledge the small mass end while the model will finally be applied rather to massive objects. Thus, finer values of these parameters should be inferred by directly fitting N-body simulations in the relevant cosmological scales.

In the present paper we are concerned with the density of objects forming or being destroyed in a given interval of time. Given the characterization of accretion and merger in the confluent system formalism, it is clear that the density of objects merging and, hence, being destroyed in a given interval of time is simply equal to the density of non-nested peaks which *become nested* along the corresponding decrement in δ. But to calculate the density of forming objects we must first characterize those mergers which contribute with *the appearance* of new objects. As just mentioned, when an object merges the non-nested peak tracing its evolution in the δ vs. R diagram experiences a discrete jump in the scale. This does not mean, of course, that every non-nested peak partaking of the same event necessarily experiences this kind of jump in the scale. The largest scale peak will the most often just keep on evolving in a continuous manner. This reflects the well-known fact in gravitational clustering that a merger from the viewpoint of one given object can be a simple accretion from the viewpoint of the most massive partner. It will sometimes happen, however, that the scale of the largest scale peak also experiences a

discrete jump. Then, it will not be possible to identify the final non-nested peak with any of its ancestrors. This appearance of a new non-nested peak therefore traces the formation of a new bound object. Therefore, to calculate the density of forming objects in a given interval of time we must compute the density of non-nested peaks which appear, in the previous sense, along the corresponding decrement of δ.

Before entering in these calculations a last remark is in order. The continuous trajectory attached to an accreting non-nested peak can be suddenly truncated (i.e., it is impossible to identify the peak at the current δ with any peak on the infinitesimally contiguous scale) without becoming nested. In the peak model framework, this kind of filtering event can only be interpreted as tracing the split of a bound virialized object in small pieces. Since this is unrealistic from the gravitational viewpoint, this kind of filtering events clearly invalidate the use of the confluent system formalism to follow the clustering process of *individual* objects. However, our aim here is not to follow the clustering of individual objects but just to own a good *statistical* description of the general clustering process. And what we only need for this to be possible is the *net* density of appearing non-nested peaks (once the density of disappearing ones has been substracted), which reflects the density of forming objects, be positive. On the other hand, peaks not only become progressively nested into each other but they can sporadically leave their hosts, which is, once again, unrealistic in terms of virialized objects. Hence, we also need the *net* density of peaks becoming nested (once the density of peaks leaving their hosts has been substracted), which reflects the density of merging objects, be positive. As shown below, these two conditions are only fulfilled for massive objects. But this shortcoming is rather formal since the validity of the model in any of its forseeable applications seems to be, in any event, guaranteed.

The reason why this model can only apply to massive enough objects is clear: for any given δ_c, the larger the scale, the higher the peak amplitude as compared to the typical density fluctuation given by $\sigma_0(R)$, and the closer is the dynamics of collapse to the spherical approximation at the base of the peak model ansatz. Indeed, the higher the peak, the more spherical its shape

and the more negligible the shear caused by the surrounding matter. Both the CDM and power-law power spectra used here to illustrate the general behavior of the model lead to hierarchical clustering (in the bottom-up fashion). In other words, their rms density contrast, σ_0, decreases with increasing scale. This implies that, on decreasing δ_c as the time goes by, the fraction of peaks with scale larger than any arbitrary fixed value tends to increase. Therefore, the nesting of smaller scale peaks tends to increase which explains that the two net densities above are usually positive. Note that, according to this argument, the steeper the power spectrum the less restrictive should the minimum mass of validity of the model be, in agreement with what is found. (This would explain the observed trend of the limiting mass with t, or δ_c, in the case of the CDM spectrum, since the characteristic wavenumber of objects collapsing at earlier times corresponds to a steeper regime of the power spectrum.) Conversely, would the power spectrum not lead to hierarchical clustering, the two net densities above would hardly be positive even for very massive objects. However, structure formation in the top-down fashion requires the action of physical processes other than just gravitational instability. So this kind of clustering is anyway outside the scope of the present model.

5.3 Growing Rates

As explained in the preceding section, objects merging (and being destroyed) in the interval dt are traced by peaks becoming nested within larger scale peaks in the corresponding range $-d\delta$. The net density of peaks with δ on scales between R and $R+dR$ becoming nested in non-nested peaks with $\delta-d\delta$ on scales between R' and $R'+dR'$, $\mathbf{N}^d(R \to R', \delta)\, dR\, dR'\, d\delta$, is calculated in Appendix B. By dividing it by $N(R,\delta)\, dR$ we obtain the conditional probability that a non-nested peak with δ on scales between R and $R+dR$ becomes nested into a non-nested peak with $\delta - d\delta$ on scales between R' and $R'+dR'$. And from this conditional probability we can readily infer the instantaneous true merger or destruction rate at t for objects of mass M per specific infinitesimal range

of mass M' ($M < M'$) of the resulting objects,

$$r^d(M \to M', t) = \frac{\mathrm{N}^d(R \to R', \delta_c)}{N(R, \delta_c)} \left(\frac{dM'}{dR'}\right)^{-1} \left|\frac{d\delta_c}{dt}\right|, \tag{5.5}$$

with R, R', and δ_c on the right hand side written in terms of M, M', and t, respectively, through equations (5.3) and (5.3).

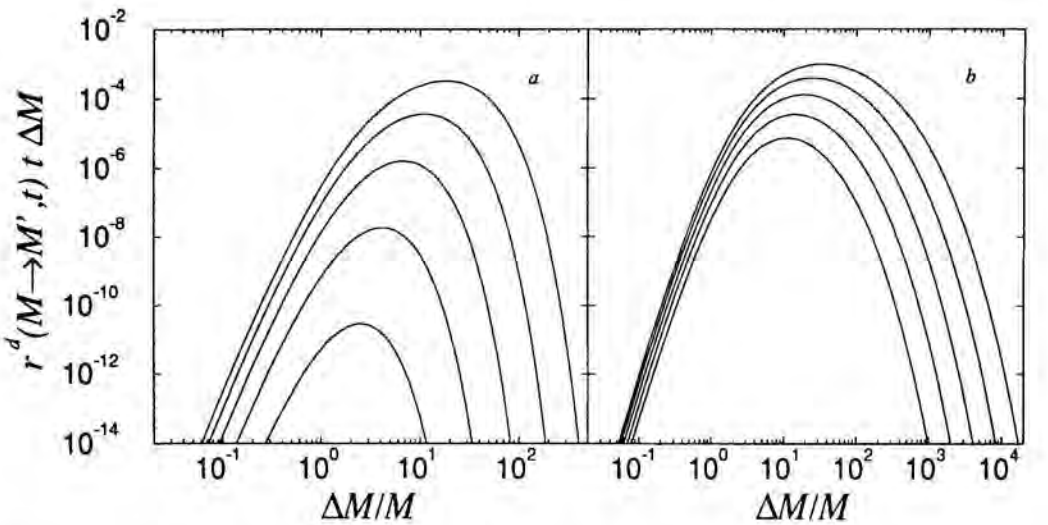

Figure 5.1: *Instantaneous destruction (or true merger) rate at the present time for an object with mass $M/M_\odot$ equal to* 0.5 10^{14} *(the lowest curve),* 10^{14}, 2 10^{14}, 4 10^{14}, *and* 8 10^{14} *(the highest curve) as a function of the mass ΔM of the merger partner for the CDM (a) and $n = -2$ power-law (b) power spectra, both normalized to $\sigma(8\,h^{-1}\,Mpc) = 0.67$ in an Einstein-de Sitter universe with $h = 0.5$.*

This true merger or destruction rate is plotted in Figure 5.1 for different masses of the initial object M and a fixed t equal to the present time. As the mass M diminishes, a small dip develops at intermediate values of the mass of the final object M' (or the mass of the merger partner $\Delta M \equiv M' - M$), which becomes more and more marked, finally reaching negative values. This therefore establishes a lower bound in M for the possible validity of

the present estimate of the merger rate. This minimum mass increases with increasing t not only in the power-law cases owing to the self-similar character of such cosmogogonies, but also in the CDM case. The latter behavior is also well understood since the smaller t, the steeper the CDM power spectrum at wavenumbers relevant for objects having previously collapsed. At the present epoch, the minimum mass is, in fact, quite small; we find $\sim 2.5\,10^9$ and $\sim 2.5\,10^8\ M_\odot$ for the CDM and $n = -2$ power law spectra, respectively) but still comparable to the mass of dwarf galaxies. And at a moderate redshift of just 1.25 it already becomes as small as $\sim 1.8\ 10^6$ and $\sim 1.1\ 10^6$, respectively, which encompasses all relevant cosmological scales. It is worthwhile mentioning that the previous results correspond to the approximate values of q and δ_{c0} quoted above. So they might appreciably change when using finer values drawn from the direct fit of N-body simulations.

These minimum masses only guarantee the self-consistency of the model for more massive objects; they do not guarantee its goodness. In fact, the true merger rate given by equation (5.5) shows a very different behavior than that obtained by LCa. As shown in Figure 5.1, the former vanishes at small ΔM while LCa's diverges (see their Fig. 1). But this does not mean that the merger rate derived here is wrong. Actually, a merger rate with a divergent behavior for vanishing partner masses as that found by LCa is not fully satisfactory because when one massive object captures a very tiny one it remains essentially unaltered during the process (in particular, the virial equilibrium is always approximately satisfied) which allows one to identify it as the same bound object before and after the capture. Hence, this capture corresponds, from the viewpoint of that massive object, to an accretion rather than a true merger in which the initial object is destroyed and a new object emerges. Consequently, the *true merger or destruction rate* should vanish for small partner masses, just as obtained from the confluent system formalism. The reason why LCa's merger rate diverges at small partner masses is simply that, as mentioned, what these authors call "merger" is any mass increase of the object whether or not this causes its destruction. It therefore includes not only true mergers but also accretion. Now, the density of tiny objects capable of being accreted by any given object diverges at the small mass end. Hence, it is well understood

that such a merger rate diverges at small partner masses in contrast with what is expected for a true merger rate. It could be argued that the correct behavior of LCa's merger rate is confirmed by N-body simulations. However, what is actually compared with simulations in LCb is not the merger rate, but the conditional probability that given an object of fixed mass at some initial epoch it is incorporated within a larger mass object at a later time. And this conditional probability does not distinguish, of course, between merger and accretion.

From the confluent system formalism making the natural distinction between accretion and merger we can also calculate the transition rate *including any kind of capture*, true mergers and accretion. Equation (5.5) gives the rate at which objects of mass M merge and are destroyed giving rise to objects of mass M'. But from the viewpoint of such resulting objects the process can be seen either as accretion if they can be identified with the initial (most massive) object partaking of each event or true merger if they cannot. Thus, the instantaneous accretion+merger, or simply capture, rate for final objects of mass M' per specific infinitesimal range of the captured mass M ($M < M'$) is

$$r^c(M' \leftarrow M, t) = \frac{r^d(M \rightarrow M', t)\, N(M, t)}{N(M', t)}, \tag{5.6}$$

with r^d given by equation (5.5). This composite rate is plotted (for masses within the validity range of the model) in Figure 5.2. As expected, it shows the same divergent behavior at small captured masses as the LCa rate. Note that these two composite rates are strictly not comparable since the merger+accretion or capture rate given by equation (5.6) refers to the fixed mass M' of the final object, while LCa's refers to the mass of the initial object. (In particular, our rate is only defined for M/M' smaller than one, while there is no such restriction in the corresponding values of $\Delta M/M$ of the LCa rate. This causes the steeper behavior of our rate as compared to LCa's.) However, that difference tends to vanish at small partner or captured masses since the masses of the initial and final object tend to be equal there. Therefore, the divergent shape of both curves in this mass regime really reflects the similar behavior of the two models when both merger and accretion events are included without distinction.

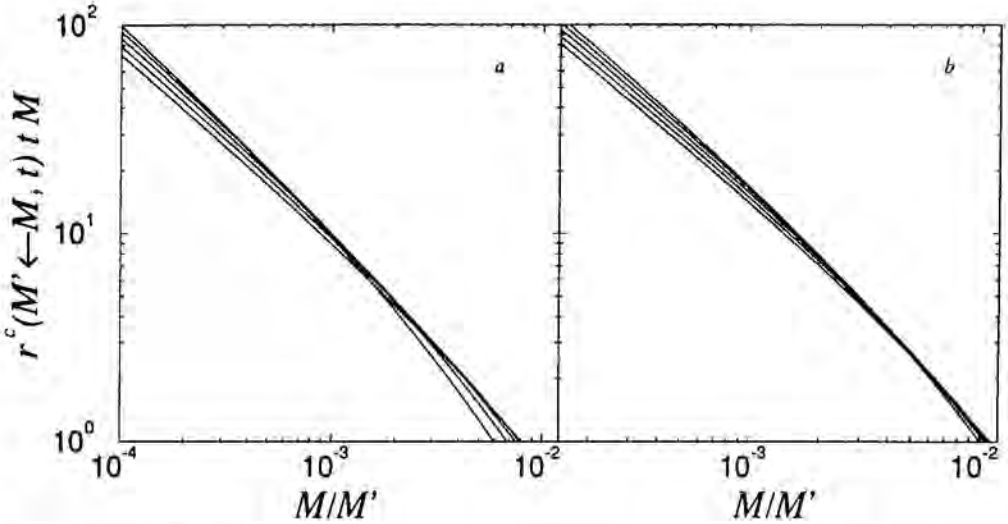

Figure 5.2: *Instantaneous capture (or accretion+merger) rate at the present time for a final object with mass* $M'/M_\odot$ *equal to* $0.5\ 10^{14}$ *(the highest curve on the left),* 10^{14}, $2\ 10^{14}$, $4\ 10^{14}$, *and* $8\ 10^{14}$ *(the lowest curve on the left) as a function of the mass* M *of the captured objects for the same cosmogonies (a) and (b) as in Fig. 4.1.*

The previous destruction and capture rates are per specific infinitesimal range of mass of the final or collected objects, respectively. To derive the respective *global* rates we must simply integrate equation (5.5) over the mass M' of the final objects,

$$r^d(M,t) = \int_M^\infty r^d(M \to M', t)\, dM', \tag{5.7}$$

and equation (5.6) over the mass M of the collected objects

$$r^c(M',t) = \int_0^{M'} r^c(M' \leftarrow M, t)\, dM. \tag{5.8}$$

Note that these global rates are obviously positive down to much smaller masses M or M' than their respective specific ones.

Let us now turn to the formation rate. Objects forming in the interval of time dt from the merger (from any viewpoint) of similarly massive objects are traced by peaks appearing in the corresponding range of density contrasts $-d\delta$ without being nested within larger scale peaks. The net density of non-nested peaks appearing between δ and $\delta - d\delta$, $\mathbf{N}^f(R,\delta)\,dR\,d\delta$, is calculated in Appendix C. By dividing it by $N(R,\delta)\,dR$ we are led to the conditional probability that a non-nested peak with scale R appears between δ and $\delta - d\delta$. Therefore, the instantaneous formation rate at t of objects of mass M is

$$r^f(M,t) = \frac{\mathbf{N}^f(R,\delta_c)}{N(R,\delta_c)}\left|\frac{d\delta_c}{dt}\right|, \tag{5.9}$$

with R and δ_c on the right hand side written in terms of M and t, respectively, through equations (5.3) and (5.4). This formation rate is plotted in Figure 5.3.

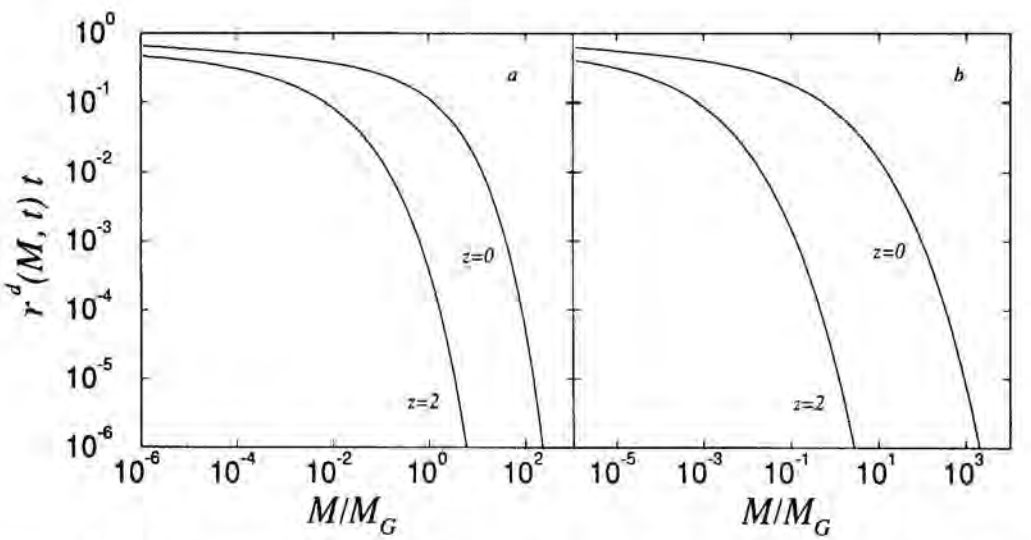

Figure 5.3: *Instantaneous formation rate at two different epochs as a function of the mass M in units of $M_G = 10^{12}\,M_\odot$ of objects for the same cosmogonies (a) and (b) as in Fig. 4.1.*

Finally, by multiplying equation (5.5) by $\Delta M = M' - M$ we obtain the specific rate at which the mass M of objects is increased at the time t ow-

ing to (true) mergers and, by integrating this latter function over M', the instantaneous typical mass increase rate owing to mergers for objects of mass M

$$r^d_{mass}(M,t) = \int_M^\infty \Delta M\, r^d(M \to M', t)\, dM'. \tag{5.10}$$

Likewise, from equation (5.6) we can obtain the instantaneous typical mass increase rate for objects of final mass M' owing to accretion and merger,

$$r^c_{mass}(M',t) = \int_0^{M'} M\, r^c(M' \leftarrow M, t)\, dM. \tag{5.11}$$

As shown in Appendix D, the idea of a *transition* rate, by accretion, similar to those given by equations (5.5) or (5.6) is meaningless because accretion is a continuous instead of a discrete process of mass increase. In contrast, the *mass increase* rate by accretion does make sense. The instantaneous mass accretion rate for objects of mass M follows from the instantaneous scale increase rate of the corresponding peaks as they evolve along continuous and derivable trajectories in the δ vs. R diagram. This latter rate depends on the particular value of the scaled Laplacian x of the peak which is being followed. However, since we are interested in the *typical* mass accretion rate for objects of mass M disregarding any other property we must average over x. This is done in Appendix D. The result we are led is

$$r^a_{mass}(M,t) = \frac{1}{< x > \sigma_2 R} \left(\frac{dR}{dM}\right)^{-1} \left|\frac{d\delta_c}{dt}\right|, \tag{5.12}$$

with R and δ_c on the right hand side written in terms of M and t, respectively, through equations (5.3) and (5.4) and $< x >$ the average mentioned in the discussion following equation (5.1).

It is important to outline that, in contrast to the transition rates (5.5) to (5.9), defined in the usual manner, i.e., normalized to the number density of objects in the state of reference, the mass increase rates (5.10) to (5.12) have not been normalized to the reference mass.

5.4 Growth Characteristic Times

From the meaning of the global merger rate, equation (5.7), we have that the density $N_{sur}(t)\,dM$ of objects surviving (i.e., having not merged but just accreted) until the time t from a typical population with masses in the range between M_0 and $M_0 + dM$ at $t_0 < t$ is given by the solution of the differential equation

$$\frac{dN_{sur}}{dt} = -r^d[M(t), t]\, N_{sur}(t), \tag{5.13}$$

with initial condition $N_{sur}(t_0) = N(M_0, t_0)$. In equation (5.13) and hereafter, the function $M(t)$ is the typical mass at t of such accreting objects, given by the solution of the differential equation

$$\frac{dM}{dt} = r^a_{mass}[M(t), t], \tag{5.14}$$

with initial condition $M(t_0) = M_0$. Indeed, from equation (5.12) we have that the typical mass of objects evolving by continuous accretion increases with time according to equation (5.14). The solution of equation (5.13) is

$$N_{sur}(t) = N(M_0, t_0) \exp\left\{ - \int_{t_0}^{t} r^d[M(t'), t']\, dt' \right\}. \tag{5.15}$$

Hence, by defining the typical survival time $t_{sur}(M_0, t_0)$ of objects with masses between M_0 and $M_0 + dM$ at t_0 as the interval of time since t_0 after which their initial density is reduced (owing to mergers) by a factor e, we are led to the equality $t_{sur} = t_d - t_0$, with the destruction time $t_d(M_0, t_0)$ given by the solution of the implicit equation

$$1 = \int_{t_0}^{t_d(M_0, t_0)} r^d[M(t'), t']\, dt'. \tag{5.16}$$

In addition, the typical mass accreted by those objects until they merge and disappear is $M[t_d(M_0, t_0)] - M_0$. (Note that what LCa called survival time would rather correspond to what here is called destruction time.)

In a fully similar manner, we can infer the typical age of objects with masses in the range between M_0 and $M_0 + dM$ at t_0, that is, the typical interval of

time since the last merger giving them rise. The density $N_{pre}(t)\,dM$ of these objects pre-existing (i.e., having just accreted matter since then) at a time $t < t_0$ is given by the solution of the differential equation

$$\frac{dN_{pre}}{dt} = r^f[M(t),t]\,N[M(t),t] - r^d[M(t),t]\,N_{pre}(t) \tag{5.17}$$

with initial condition $N_{pre}(t_0) = N(M_0,t_0)$. The solution of equation () is

$$\begin{aligned} N_{pre}(t) &= N(M_0,t_0)\,\mathrm{e}^{\int_t^{t_0} r^d[M(t'),t']\,dt'} \\ &\times \left\{1 - \int_t^{t_0} dt'\,\frac{N[M(t'),t']}{N(M_0,t_0)}\,r^f[M(t'),t']\,\mathrm{e}^{-\int_{t'}^{t_0} r^d[M(t''),t'']\,dt''}\right\} \end{aligned} \tag{5.18}$$

Thus, by defining the typical age $t_{age}(M_0,t_0)$ of objects with masses between M_0 and M_0+dM at t_0 as the interval of time until t_0 before which their density (owing to their progressive formation) was a factor e smaller, we are led to the equality $t_{age} = t_0 - t_f$, with the formation time $t_f(M_0,t_0)$ given by the solution of the implicit equation

$$\begin{aligned} 1 &= \mathrm{e}^{-1-\int_{t_f(M_0,t_0)}^{t_0} r^d[M(t'),t']\,dt'} \\ &+ \int_{t_f(M_0,t_0)}^{t_0} dt'\,\frac{N[M(t'),t']}{N(M_0,t_0)}\,r^f[M(t'),t']\,\mathrm{e}^{-\int_{t'}^{t_0} r^d[M(t''),t'']\,dt''}. \end{aligned} \tag{5.19}$$

And the typical mass accreted by these objects since they formed is $M_0 - M[t_f(M_0,t_0)]$.

These typical ages and survival times are plotted in Figures 5.4 and 5.5, respectively. As can be seen, the larger the mass of the object, the smaller the typical age. This reflects the well-known fact that in hierarchical clustering larger mass objects form later on. The same trend was found by LCa. A more surprising result because showing the opposite trend from LCa's is that the larger the mass of the object, the larger its survival time. In fact, our estimates of the typical ages and survival times are not comparable to those of LCa. The natural definitions of the typical age and survival time considered here, i.e., the time spent until the next true merger when the object will be destroyed and the time spent since the previous true merger when the object was formed, respectively, are meaningless in the approach followed by those authors because

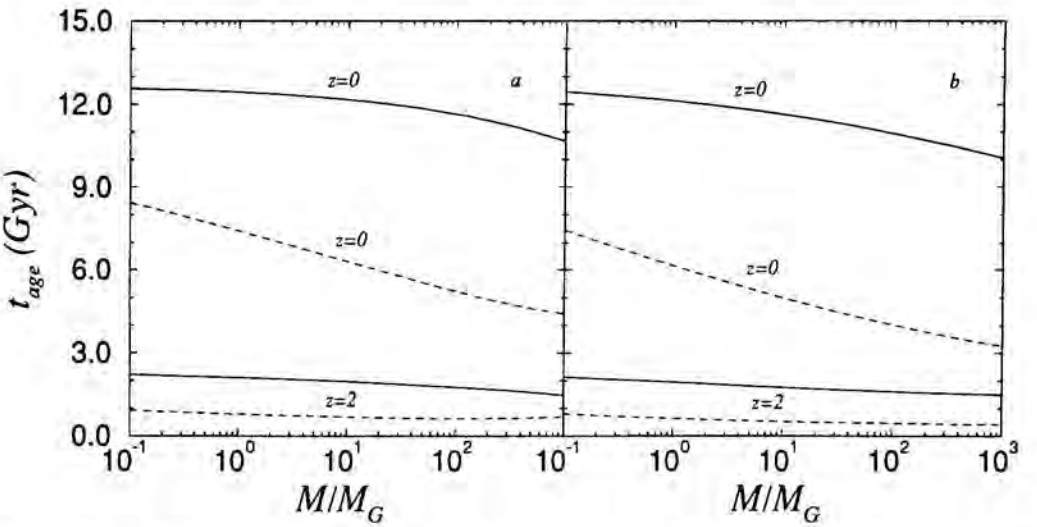

Figure 5.4: *Typical age (full lines) and accretion-age (dashed lines) of objects of mass M in units of $M_G = 10^{12}\,M_\odot$ for the quoted values of the redshift corresponding to the same cosmogonies (a) and (b) as in the preceding figures.*

it does not distinguish between merger and accretion. What LCa adopted as the typical age and survival time (or formation and destruction times) are two quantities which also report on the past and future history of objects but which have a very distinct meaning: the interval of time spent since the mass of some parent object was half the current value for the object and the interval of time required by the object to double its current mass, respectively. The theoretical expressions derived by LCa were checked, in LCb, to correctly estimate the same quantities as inferred from N-body simulations, but this does not mean, of course, that they really reflect the times suggested by their names.

In Figures 5.4 and 5.5 we plot, for comparison, a new version of the age and survival times of objects of given mass at a given time. These new times, which can be called accretion-age and accretion-survival-time, have been derived from our model and are, in some sense, complementary to the previous ones. They are defined as the interval of time spent since the mass of an ob-

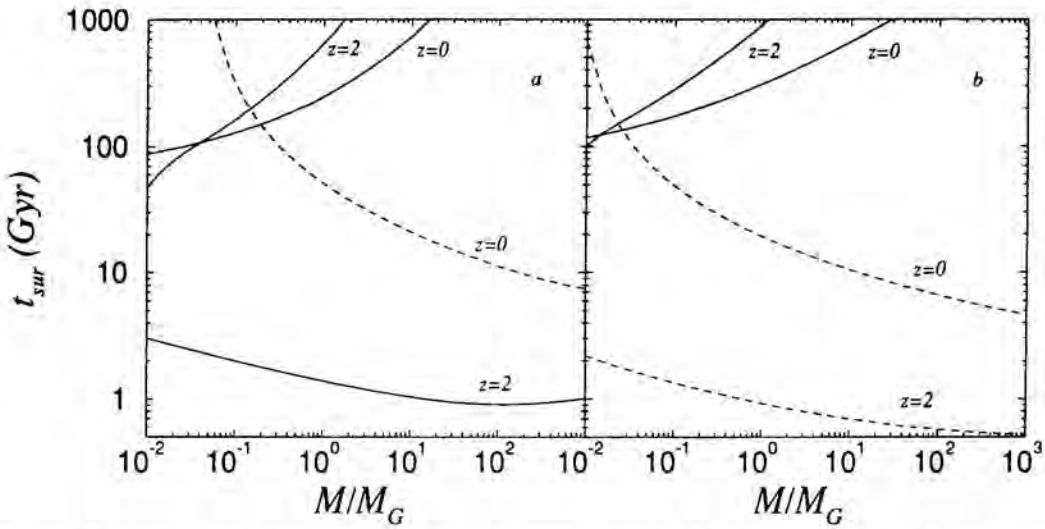

Figure 5.5: **Typical survival time (full lines) and accretion-age (dashed lines) of objects of mass M in units of $M_G = 10^{12}\,M_\odot$ for the quoted values of the redshift corresponding to the same cosmogonies (a) and (b) as in the preceding figures.**

ject was half its current mass and the interval of time required by an object to double its current mass, respectively, and since they refer to the mass evolution of *a given object* they only include accretion. They are therefore readily obtained from the function $M(t)$ solution of equation (5.14). Notice that as far as the new times are smaller than the respective previous ones the mass increase of objects of that mass will be really dominated by accretion. Therefore, these new accretion-times should essentially coincide, in this regime, with those calculated by LCa. As can be seen from Figures 4 and 5, they show, indeed, the same trend as LCa's estimates. In particular, they both decrease with increasing mass of the object. From the behavior shown by these two complementary time estimates we arrive to the interesting conclusion that the clustering of small mass objects is dominated by mergers while that of very massive ones, once they have formed, is dominated by accretion.

Finally, from the typical age and surviving time of objects with masses between M_0 and $M_0 + dM$ at t_0 calculated above, we can readily calculate their typical lifetime (or intermerger period). This is simply

$$t_{life}(M_0, t_0) = t_{age}(M_0, t_0) + t_{sur}(M_0, t_0) = t_m(M_0, t_0) - t_f(M_0, t_0). \quad (5.20)$$

And connected with this latter quantity, there is the total mass typically accreted by those objects during their whole life, given by $M[t_m(M_0, t_0)] - M[t_f(M_0, t_0)]$.

5.5 Summary and Conclusions

A fundamental result of Chapter 4 was that the confluent system formalism fixes the filtering window and the $M(R)$ and $\delta_c(t)$ relations that are consistent with the peak model ansatz and allows one to account for the cloud-in-cloud effect so that a mass function can be obtained which is in overall agreement with N-body simulations. In the present paper we have calculated the rates and characteristic times of growth of bound objects. As far as we can tell from the comparison achieved between our model and that constructed by LCa, the two models seem to yield a similarly good description of clustering provided no distinction is needed between merger and accretion. The interest of our model precisely relies on the fact that it can make that practical distinction which enables one to calculate several important quantities connected with the growth history of objects which are not available from the LCa model. The statistic which puts the most severe limitation to the applicability of our model (i.e., which establishes the largest minimum mass of validity at a given epoch) is the merger rate per specific mass of the final object. But the model can still apply to smaller masses if we resign ourselves to less detailed information. For example, there is, in principle, no restriction at whatever redshift if one uses the confluent system formalism just to infer the mass function of objects. A thourough comparison between our model and N-body simulations as that carried out in LCb with their own model is however needed in order to draw more definite quantitative conclusions on its general as well as detailed validity.

The idea that our clustering model relying just on the peak formalism provides a good description of hierachical clustering is at variance with the rather extended opinion that peaks are not good seeds of bound objects. Detailed N-body simulations of the gravitational evolution of individual density maxima show, indeed, that if their initial amplitude is small they can be easily disrupted before collapsing (van de Weygaert & Babul 1993). While Katz, Quinn, & Gelb (1993) have found that even high amplitude peaks seem to be poor tracers of bound objects, and this individually as well as statistically. The reason why this would be so is that peaks are not spherical in general, nor are they isolated. So their non-linear evolution will markedly deviate from the spherical approximation at the base of the peak model ansatz. However, there is the counterargument that the higher the peak relative to the typical density fluctuation on that scale, the more spherical it is and the less important is the shear caused by the surrounding density fluctuations, particularly if the power spectrum is steep enough to guarantee that large mass fluctuations have much less typical amplitude. In fact, this idea has been recently confirmed by Bernardeau (1994) who has rigurously shown that the evolution of high amplitude peaks (with $\nu \geq 2$) in a Gaussian random density field is correctly described by the spherical model provided only the logarithmic slope of the power spectrum is smaller than $n = -1$. On the other hand, the conclusion drawn from the above mentioned N-body simulations dealing with peak statistics is somewhat precipitated because of the unknown effects of the use of unappropriate $M(R)$ and $\delta_c(t)$ relations, and the lack of any correction for the cloud-in-cloud effect. Thus, we should not be surprise, after all, that for realistic (relatively steep, at the relevant scales) power spectra and massive enough objects (high enough initial peaks for any fixed t) the peak model with adequate filtering window, $M(R)$ and $\delta_c(t)$ relations, and after correction for the nesting effect can provide a good description of the clustering process.

6

CONCLUSIONS AND FUTURE PROSPECTS

In this work we have discussed the foundations of a new formalism for the construction of a detailed model of hierarchical clustering via gravitational instability from an initial random Gaussian field of density fluctuations. Similarly to other formalisms the new one also deals with clustering through the filtering process of the density field at an arbitrary fixed early epoch, but it focus its attention on maxima instead of normal points. The conexion between peaks and collapsed objects is made through the peak model ansatz, a prescription inspired in the spherical collapse, which states that objects at a time t emerge from peaks with a fixed linear overdensity δ_c in the smoothed, on any scale R, density field at the arbitrary initial time t_i. The critical overdensity would be a monotonous decreasing function of t, and the mass M of collapsing clouds associated with peaks a monotonous increasing function of R.

The peak model ansatz is, in principle, a suitable framework for the construction of a good clustering model. The true dynamics of collapse are well approximated by the spherical model for high amplitude peaks or, equivalently, massive objects (in hierarchical models, the rms. density fluctuation decreases

with increasing R), and the main effects of such simple dynamics are *implicitly accounted for* by that ansatz. So the question is whether or not there is enough room left by the only freedom we have, namely the shape of the filter and the monotonous functions $M(R)$ and $\delta_c(t)$, for the filtering process to be able to statistically reproduce the gravitational clustering, i.e., the rate at which mergers and accretion proceed according to those unknown dynamics, and, if so, whether the problem is well constrained.

The identification of peaks on slightly different scales proposed in § 4.2.1 allows us to draw the trajectory $\delta(R)$ followed by the evolving peack attached to any individual accreting object in the filtering process. The form of the total derivative of peak trajectories, which coincides with $\partial_R\delta$, and very general properties of the Fourier transformation lead to the important conclusion that *only the Gaussian window is able to recover*, in any realistic density field, *such a fundamental property of gravitational clustering as the systematic growth, by accretion, of the mass of objects.* We have not yet required accretion to proceed at the correct rate, that is, accreting peaks to follow tracks in the δ vs. R diagram statistically consistent with the real collapse dynamics. In principle, the two functions $M(R)$ and $\delta_c(t)$ can be adjusted in order to satisfy this constraint. But can we separately recover the rate at which mergers proceed?

Mergers are in both gravitational and filtering clustering the natural consequence of the mass increase of accreting objects or peaks and the fact that the total available mass is fixed. Objects and peaks accrete at the expence of smaller mass objects which merge into them and new objects form or new peaks appear (they cannot be identified with any preceding peak) whose mass or volume subtends that previously subtended by objects or peaks with similar masses or scales. Therefore, mergers and accretion are not to be separately reproduced by the filtering process. The fine tuning between these two competing events will be automatically satisfied provided we have the correct spatial coverage by peaks (properly corrected from nesting) or, more exactly, their associated collapsing clouds at any δ_c.

To derive the mass function of objects at any given t in the peak model framework we should follow the peak trajectories tracing the mass evolution of bound objects in the δ vs. R diagram, calculate the density of such trajectories upcrossing the corresponding overdensity in the infinitesimal range of scales, $N_{pk}(R, \delta_c)\, dR$, correct it for cloud-in-cloud configurations, and transform the result to the mass function of objects at that time, $N(M, t)\, dM$, through the appropriate $M(R)$ and $\delta_c(t)$ relations. These two functions therefore determine the shape of the mass function at every time or, equivalently, the rates at which filtering accretion and mergers proceed according to the true collapse dynamics (the fine tuning among these two competing events being guaranteed by the correct normalization of the mass function). So the question finally reduces to whether there is enough room to fit the correct mass function and whether this constraint is enough to fix the functions $M(R)$ and $\delta_c(t)$. By imposing some consistency arguments in an Einstein-de Sitter universe ($\Omega = 1$, $\Lambda = 0$) and a density field endowed with a power-law power spectrum we can restrict the form of these two functions. Since, in this scenario, the gravitational clustering proceeds in a self-similar way, then the relations $M(R)$ and $\delta_c(t)$ adopt the forms given by equations (5.3) and (5.4) respectively, which are exact for the scale-free case and approximate for other cosmogonies. The resulting mass function gives good fits to the PS one at any epoch for $\delta_{c0} \approx 6.4$ and 8.4 and $q \approx 1.45$ and 1.45 in the CDM and the $n = -2$ power-law cases. (It can be shown that there is no degeneracy in the values of these parameters.)

The natural prolongation of the model includes the calculation of quantities related to the growth of objects, in particular typical rates and characteristic times. With the aid of the confluent system formalism, we have derived the net density of non-nested peaks becoming nested, the net density of non-nested appearing peaks (both in an element of the δ–R diagram), and the mass accretion rate. The first density leads to the instantaneous merger rate of objects of mass M per infinitesimal range of mass M' of the resulting object, which is used to obtain the capture (accretion plus merger) rate for final objects of mass M' per infinitesimal range of the captured mass M, and, by integrating over M' and M, the respective global rates, whereas the second density allows one to deduce the instantaneous formation rate of objects of mass M. The

variation in the number density of survival objects (owing to mergers) and pre-existing objects (due to mergers and formations) has been implemented as a criterion to set the destruction and formation times respectively, both referred to a specific epoch. The survival time for an object of a given mass corresponds to the interval elapsed until it is destroyed, and the typical age to the interval elapsed since it was formed. The difference between the destruction and formation times gives the intermerger period, or the object lifetime.

We have compared our specific merger rate, the survival time and the typical age with the analog quantities derived in the excursion set formalism framework (LCa) and checked by means of N-body simulations (LCb) by Lacey & Cole. The agreement is good as long as we are not concerned with the distinction between merger and accretion. However, the confluent system formalism is able to do such a distinction, allowing the derivation of relevant quantities connected with the gravitational clustering which are not avalaible from the LCa model.

To summarize, the peak model ansatz with monotonous relations $M(R)$ and $\delta_c(t)$ is appropriate to describe the gravitational clustering of objects through the filtering of the initial density field. A fully consistent description of gravitational clustering can be obtained, indeed, leaving one or two free parameters, depending on the particular cosmogony assumed, which can be used to fit the real mass function whatever its exact shape. As long as the true unknown dynamics of collapse are not be far from the spherical model, at least when dealing with massive objects, it is not surprising that a good fit can be obtained at any epoch for appropriate values of the free parameters. Moreover, both mergers and accretion can be simultaneously followed which is crucial for the obtention of an accurate clustering model as far as the own definition of bound objects involves the distinction between those two kinds of events.

The model, which has already yielded three papers in refereed journals (Manrique, & Salvador-Sole 1995a, Salvador-Solé, & Manrique 1995, and Manrique, & Salvador-Sole 1995b), has a wide range of applicability. Its extension to other cosmogonies, apart from the Einstein-de Sitter univers, will allow to

study the role played by the cosmological parameters in gravitational clustering and, by comparing with observations, constrain their values. We intend to perform the same calculations for two low density models, one filled with baryonic matter and $\Omega_0 = 0.2$, and the other with CDM and a cosmological constant such that $\Omega_0 + \Omega_\Lambda = 1$.

In a medium term we plan to apply the model to several fields on which our group has been deeply concerned:

- Morphological se gregation.
  It is well known that galaxies of different morphological types dwell in different environments. This observational fact suggests that the galaxy shapes can change due to interactions with the environment (Solanes, Salvador-Solé, & Sanromà 1989; Salvador-Solé, Sanromà, & Jordana 1989; Sanromà, & Salvador-Solé 1990; Solanes, & Salvador-Solé 1992). However, the evolutive interpretation is currently challenged by an alternate explanation which claims that the shape does not change but it is determined by the environment before galaxy formation. This would be the case if earlier type galaxies arise from higher peaks of the linear density field. We think of using our model to find the population fraction and galaxy luminosity function inside and outside virialized structures at different redshifts. The thresholds for the morphological types could be obtained by assuming that galaxies with a lifetime shorter than the characteristic formation time of a disk ($\sim$ 2 Gyr) are ellipticals, and spirals or S0's otherwise.

- Modeling galaxy clusters.
  Present models of galaxy clusters account for some generic properties of these systems at the present time (Solanes, & Salvador-Solé 1990), any evolutionary model being still very rough. A complete theoretical description of galaxy clusters, including features of the galaxy population (the total number of galaxies above some limiting magnitude, the galaxy luminosity function, and the population fraction) at different epochs, can be achieved with the aid of our model.

- Detection and characterization of substructure.
  Clusters of galaxies often show substructure. Provided the knowledge of its dynamical survival time, the observed frequency and characteristics of the detected clumpiness informs us on the rate of clusters mergers and accretion of groups onto clusters (Salvador-Solé, Sanromà, & González-Casado 1993; Salvador-Solé, González-Casado, & Solanes 1993; González-Casado, Solanes, & Salvador-Solé 1993; Gonzalez-Casado, Mamon, & Salvador-Solé 1994; Gonzalez-Casado, Serna, Alimi, & Salvador-Solé 1995). It is clear that our gravitational clustering model can make the link between such observations and the correct cosmogonical scenario.

7

REFERENCES

Adler, R.J. 1981. The Geometry of Random Fields. (New York: John Wiley)

Alcock, C. et al. 1993, Nature, 365, 621

Appel, L., & Jones, B.J.T. 1990, MNRAS, 245, 522 (AJ)

Aubourg, E. et al. 1993, Nature, 365, 623

Bahcall, N.A., & Cen, R. 1993, ApJ, 407, L49

Bardeen, J.M., Bond, J.R., Kaiser, N., & Szalay, A.S. 1986, ApJ, 304, 15 (BBKS)

Bernardeau, F 1994, ApJ, 427, 51

Bertschinger, E., & Dekel, A. 1989, ApJ, 336, L5

Bond, J.R. 1988, in Large-Scale Motions in the Universe, eds. Rubin, V.C., & Coyne, G.V. (New Jersey: Princeton Series), p. 419

Bond, J.R. 1989, in Frontiers in Physics. From Colliders to Cosmology, eds. Astbury, A., Campbell, B.A., Israel, W., & Khanna, F.C. (Singapore: World Scientific), p. 182

Bond, J.R., Cole, S., Efstathiou, G., Kaiser, N. 1991, ApJ, 379, 440 (BCEK)

Bond, J.R., & Myers, S.T. 1993a, CITA, preprint 93/27

Bond, J.R., & Myers, S.T. 1993b, CITA, preprint 93/28

Bower, R.J., 1991, MNRAS, 248, 332

Carlberg, R.G., & Couchman, H.M.P. 1989, ApJ, 340, 47

Colafrancesco, S., Lucchin, F., & Matarrese, S. 1989, ApJ, 345, 3

Coles, P. 1989, MNRAS, 238, 319

Couchman, H.M.P. 1987, MNRAS, 225, 795

Dekel, A., Bertschinger, E., & Faber, S. 1990, 364, 349

Dekel et al. 1993, ApJ, 412, 1

Dekel, A. 1994, Ann. Rev. Astron. Astropys. 32, 371

Doroshkevich, A.G. 1970, ApJ, 6, 581

Doroshkevich, A.G., & Shandarin, S.F. 1978, MNRAS, 182, 27

Efstathiou, G., Frenk, C.S., White, S.D.M., & Davis, M. 1988, MNRAS, 235, 715

Efstathiou, G., & Rees, M.J. 1988, MNRAS, 230, 5p

Fort, B., & Mellier, Y. 1995, Ann. Rev. Astron. Astropys.

González-Casado, G., Solanes, J.M., & Salvador-Solé, E. 1993, 410, 15

González-Casado, G., Mamon, G., & Salvador-Solé, E. 1994, ApJ, 433, L61

González-Casado, G., Serna, A., Alimi, J.-M., & Salvador-Solé, E. 1995, ApJ, submitted

Heavens, A.F., & Peacock, J.A. 1988, MNRAS, 232, 339

Jedamzik, K. 1994, ApJ, in press

Katz, N., Quinn, T., & Gelb, J.M. 1993, MNRAS 265, 689

Kauffmann, G. 1994, MNRAS, in press

Kauffmann, G., & White, S.D.M., 1993, MNRAS, 261, 921

Kauffmann, G., & White, S.D.M., & Guiderdoni, B. 1993, MNRAS, 264, 201

Kaiser, N. 1984, ApJ, 284, L9

Katz, N., Quinn, T., & Gelb, J.M. 1993, MNRAS 265, 689

Kneib, J.-P., et al. 1995 A&A, in press

Lacey, C., & Cole, S. 1993, MNRAS, 262, 627

Lacey, C., & Cole, S. 1994, MNRAS, 271, 676

Manrique, A., & Salvador-Solé, E. 1995a, ApJ, in press

Manrique, A., & Salvador-Solé, E. 1995b, ApJ, submitted

Mellot A.B., Pellman, T.F., & Shandarin 1994, MNRAS, to appear in the 10 June issue

Monaco, P. 1994, ApJ, submitted

Nolthenius, R., & White, S.D.M. 1987, MNRAS, 225, 505

Peacock, J.A., & Heavens, A.F. 1985, MNRAS, 217, 805

Peacock, J.A., & Heavens, A.F. 1990, MNRAS, 243, 133

Misner, C.W., Thorne, K.S., & Wheeler, J.A. 1973, Gravitation (San Francisco: W.H. Freeman and Company)

Peebles, P.J.E. 1993, Principles of Physical Cosmology (Princeton: Princeton University Press)

Peebles, P.J.E. 1980, Principles of Physical Cosmology (Princeton: Princeton University Press)

Press, W.H., & Schechter, P. 1974, ApJ, 187, 425

Richstone, D., Loeb, A., & Turner E. 1992, ApJ, 393, 477

Salvador-Solé, E., Sanromà, M., & Jordana, J.J.R. 1989, ApJ, 337, 636

Salvador-Solé, E., Sanromà, M., & González-Casado 1993, 402, 398

Salvador-Solé, E., González-Casado, G., & Solanes, J.M. 1993, 410, 1

Salvador-Solé, E., & Manrique, A. 1994, in Clusters of Galaxies, eds. F. Durret, A. Mazure, & J. Tran Thanh Van (Gif-sur-Yvette: Frontières), p. 297

Salvador-Solé, E., & Manrique, A. 1995, ApLC, submitted

Sanromà, M., & Salvador-Solé, E. 1990, ApJ, 360, 16

Solanes, J.M., Salvador-Solé, E., & Sanromà, M. 1989, AJ, 98, 798

Solanes, J.M., & Salvador-Solé, E. 1990, Ap&SS, 171, 9

Solanes, J.M., & Salvador-Solé, E. 1992, ApJ, 395, 61

Toth, G., Ostriker, J.P. 1992, ApJ, 389, 5

Udalski, A. *et al.*1993, Acta Astron, 43, 289

van de Weygaert, R., & Babul, A. 1993, Cita preprint, CITA 93/47

White, S.D.M., Efstathiou, G., & Frenk, C.S. 1993, MNRAS, 265, 727

Weinberg, S. 1972, Gravitation and Cosmology (New York: John Wiley and Sons).

Zel'dovich Ya.B., & Novikov, I.D. 1983, The Structure and Evolution of the Univers (Chicago: The University of Chicago Press).

Zel'dovich Ya.B. 1970, A&A, 5, 20

A

Nesting Probabilities

Collapsing clouds associated to non-nested peaks with fixed δ yield a partition of space which makes the mass function of objects at t be correctly normalized (see Chapter 4). This implies that the volume fraction occupied by disjoint backgrounds with δ on filtering scales between R' and $R' + dR'$ or, equivalently, the probability to find a point in any such backgrounds is $M(R')\,\rho^{-1}\,N(R',\delta)\,dR'$. Therefore,

$$P(R',\delta|R,\delta)\,dR' = \frac{M(R')}{\rho}\,N(R',\delta)\,dR'\,\frac{N_{pk}(R,\delta|R',\delta)}{N_{pk}(R,\delta)}. \qquad \text{(A.1)}$$

gives the probability that a typical peak with δ on scale R is nested within some non-nested peak with identical density contrast but on a scale between R' and $R' + dR'$ ($R < R'$), hereafter simply called the (differential) nesting probability of a peak. This was used, in Chapter 4, to derive equation (4.18). Likewise, the nesting probability of peaks with given values of variables δ, x, and any set of variables v_i ($i = 2, ..., n$ with arbitrary n) is

$$P(R',\delta|R,\delta,x,v_2,...v_n)\,dR' = \frac{M(R')}{\rho}\,N(R',\delta)\,dR'\,\frac{N_{pk}(R,x,v_2,...,v_n,\delta|R',\delta)}{N_{pk}(R,x,v_2,...,v_n,\delta)}, \qquad \text{(A.2)}$$

with $N_{pk}(R,x,v_2,...,v_n\delta|R',\delta)$ the conditional density function analogous to $N_{pk}(R,\delta|R',\delta)$ in equation (A.1) but per infinitesimal ranges of the extra vari-

ables $x, v_2, v_3, ..., v_n$. The last factor on the right-hand member of equation (A.2) satisfies the relation (see § 3.2.3)

$$\frac{N_{pk}(R, x, ..., v_n, \delta | R', \delta)}{N_{pk}(R, x, ..., v_n, \delta)} = \frac{\mathcal{P}(\nu', R' | \nu, x, ...v_n, R)\, \mathcal{N}_{pk}(\nu, x, ...v_n, R) x\sigma_2 R/\sigma_0}{\mathcal{P}(\nu', R')\, \mathcal{N}_{pk}(\nu, x, ...v_n, R) x\sigma_2 R/\sigma_0}$$
$$= \frac{\mathcal{P}(\nu', R' | \nu, x, ..., v_n, R)}{\mathcal{P}(\nu', R')}, \qquad (A.3)$$

with $\nu' \equiv \delta/\sigma_0'$, $\mathcal{P}(\nu', R'|\nu, x, v_2, ..., v_n, R)\, d\nu'$ defined in equation (3.63), and $\mathcal{P}(\nu, R)\, d\nu$ the Gaussian probability to find the scaled density contrast on scale R between ν and $\nu + d\nu$. Notice that, for identical reasons as for the conditional probability in equation (3.65), the conditional probability given in equation (A.2) applies, in fact, to points. Note also that we are using the same convention for the notation of the conditional probabilities as for the density functions: they are denoted by a caligraphic capital p (in contrast with the notation used in Chapter 2) when they are per infinitesimal range of ν at a fixed R, and by a roman capital p when they are per infinitesimal range of R at a fixed δ. Finally, it is worthwhile mentiong that, contrary to what is suggested by the present notation, we can write ν or δ, indistinctly, when specifying the condition.

From equation (3.65), it is clear that the nesting probability given by equations (A.2) and (A.3) will depend on variables v_i provided only that these variables have non-null correlations with ν (or δ) and x on scale R or any explicit variable correlating with them. This is what happens with the variables v_i defined in equation (3.67) involving the different order scale derivatives of the density contrast. Thus, to accurately infer the density of nested peaks in any given peak population one must calculate the distribution of these *infinite* variables in that population. The only noticeable exception concerns the *typical population* of peaks. The density of typical peaks at δ with values of v_i $(i = 1, ..., n)$ in infinitesimal ranges, $N_{pk}(R, x, v_2, ...v_n, \delta)\, dR\, dx\, dv_2 ...dv_n$, times the nesting probability $P(R', \delta | R, \delta, x, v_2, ...v_n)\, dR'$ integrated over any subset of variables v_i coincides with the product of these two functions without the explicit dependence on the integrated variables, as readily seen from equation (A.2) valid for any arbitrary values of the subindexes. In particular, the integral over all v_i for $i \geq 1$ is equal to the product of $N_{pk}(R, \delta)\, dR$ times the

reduced nesting probability $P(R', \delta | R, \delta)\, dR'$ given in equation (A.1), which justifies this latter expression and equation (4.18).

The conditional probability $\mathcal{P}(\nu', R' | \nu, x, v_2, v_3, ..., R)\, d\nu'$ extended to the infinite set of variables v_i defined in equation (3.67) can be obtained according to equation (3.65). After some lenghty algebra using intermediate variables which only correlate with themselves (found by means of the Gramm-Schmidt method) we arrive to the expression

$$\mathcal{P}(\nu', R' | \nu, x, v_2, v_3, ..., R)\, d\nu' = \frac{1}{\sqrt{2\pi}\,\sigma_{\nu'}} \exp\left[-\frac{(\nu' - \bar{\nu})^2}{2\,\sigma_{\nu'}^2}\right] d\nu' \qquad \text{(A.4)}$$

with

$$\bar{\nu} = \alpha_0 \nu + \alpha_1 x + \alpha_2 v_2 + ...,$$

$$\begin{aligned} \alpha_i &= \sum_{j=0}^{\infty} B_j\, \beta_{i\,j-i} \sum_{k=0}^{j} \beta_{k\,j-k}\, \langle v_0'\, v_k \rangle \\ \sigma_{\nu'}^2 &= 1 - \sum_{j=0}^{\infty} B_j \left[\sum_{k=0}^{j} \beta_{k\,j-k}\, \langle v_0'\, v_k \rangle \right]^2 \end{aligned} \qquad \text{(A.5)}$$

($i \geq 0$), where a prime denotes the scale R', the correlations in angular brackets are given by equation (3.68), and coeffecients B_j and $\beta_{k\,j-k}$ are defined as

$$(B_j)^{-1} = 1 + \sum_{k=0}^{j-1} \beta_{k\,j-k} \left(\beta_{k\,j-k} + 2 \sum_{l=0}^{j-1-k} \beta_{j-l\,l}\, \langle v_k\, v_{j-l} \rangle \right)$$

$$\beta_{i\,j-i} = -\sum_{k=0}^{j-1} C_{i\,j-i}^{k}\, \langle v_j\, v_k \rangle, \qquad \text{(A.6)}$$

($j \geq 1$ and $i \neq j$) in addition to $B_0 = 1$ and $\beta_{i0} = 1$. In equations (A.6) we have used the notation

$$C_{i1}^{k} \equiv B_i\, \beta_{k\,i-k} \qquad\qquad C_{i\,j-i}^{k} \equiv \sum_{l=k}^{j-1} B_l\, \beta_{k\,l-k}\, \beta_{i\,l-i} \qquad \text{(A.7)}$$

for $i \leq k$ and $C_{i\,j-i}^{k} \equiv C_{k\,j-k}^{i}$ for $i > k$.

From the general expressions of $\bar{w}$ and σ_w^2, equation (3.65), it can be shown, through the intermediate use of variables $\bar{\nu}^{(n)}$ defined as $\bar{\nu}$ but for just the first arbitrary $n+1$ variables v_i, that

$$\langle \bar{\nu}\, v_i \rangle = \langle \nu'\, v_i \rangle \equiv (-1)^{i+1+\delta_{0i}} \frac{\sigma_{ih}^2}{\sigma_0'\, \sigma_{2i}}, \tag{A.8}$$

$(i \geq 0)$ which implies, on its turn, a similar relation for any (finite or infinite) linear combination of v_i, in particular,

$$\langle \bar{\nu}^2 \rangle = \langle \nu'\, \bar{\nu} \rangle = 1 - \sigma_{\nu'}^2. \tag{A.9}$$

On the other hand, taking into account that the correlation between two variables is equal to the integral of the product of their Fourier transforms taken at $\mathbf{r} = \mathbf{0}$ and defining the new variable $\bar{x}$ as $-(\sigma_2\, R)^{-1}\, \partial_R(\sigma_0'\, \bar{\nu})$ we have

$$\langle \bar{x}\, v_i \rangle = \frac{\sigma_0'}{\sigma_2} \left(\frac{\sigma_{2i+1}^2}{\sigma_{2i}^2} - \frac{1}{R}\, \partial_R \right) \langle \bar{\nu}\, v_i \rangle + (-1)^{\delta_{i0}}\, \frac{\sigma_0'\, \sigma_{2(i+1)}}{\sigma_2\, \sigma_{2i}}\, \langle \bar{\nu}\, v_{i+1} \rangle \tag{A.10}$$

$(i \geq 0)$ and

$$\langle \bar{x}\, \bar{\nu} \rangle = -\frac{\sigma_0'}{\sigma_2}\, \frac{1}{2\, R}\, \partial_R \langle \bar{\nu}^2 \rangle. \tag{A.11}$$

By substituting the correlations in equation (A.8) into equation (A.10) we obtain

$$\langle \bar{x}\, v_i \rangle = 0 \tag{A.12}$$

$(i \geq 0)$ which also implies

$$\langle \bar{x}\, \bar{\nu} \rangle = 0 \qquad\qquad \langle \bar{x}^2 \rangle = 0. \tag{A.13}$$

Thus, $\langle \bar{\nu}^2 \rangle$ and $\sigma_{\nu'}$ do not depend on R (see equations [A.9] and [A.11]) which ultimately implies that $\sigma_{\nu'}$ is null and $\langle \bar{\nu}^2 \rangle$ equal to unity. Indeed, according to its definition, equation (A.5), $\sigma_{\nu'}$ is null for $R' = R$ and since it does not depend on R it is necessarily null for any value of R'. Then, equation (A.4) leads to

$$\mathcal{P}(\nu', R' | \nu, x, v_2, v_3, ..., R)\, d\nu' = \delta(\nu' - \bar{\nu})\, d\nu'. \tag{A.14}$$

This result is not surprising since fixing the values of the density contrast and every order scale derivative of it on a given scale R automatically fixes, through

the Taylor series expansion of δ as a function of the filtering scale, the value of the density contrast in any other scale R'. Finally, by substituting $\mathcal{P}$ given by equation (A.10) into equation (A.3) and the latter into (A.2) we arrive to the following expression for the nesting probability

$$P(R', \delta | R, \delta, x, v_2, ...)\, dR' \equiv P(R', \delta|\bar{\nu})\, dR' = \frac{M(R')}{\rho} N(R', \delta)\, dR' \frac{\delta(\nu' - \bar{\nu})}{\mathcal{P}(\nu')}, \tag{A.15}$$

with $\nu' = \delta/\sigma_0'$.

B

Net Density of Peaks Becoming Nested

The density of peaks at $\delta_f \equiv \delta - \Delta\delta$, with $\Delta\delta$ positive and arbitrarily small, on scales between R_f and $R_f + dR_f$ and variables $x_f, v_{2f}, v_{3f}, ...$ in infinitesimal ranges, which result by continuous evolution from peaks at δ on scales between R and $R + dR$ and $x, v_2, v_3, ...$ in infinitesimal ranges is

$$N_{pk}^{evu}(R_f, x_f, v_{2f}, ..., \delta_f)\, dR_f\, dx_f\, dv_{2f} ... = N_{pk}(R, x, v_2, ..., \delta)\, dR\, dx\, dv_2 ..., \tag{B.1}$$

with

$$R_f \approx R + \frac{\Delta\delta}{x\,\sigma_2\,R} \tag{B.2}$$

$$\begin{aligned} x_f &\approx x + \left(v_2\,\frac{\sigma_4}{\sigma_2} + x\,\frac{\sigma_3^2}{\sigma_2^2}\right)\frac{\Delta\delta}{x\,\sigma_2} + \left(\sum_i \frac{\partial_R \eta_i}{\lambda_i}\,\partial_i x\right)\frac{\Delta\delta}{x\,\sigma_2\,R} \\ v_{2f} &\approx v_2 + \left[v_3\,\frac{\sigma_6}{\sigma_4} + v_2\left(\frac{\sigma_5^2}{\sigma_4^2} - \frac{1}{R^2}\right)\right]\frac{\Delta\delta}{x\,\sigma_2} + \left(\sum_i \frac{\partial_R \eta_i}{\lambda_i}\,\partial_i v_2\right)\frac{\Delta\delta}{x\,\sigma_2\,R} \end{aligned} \tag{B.3}$$

...

to first order in $\Delta\delta$. Equation (B.1) states that the density $N_{pk}(R, x, v_2, v_3, ..., \delta)$ $dR\,dx\,dv_2\,dv_3$... of peaks is conserved through continuous evolution from δ to δ_f. There likely is a small amount of peaks which disappear in that infinitesimal range of δ but, as shown in Appendix A.1, these are not counted in N_{pk}. Equations (B.2) and (B.4) give the shift from δ to δ_f in the values of all the relevant variables. It is important to outline that we need to know, indeed, the values of all variables R and v_i ($i \geq 1$) at δ_f in order to calculate the density of evolved peaks which are nested since, as explained in Appendix A, the nesting probability depends explicitly on all these variables differently distributed in N_{pk}^{ev} than in N_{pk} at δ_f. Equation (B.2) arises from the derivative $dR/d\delta$ along continuous peak trajectories, equal to $-(x\,\sigma_2\,R)^{-1}$ (see § 4.2.1). While the shift in the variables v_i, equations (B.4), is equal to the sum of two terms: one coming from the scale derivative of each particular variable, and a second one coming from the scalar product of its spatial gradient times the shift in position of the new peak relative to the old one (equation [3.44]). However, the nesting probability does not depend on the variables $\partial_R\eta_i$ since these variables do not correlate with $\nu, x, v_2, v_3, ...$ (see Appendix A). Thus, in averaging below over all variables, these second terms will contribute with a null mean (the distribution of $\partial_R\eta_i$ for peaks is the same as for arbitrary points). Consequently, we can drop these second terms which is equivalent to taking an effective location for each evolved peak equal to the mean expected value, that is, the same location as the original peak.

From equation (B.1) we have that the density of peaks at δ per infinitesimal ranges of R and x, v_2, v_3,... which, after evolving to δ_f, are found to be nested (although not necessarily just become nested) into non-nested peaks with scales between R' and $R' + dR'$ ($R \leq R_f < R'$) is

$$N_{pk}^{nest}(R \to R', x, v_2, ..., \delta \to \delta_f)\,dR\,dR'\,dx\,dv_2, ...$$
$$= N_{pk}(R, x, v_2, ..., \delta)\,dR\,dx\,dv_2, ...\,P(R', \delta_f | R_f, \delta_f, x_f, v_{2f}, ...)\,dR' \quad \text{(B.4)}$$

with R_f, x_f, v_{2f}, v_{3f},... on the right hand side in terms of R, x, v_2, v_3,... and $\Delta\delta$ through equations (B.2) and (B.4), and the specific nesting probability P given in Appendix A. To obtain $N_{pk}^{nest}(R \to R', \delta \to \delta_f)\,dR\,dR'$ giving the density of peaks at δ per infinitesimal range of R which are nested at δ_f into non-nested

peaks on scales between R' and $R'+dR'$, we must integrate equation (B4) over variables $x, v_2, v_3, \ldots$. Given the simple expression of the nesting probability appearing in equation (B.4) in terms of the variable $\bar{\nu}$ (equation [A.8]) it is convenient to first transform v_2 and v_3 to $\bar{\nu}$ and $\bar{x}$. This can be done by repeated application of the scheme given in § 2.3.2. Taking into account the correlations (A.8) and (A.9) and the fact that $\sigma^2_{\nu'} = 0$ (see the discussion after equation [A.11]) we first obtain

$$N_{pk}(R, x, \bar{\nu}, R', \delta)\, dR\, dx\, d\bar{\nu} = N_{pk}(R, x, \delta)\, dR\, dx\, \frac{\exp\left[-\dfrac{(\bar{\nu}-\bar{\nu}_*)^2}{2\sigma^2_{\bar{\nu}}}\right]}{\sqrt{2\pi}\,\sigma_{\bar{\nu}}}\, d\bar{\nu}, \quad \text{(B.5)}$$

with $N_{pk}(R, x, \delta) = \mathcal{N}_{pk}(\nu, x, R)\, x\, \sigma_2\, R/\sigma_0$ in terms of the density function given in equation (3.23) and

$$\begin{aligned} \bar{\nu}_* &= \alpha_{\bar{\nu}0}\frac{\delta}{\sigma_0} + \alpha_{\bar{\nu}1}\, x & \sigma^2_{\bar{\nu}} &= 1 - \epsilon^2\left[\frac{(1-\gamma^2 r_1)^2}{1-\gamma^2} + r_1^2\right] \\ \alpha_{\bar{\nu}0} &= \frac{\epsilon(1-\gamma^2 r_1)}{1-\gamma^2} & \alpha_{\bar{\nu}1} &= -\frac{\epsilon\gamma(1-r_1)}{1-\gamma^2} \end{aligned} \quad \text{(B.6)}$$

with $\epsilon \equiv \sigma^2_{0h}/(\sigma_0\,\sigma'_0)$ and $r_1 \equiv \sigma^2_{1h}\,\sigma^2_0/(\sigma^2_{0h}\,\sigma^2_1)$ already used in § 3.2.2. Then, from correlations (A.12) and (A.13) we obtain

$$N_{pk}(R, x, \bar{\nu}, \bar{x}, R', \delta)\, dR\, dx\, d\bar{\nu}\, d\bar{x} = N_{pk}(R, x, \bar{\nu}, R', \delta)\, dR\, dx\, d\bar{\nu}\; \delta(\bar{x})\, d\bar{x}. \quad \text{(B.7)}$$

This result is well understood. As shown in Appendix A, variable $\bar{\nu}$ can only take the same value as ν' and, hence, $\sigma'_0\,\bar{\nu}$ can only depend on R' so that $\bar{x} \equiv -(\sigma_2\, R)^{-1}\,\partial_R(\sigma'_0\,\bar{\nu})$ must be null. Finally, following the same procedure we can infer the density of peaks for the remaining infinite series of variables $v_4, v_5, \ldots$ in infinitesimal ranges. But this is actually not necessary since the integration of equation (B.4) over these latter variables not entering in P is trivial, leading to

$$\begin{aligned} N^{nest}_{pk}(R \to\ R', x, \bar{\nu}, \bar{x}, \delta\ \to \delta_f)\, dR dR' dx d\bar{\nu} d\bar{x} &= N_{pk}(R, x, \bar{\nu}, \bar{x}, R', \delta) \\ &\times P(R', \delta_f|\bar{\nu}_f)\, dR dR' dx d\bar{\nu} d\bar{x}, \end{aligned} \quad \text{(B.8)}$$

with $\bar{\nu}_f = \bar{\nu} - \bar{x}\,\Delta\delta/(x\,\sigma'_0)$. Then, by integrating equation (B8) over $\bar{x}$, and $\bar{\nu}$, keeping the first order terms in $\Delta\delta$ and then integrating over x (in the positive

range) we arrive to

$$N_{pk}^{nest}(R \to R', \delta \to \delta_f)\, dR\, dR' = N_{pk}(R, \delta)\, P(R', \delta | R, \delta) \times \left\{1 - \partial_{\delta_f} \ln[N(R', \delta_f)\, N_{pk}(R, \delta | R', \delta_f)]\Big|_{\delta_f = \delta} \Delta\delta\right\} dR\, dR'. \quad \text{(B.9)}$$

Equation (B.9) can also be written in the form

$$N_{pk}^{nest}(R \to R', \delta \to \delta_f)\, dR\, dR' = N_{pk}(R, \delta)\, dR\, P(R', \delta_f | R, \delta)\, dR', \quad \text{(B.10)}$$

with

$$P(R', \delta_f | R, \delta)\, dR' = \frac{M(R')}{\rho}\, N(R', \delta_f)\, dR'\, \frac{N_{pk}(R, \delta | R', \delta_f)}{N_{pk}(R, \delta)} \quad \text{(B.11)}$$

therefore giving the probability (only for $R' > R$; the case $R' = R$ being excluded) that a peak with δ on scale R is located on a disjoint background with δ_f on scales between R' and $R' + dR'$. The expression for that probability given by equation (B.11) is just what one would expect from the same arguments leading to the nesting probability (A.1). Notice that, in contrast to the case $\delta_f = \delta$, the probability given by the left-hand member of equation (B.11) would now include not only the nesting effect but also direct filtering evolution, while, by construction, the right-hand member of equation (B.9) only includes the nesting effect. However, as readily seen from a similar development as that leading to N_{pk}^{nest}, the density of peaks with R at δ which, by direct evolution, are found with R' at δ_f is of high order in $\Delta\delta/(R' - R)$. So, to first order in $\Delta\delta$ and provided $R' - R$ is not too small, there is no difference, in practice, between these two expressions. Note also that the spatial shift of evolving peaks makes the different order scale derivatives of the density contrast of the evolved peak at δ_f deviate from those of the initial point at the same δ_f for arbitrarily large values of $\Delta\delta$ (see equation [B.4]). The equality only holds to first order in $\Delta\delta$. Therefore, the probability to find a peak with R at δ located in a disjoint background with R' at δ_f is different, in general, from the probability that the corresponding evolved peak at δ_f is located in that background.

We are now ready to calculate the net density of peaks with δ on scales between R and $R + dR$ *becoming nested into* (being destroyed in a merger

giving rise to) non-nested peaks with $\delta_f \equiv \delta - \Delta\delta$ on scales between R' and $R' + dR'$, $N^d(R \to R', \delta \to \delta_f)\, dR\, dR'$. (Superindex d stands for destruction since we are dealing with true mergers.) To do this we must simply correct the density of peaks which, after evolving from δ to δ_f, turn out to be nested into non-nested peaks with such larger scales for nesting at the initial δ in the ancestrors of those disjoint backgounds at δ_f. (Note that these ancestrors concern, in principle, any kind of evolution, although the contribution of direct evolution can be ignored in practice since being of higher order in $\Delta\delta$). This correction can be readily performed following the same procedure as leading to equation (5.1). The result is the integral equation

$$N^d(R \to R', \delta \to \delta_f) = N_{pk}^{nest}(R \to R', \delta \to \delta_f) - \int_R^{R'} dR'' \, \frac{M(R'')}{\rho} \, N^d(R'' \to R', \delta \to \delta_f)\, N_{pk}(R, \delta | R'', \delta) \quad \text{(B.12)}$$

for the unknown function $N^d(R \to R', \delta \to \delta_f)$ in terms of $N_{pk}^{nest}(R \to R', \delta \to \delta_f)$ (equation [B.12]) and $N_{pk}(R, \delta | R'', \delta)$ (see equation [5.1]).

But we do not need to solve equation (B.12). Given the meaning of N^d and N, we have $N^d(R'' \to R', \delta \to \delta) \equiv N(R', \delta)\, \delta(R' - R'')$. (Notice that R'' reaches the value R' inside the integral of eq. [B12].) And since $N_{pk}^{nest}(R \to R', \delta \to \delta)$ is equal to $N_{pk}(R, \delta)\, P(R', \delta | R, \delta)$ (see eq. [B9]) we are led to $N^d(R \to R', \delta \to \delta) \equiv 0$ (for $R < R'$ as in the present case). Thus, equation (B.12) reduces to a simple relation between first order terms in $\Delta\delta$. By dividing this relation by $\Delta\delta$ we are led (see eqs. [B9] and [A13]) to the Volterra type integral equation of the second kind

$$\mathbf{N}^d(R \to R', \delta) = -\frac{M(R')}{\rho} \, \partial_{\delta_f} [N(R', \delta_f)\, N_{pk}(R, \delta | R', \delta_f)]_{\delta_f = \delta} - \int_R^{R'} dR'' \, \frac{M(R'')}{\rho} \, \mathbf{N}^d(R'' \to R', \delta)\, N_{pk}(R, \delta | R'', \delta), \quad \text{(B.13)}$$

whose solution gives the wanted net density $\mathbf{N}^d(R \to R', \delta)\, dR\, dR'\, d\delta$ of non-nested peaks at δ with scales between R and $R + dR$ becoming nested (merging) into non-nested peaks with scales between R' and $R' + dR'$ in the next $-d\delta$. Equation (B.13) can be solved numerically by iteration from the initial

approximate solution $-M(R')\,\rho^{-1}\,\partial_\delta[N_{pk}(R',\delta)\,N(R,\delta|R',\delta)]$. Actually, this latter function is a very good approximation to the wanted solution, at least for all power spectra analyzed. Thus, we can simply take

$$\mathbf{N}^d(R \to R',\delta) \approx -\frac{M(R')}{\rho}\,\partial_{\delta_f}[N(R',\delta_f)\,N_{pk}(R,\delta|R',\delta_f)]_{\delta_f=\delta}, \qquad \text{(B.14)}$$

with $\partial_\delta N(R',\delta)$ given by numerical differentiation of the scale function $N(R',\delta)$ or, what is more accurate, by the numerical solution of the new Volterra type integral equation

$$\begin{aligned}\partial_\delta N(R',\delta) &= \left[\partial_\delta N_{pk}(R',\delta) - \int_{R'}^{\infty} dR''\,\frac{M(R'')}{\rho}\,N(R'',\delta)\,\partial_\delta N_{pk}(R',\delta|R'',\delta)\right] \\ &- \int_{R'}^{\infty} dR''\,\frac{M(R'')}{\rho}\,\partial_\delta N(R'',\delta)\,N_{pk}(R',\delta|R'',\delta), \qquad \text{(B.15)}\end{aligned}$$

resulting from differentiation of equation (5.1).

C

Net Density of non-Nested Appearing Peaks

The net density of peaks appearing at δ with scales between R and $R + dR$ and variables x, v_2,v_3,... in infinitesimal ranges is equal to the density of peaks found with these characteristics minus the density of those of them arising by continuous evolution from peaks at $\delta_i \equiv \delta + \Delta\delta$, with $\Delta\delta$ positive and arbitrarily small. Therefore, the net density of *non-nested* peaks appearing (forming) with the previous characteristics is

$$\mathbf{N}^f(R,\delta,x,v_2,v_3,...)\,\Delta\delta\,dR\,dx\,dv_2\,dv_3\,.... = \Big[1 - P(R,\delta,x,v_2,v_3,...)\Big]$$

$$\times \Big[N_{pk}(R,x,v_2,v_3,...,\delta) - N_{pk}^{ev}(R,x,v_2,v_3,...,\delta)\Big]\,dR\,dx\,dv_2\,dv_3\,..., \qquad \text{(C.1)}$$

with $P(R,\delta,x,v_2,v_3,...)$ the integral (over $R' > R$) of the differential nesting probability given by equation (A.2) and $N_{pk}^{ev}(R,x,v_2,v_3,...,\delta)\,dR\,dx\,dv_2\,dv_3\,...$ the density of evolved peaks, equal to

$$N_{pk}^{ev}(R,x,v_2,...,\delta)\,dR\,dx\,dv_2\,... = N_{pk}(R_i,x_i,v_{2i},...,\delta_i)\,dR_i\,dx_i\,dv_{2i}\,... \qquad \text{(C.2)}$$

Equation (C.2) is but equation (B.1) for the present values of the initial and final density contrasts, while the present relations between variables with and

without subindex i are just the inverse of those given in equations (B.2) and (B.4). Note that, for the same reasons as in Appendix B, we are forced to follow the evolution of the whole infinite set of variables $x, v_2, v_3, ...$

From equations (C) and (C.2) we have

$$\mathbf{N}^f(R,\delta,x,v_2,v_3,...)\,\Delta\delta\,dR\,dx\,dv_2\,dv_3\,... = \Big[1 - P(R,\delta,x,v_2,v_3,...)\Big]$$

$$\times\,\Big[N_{pk}(R,x,v_2,v_3,...,\delta) - N_{pk}(R_i,x_i,v_{2i},...,\delta_i)|J|\Big]\,dR\,dx\,dv_2\,dv_3\,... \quad \text{(C.3)}$$

with J the Jacobian of the transformation from variables with subindex i to variables without subindex. Thus, by integrating equation (C.3) over all intermediate variables we obtain

$$\mathbf{N}^f(R,\delta)\,\Delta\delta\,dR = \Big\{N(R,\delta) - N_{pk}(R,\delta)$$

$$+ \int N_{pk}(R,x,v_2,v_3,...,\delta)\,P(R_f,\delta_f,x_f,v_{2f},...)\,dx\,dv_2\,dv_3\,...\Big\}\,dR \quad \text{(C.4)}$$

In deriving equation (C.4) we have used the fact that $N_{pk}(R,\delta)$ times the probability that a peak with δ on scale R be nested, $P(R,\delta)$, is just equal to the difference $N_{pk}(R,\delta) - N(R,\delta)$ (equations [A.1] and[5.1]). We have also transformed the variables at δ in the integral on the right hand side to variables at δ_i, which balances the Jacobian $|J|$, and then dropped subindexes i for the new variables while written subindex f for the old ones, which makes them be related within each other just through equations (B.2) and (B.4).

For identical reasons as in Appendix B, it is convenient to express N_{pk} and the nesting probability P in equation (C.4) in terms of variables $\bar{\nu}$ and $\bar{x}$ instead of v_2 and v_3. After this substitution, the integrals over variables $v_4, v_5, ...$ in equation (C.4) become trivial, while those involving $\bar{x}, \bar{\nu}$ and x have been calculated in Appendix B (equations [B.8] and [B.9] for the differential nesting probability, equation [A.1], instead of the integral form used here). The final result after taking the limit $\Delta\delta \to 0$ is

$$\mathbf{N}^f(R,\delta)\,dR\,d\delta = \partial_\delta[N(R,\delta) - N_{pk}(R,\delta)]\,dR\,d\delta, \quad \text{(C.5)}$$

with $\partial_\delta N(R,\delta)$ given in equation (B.14).

D

Mass Accretion Rate

From equation (B.2) we have that the mass accreted from δ to $\delta_f \equiv \delta - \Delta\delta$, with $\Delta\delta$ positive and arbitrarily small, by any non-nested peak with initial scale between R and $R + dR$ and variable x in an infinitesimal range is

$$\Delta M = \frac{dM}{dR}\,\frac{1}{x\,\sigma_2\,R}\,\Delta\delta. \tag{D.1}$$

The density of such accreting non-nested peaks is

$$N^a(R, x, \delta)\,dR\,dx = N(R, x, \delta)\,dR\,dx. \tag{D.2}$$

In writing equation (D.2) we have taken into account that the density of non-nested peaks not accreting because merging from δ to $\delta - \Delta\delta$ is a higher order correction (see the discussion leading to equation [eq:apb13]). Therefore, by dividing the density (D.2) by $N(R, \delta)\,dR$ we obtain the conditional probability $p(x, R|\delta, R)\,dx$ that an accreting non-nested peak at δ with scale R has the appropriate value of x in order to increase its mass by ΔM given by equation (D.1) in the passage from δ to $\delta - \Delta\delta$. From equation (5.1) but for peaks with variable x in an infinitesimal range (or, equivalenly, from eq. [A14], after integrating the product $N_{pk}\,P$ over the remaining variables) this conditional probability takes the form

$$p(x, R|\delta, R)\,dx \;=\; \frac{dx}{N(R, \delta)}\Big[N_{pk}(R, x, \delta)$$

$$- \int_R^\infty dR' \frac{M(R')}{\rho} N(R', \delta)\, N_{pk}(R, x, \delta | R', \delta)\Big], \qquad \text{(D.3)}$$

with the densities $N_{pk}(R, x, \delta) = \mathcal{N}_{pk}(\nu, x, R)\, x\, \sigma_2\, R/\sigma_0$ and $N_{pk}(R, x, \delta | R', \delta) = \mathcal{N}_{pk}(\nu, x, R|\nu, R')\, x\, \sigma_2\, R/\sigma_0$ in terms of the analogous density functions calculated in Chapter 3.

By changing variable x into $M' = M + \Delta M$ we can compute the instantaneous accretion rate of objects of mass M per specific range of mass M' of the final object similar to the merger rate (5.6). By doing so we arrive to the fact that this transition rate is identically null. The reason for this is that, as mentioned in Appendix B, the density of peaks with scales between R and $R + dR$ at δ which directly evolve into peaks with scales between R' and $R' + dR'$ at δ_f is of higher order than one in $\Delta\delta = \delta_f - \delta$. This result is well understood. From the viewpoint of the accreting object, the process is not a transition between two different masses but as a continuous mass increase. Consequently, no discrete increment ΔM can be achieved in the limit $\Delta\delta \to 0$. Of course, such a continuous evolution of the accreting object during the small interval Δt necessarily causes (is made at the expense of) the merger (capture) of a number of tiny objects which do make a finite transition in mass. And it is taking the limit for vanishing Δt of the change in the number density of these latter objects that one obtains a non-vanishing accretion(+merger) rate (see § 5.3).

In any event, there is no problem, even from the viewpoint of accreting objects, in obtaining the instantaneous *mass accretion* rate at t for objects of mass M. Equation (D.1) tells us that the instantaneous mass increase rate, by accretion, for objects arising from peaks with δ and the specific value of x is

$$\frac{dM}{dt} = \frac{dM}{dR} \frac{1}{x\, \sigma_2\, R} \left| \frac{d\delta_c}{dt} \right|. \qquad \text{(D.4)}$$

Therefore, the instantaneous mass accretion rate, at t, for objects of mass M (disregarding any other particularity) is the average of the specific rate (??) for the probability function (D.3) with R and $\delta = \delta_c$ expressed in terms of M and t through equations (5.3) and (5.4). Given the form of functions $N_{pk}(R, x, \delta)$,

$N_{pk}(R, x, \delta | R', \delta)$ and the expression of $N(R, \delta)$ (equation [5.1]), we arrive to

$$r^a_{mass}(M,t) = \frac{dM}{dR} \frac{1}{< x > \sigma_2 R} \left| \frac{d\delta_c}{dt} \right|. \qquad \text{(D.5)}$$